ITER TECHNICAL REPORT

REPORT NO.

ITR-IEBH-206-1 v1.0

TITLE

ITER Engineering Basis Handbook

Vol. 2: Anatomy of the Plant

Chapter 6 - All the pieces of the puzzle

Section 1 - Magnets Systems Including Vessel Coils

CHIEF EDITOR

Dr. Gianfranco Federici

CHIEF EDITOR'S EMAIL

gianfranco.federici@euro-fusion.org

August 8th, 2026

This work has been carried out within the framework of the EUROfusion Consortium, funded by the European Union via the Euratom Research and Training Programme (Grant Agreement No 101052200 – EUROfusion). Views and opinions expressed are however those of the author(s) only and do not necessarily reflect those of the European Union or the European Commission. Neither the European Union nor the European Commission can be held responsible for them.

www.iter.org

About the ITER Basis Engineering Handbook

This handbook consists of two volumes which describe the ITER design from its inception up to the design, construction and assembly in 2025.

The handbook is not designed to be read as a continuous sequence of chapters. Instead, it is composed of focused, self-contained sections that address specific topics. Each chapter can be read and understood independently, allowing readers to engage with the material most relevant to their needs without requiring familiarity with preceding chapters. As a result, the reader will find certain overlapping content in chapters.

It is to be noted that at the time of writing, the design for some systems is still on-going. Therefore, the reader should consider that whilst there is significant value of this important point-in-time study, an update would be required as the Project progresses.

A broad Project overview is given in the first volume, to provide the reader with background information necessary to understand the context in the subsequent more-detailed chapters of the second volume, dedicated to the individual systems composing ITER.

For the overall table of contents of the Handbook and to access each one of the chapters, please refer to https://www.iter.org/scientists/iter-technical-reports.

Authors and Contributors of this Chapter

This chapter is authored by Neil Mitchell.

Volume 2
ANATOMY OF THE PLANT

Chapter 6
ALL THE PIECES OF THE PUZZLE

Section 1

MAGNETS SYSTEMS INCLUDING VESSEL COILS

Table of Contents

Chapter 6

All the pieces of the puzzle

6.1 Magnet Systems Including Vessel Coils

6.1.1 Overview

The magnet system comprises, in its as-built form (2024), as shown in Figure 6.1-1:

- 18 toroidal field (TF) coils using Nb_3Sn superconductor and operating at a maximum (conductor) current of 68kA provide a toroidal magnetic field on the plasma axis of up to 5.3T, with a maximum field in the inboard length of 11.8T. The TF coils come with a set of structures (cases and intercoil keys) together with gravity supports (one per coil) and a set of pre-compression rings.
- A central solenoid (CS), assembled from 6 modules fabricated from Nb_3Sn superconductor, operating at up to 45kA and producing a maximum field of 13T, capable to provide 30,000 full flux swings (i.e. from maximum negative to maximum positive conductor current) with a maximum rate of field swing of ~1.2Ts^{-1} over the device lifetime. The CS includes upper and lower segmented flanges (key blocks) and a set of inner and outer tie plates used to pre-load the modules.
- 6 poloidal field (PF) coils fabricated from NbTi superconductor, having diameters of up to 25m, and producing maximum fields (at the conductor) of ~6T at operating currents of up to 45kA. The PF coils have clamps which connect them to the TF coils.
- 18 error field correction coils (CC), also fabricated from NbTi superconductor. The CC have clamps which connect them to the TF coils, with 3 in the poloidal direction (lower, side and upper) and 6 around the torus.

- An extensive set of feeders leading current (with NbTi superconductor), cryogen and instrumentation supplies from outside the cryostat into the coils.
- Two copper/MgO insulated vertical stability control coils on the inner surface of the vacuum vessel.
- 27 copper/MgO insulated ELM control coils mounted on the inner surface of the vacuum vessel, 3 poloidally and 9 toroidally.
- A set of feeders for the in-vessel coils providing current and water cooling.

The ITER design activities eventually produced, in the 2001 FDR, what is essentially the present ITER design. This shared many design concepts with ‘next step’ devices explored in earlier years by the ITER partners (e.g. the EU NET device of the late 1980s). The magnet and conductor concepts in the 2001 design for ITER, developed over the previous 10 years, were also substantially utilized in the KSTAR and EAST devices, both of which became operational during the 2000s with both design groups being involved in contacts to the ITER magnet group at Naka up to 2006. Both tokamaks exploited the cable-in-conduit conductor development that led up to the ITER model coil program, section 3.3.2. More recently in 2024, the BEST tokamak in China and the DTT (Diverter Test Tokamak) in Italy are closely following the ITER magnet and Nb_3Sn conductor designs.

Between 2001 – 2006 (i.e. from the issuing of the ITER Final Design Report until the signature of the ITER Agreement) ITER activities were not covered by a formal agreement among the partners, and therefore all R&D was undertaken by the partners on a voluntary basis. The continuing analysis enabled three major improvements to be introduced in the magnet area: fixing the copper to non-copper ratio in the Nb_3Sn strands at 1.0 (and abandoning conventional NbTi stability theory), adopting the use of High Temperature Superconductors in the Current Leads and adopting a cyanate ester blend of resin in place of epoxy DGEBA/F type for the insulation systems.

Following signature of the ITER Construction Agreement in 2007, the project entered the Construction Phase, led in the tokamak area by magnets, where the first procurement contracts for the superconducting strands were placed in 2008. Design developments continued after this, and realisation of realistic manufacturing routes also required changes. Performance shortfalls also drove some modifications. Major changes had to be introduced in the Feeders, because of seismic assessments arising from nuclear safety requirement changes after the Fukushima accident in 2011, with a major change in the cryostat base and gravity support system. The in-vessel coil system, much discussed even before 2001, was not implemented until 2011 when it became obvious that plasma control (and especially near-elimination of VDEs) could not be achieved with a low resistance fully welded vacuum vessel and superconducting coils outside it.

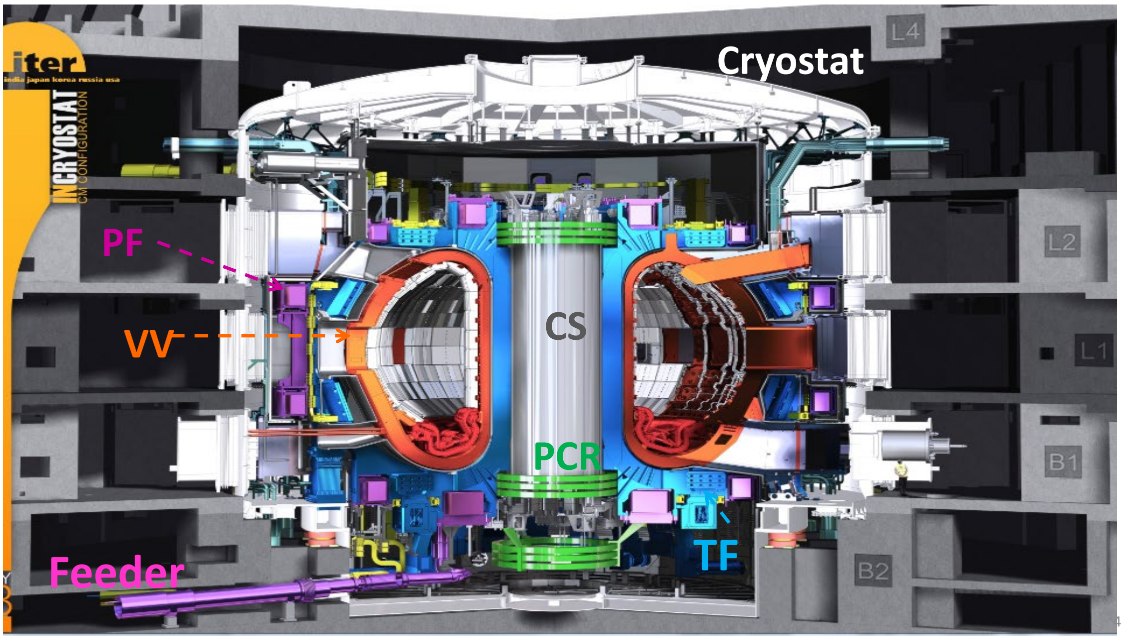

Fig. 6.1-1: The ITER Magnet System

6.1.2 Magnet System as Built

In this section the evolution of the ITER magnet system from the 2001 FDR through to the 2024 as-manufactured configuration is described.

6.1.2.1 Superconductors

The basic conductor used in the superconducting coils is a rope-type cable-in-conduit type using Nb_3Sn (TF, CS) or NbTi (Feeders, PF, CC) superconductor and cooled by a forced flow of supercritical helium, Figure 6.1-2. The cable is formed by multi-stage cabling of superconducting strands, with the final stage (except for the CC) consisting of 6 bundles twisted around a central cooling channel, Figure 6.1-3. The TF conductor has an external circular jacket (Figure 6.1-2) and the CS and PF conductors a square jacket.

The cable is a mix of superconductor strands and pure copper, with the copper providing the thermal protection against quench.

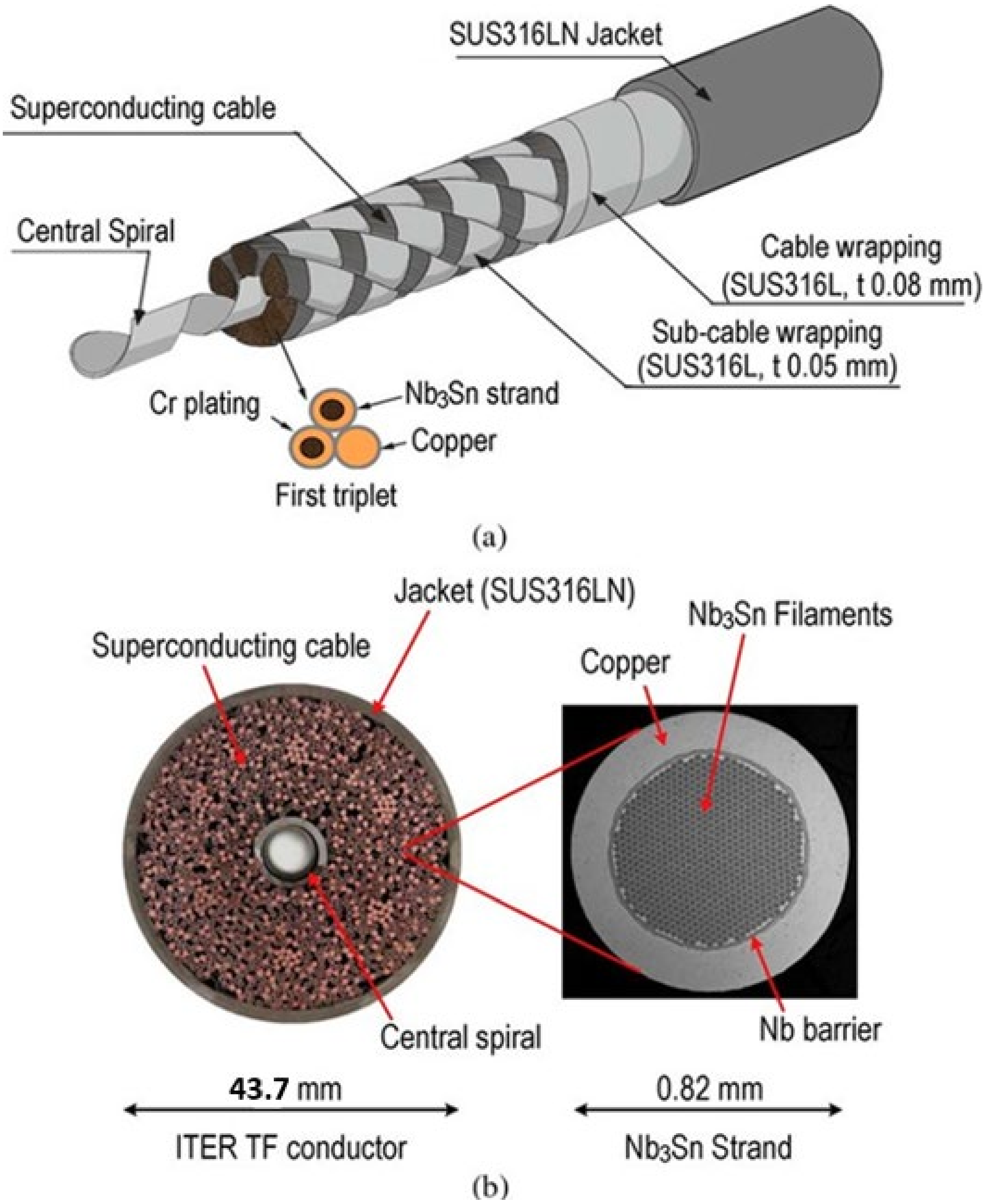

Fig. 6.1-2: ITER Cable in Conduit Conductors

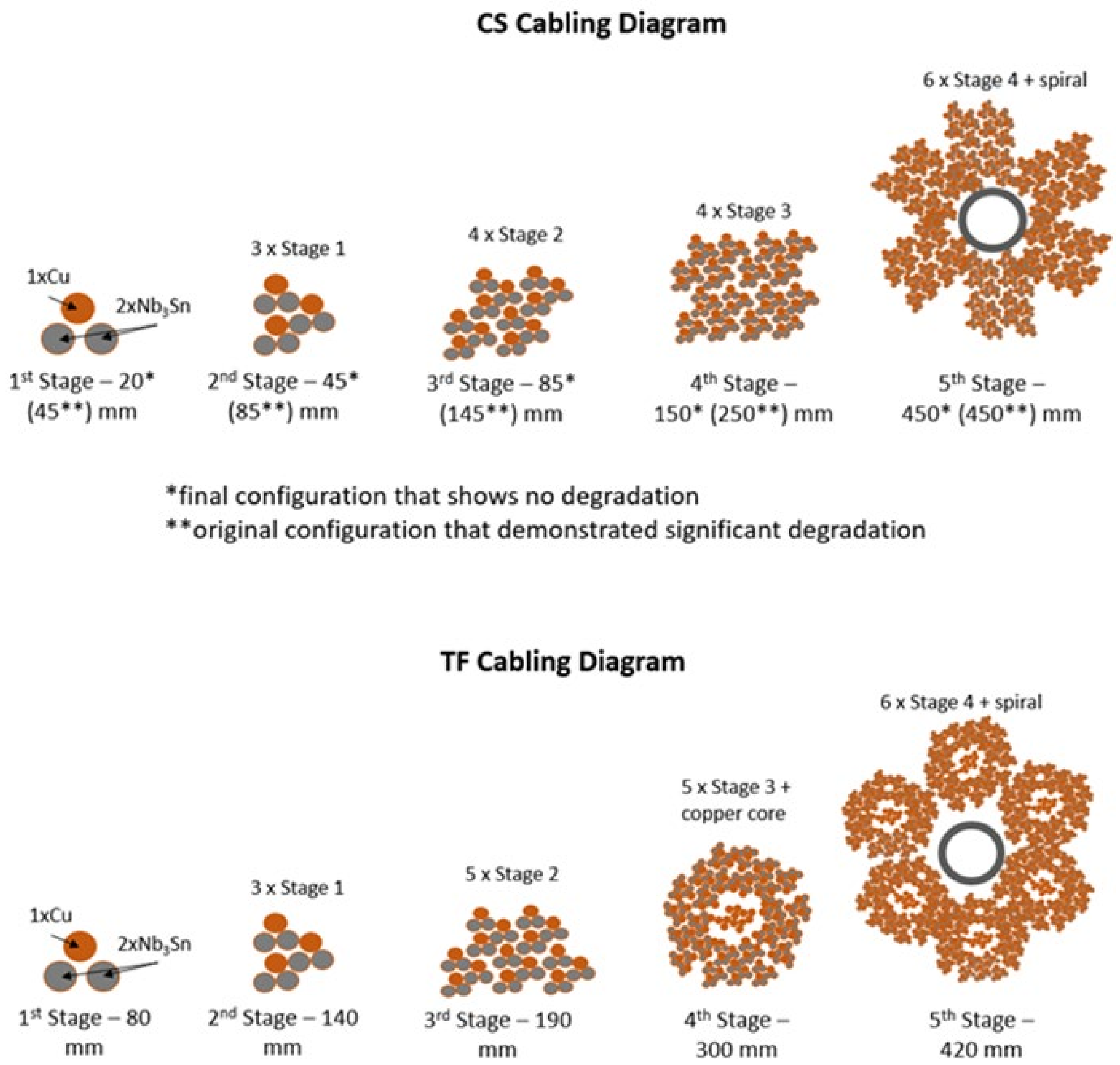

Fig. 6.1-3: CS and TF cable designs. The CS cable pitch lengths were modified in 2010-11 to solve a degradation issue, as described in section 3.3.2.

6.1.2.2 TF Coils, Supports and Structures

The 18 TFCs are 'D' shaped as shown in Figure 6.1-4 and consist of a winding pack enclosed in a thick steel case, the Toroidal Field Coil Case (TFCC) Figure 6.1-5, and made up of 4 welded sub-assemblies as shown in Figure 6.1-6. The coils are wedged together along the inner straight leg, Figure 6.1-4.

6.1.2.2.1 Winding Pack (WP)

The WP, Figure 6.1-5, is a bonded structure of 7 Double Pancakes (DP) each made up of a steel radial plate (RP), which houses the reacted Cable in Conduit Conductor (CICC), with an outer ground insulation of 7mm thickness. The coil terminals protrude from the TFCC at its lower curved part with the 6 DP joints (i.e. the joints linking adjacent DPs) and the helium feeder manifolds, Figure 6.1-4.

6.1.2.2.2 Case

Each leg of the TFCC is formed by a sub-assembly with a U-section and a closure plate sub-assembly, Figure 6.1-6. Both U-section sub-assemblies have numerous integral structural attachments such as the Intercoil structures, the pre-compression flanges, the TFC support leg, and attachments for the CS, PFC, CC, vacuum vessel thermal shield (VVTS) supports and machine assembly tooling (some are labelled in Figure 6.1-4).

In operation, the centring force on each TFC is reacted by toroidal hoop pressure in the central "arch" formed by the straight inboard legs of the 18 coils. The TFCC inboard legs are wedged over their full radial thickness and about half of the centring force is reacted in toroidal direction through the WP, while the other half is reacted by the case. The front part or "nose" of each TFCC is thicker to take the case part of this load.

When the TFCs are energized, the WP also pushes outward all-round the case and tends to shrink slightly in the toroidal and radial directions due to the Poisson effect and magnetic compression. A small gap between WP and TFCC opens on the inside (facing the plasma). This gap may locally close due to torsion of the coil under out-of-plane forces when the CS and PFC are pulsed. A positive consequence of this gap is to reduce the heat conduction from the TFCC to the plasma-facing side of the WP. This "thermal barrier" is supplemented by the electrical insulation layer on the plasma facing side of the WP and the WP-to-TFCC fill material; the cooling pipes in grooves on the inner surface of the TFCC also act as a thermal screen, with pipe spacing chosen to minimize heat transfer from the case even in the case of full thermal contact. In the inboard leg, the wedging pressure forces the winding pack against the case and tends to suppress the side gaps. On the outboard leg, there is a small amount of slip between WP and TFCC through the plasma pulse as the out-of-plane forces change.

In the inboard curved regions above and below the straight leg, the case thickness increases rapidly to provide adequate out-of-plane support. The peak stresses occur at the point where the straight leg ends, and they are sensitive to the minimum wall thickness of the case at this point (this determines its torsional rigidity which is required to support the loads as the wedging stops).

6.1.2.2.3 Intercoil Structures including Precompression Rings

The ITER designs of the 1990s included elaborate methods to support the overturning moments on the TF coils, partly because of the high plasma current (the moment is proportional to the current) and because of the use of a bucked design where torsion of the CS had to be limited. This extended to full keying of the TF coils to each other in the inner leg region. The difficulty of manufacturing this to the required tolerances and then assembling it was one of the insurmountable problems that led to the wedged design to be chosen instead. By the 2001 FDR, these links between the individual TF coils had relaxed to 4 sets of support systems, the Inner Leg Intercoil Structure (ILIS), the Inner Intercoil Structure (IIS) keys, the OIS (outer intercoil structure) and the IOIS (intermediate OIS), plus the Pre-Compression Rings (PCRs).

In the wedged design the TF coil inner legs touch and support the overturning moment by friction. This was addressed rather simplistically until 2017 without a proper design of the interface surfaces. The IIS, OIS and IOIS all went through a detailed design phase in 2010-2012. The changes were substantial and largely addressed the issue of absorbing tolerance between the coils (match machined shells for the IIS and off set inserts and expansion bolts/pins for the OIS). The IOIS had more significant performance problems (load distribution and stress concentrations) and was completely changed, twice, from the 2001 FDR design before the present system of large pins, match machined inserts and plates was developed.

The ILIS had to combine the functions of a shim (to adjust the gaps between the TF coils to achieve the required average value of 2mm for each gap (see the section below on tolerances) and to remain fixed to the coil surfaces when they are de-energised (with the risk of falling down the gap and creating a severe non-uniformity in the wedging stresses), and also to provide a low voltage insulation against eddy currents. Finally, a system of variable thickness steel plates on one side and G11 high strength boards on the other, both fixed with washers, was adopted in 2018. Attaching these plates was eventually performed in a separate facility on site (building 73.2), partly because the design was finalised too late to be included in the work at the suppliers and partly to leave flexibility in case the ILIS needed to be customised during assembly.

The original intent was that the coils could be shimmed as required (i.e. as determined by the on-going build up in the cryostat) while on the SSAT, at the last minute. This has not been possible due to access and orientation and all the TF coils have been prepared in the same way. It is fortunate that it seems from the manufacturing experience and the initial assembly of sector 6, that the TF manufacturing and SSAT adjustment capability is sufficiently good to avoid the need for variable ILIS shimming and the early pre-preparation will be acceptable.

The Pre-Compression Rings as originally conceived were a sort of replacement of the 'crown rings' of the 1998 FDR concept, with the idea that a pre-load in the region of the top and bottom of the inner leg is needed to maintain the IIS keys in compression and prevent gaps opening, with severe consequences on the case fatigue. The development created many problems but also, as seen in 2024, the rings are not as design critical as was thought in 2001. Adjustments of the local coil surface at the keys, and an improved (i.e. more limited) gap range between the TF coils of 0.5-2.5mm on average is sufficient to keep the IIS in compression, also without the PCRs. The PCRs do however have an important function to reduce the toroidal tension loads carried by the IOIS. It seems possible that more effort on the TF coil case thicknesses could have also provided the same functionality without the PCRs, but there was little time or resources for structural optimisation from 2001-2007.

The designs of the ITER TF intercoil structure system have been more or less repeated in BEST and DTT magnet systems (without apparently a PCR equivalent being needed).

6.1.2.2.4 Gravity Supports (GS)

A GS supports the leg attached to the lower outer curved region of each TFC, Figure 6.1-7. The GS includes a flexible plate assembly (FPA), clamping bars, studs and bolts. The FPA is pre-assembled in the factory from 21 flexible plates (with cooling pipes and thermal shields sections attached), separated by 20 short spacer plates at top and bottom. The FPA components are pressed together at top and bottom between pairs of horizontal pre-stressing bars by tie-rods. The FPA is designed with sufficient pre-compression and friction to prevent both sliding and separation between its components.

The FPA of each GS flexes to accommodate the radial thermal contraction of the TFC assembly. But the GS is rigid versus cyclic out-of-plane bending caused by TFC torsion during plasma operation, and versus vertical and horizontal forces parallel to the flexible plates due to deadweight, asymmetric plasma VDE and earthquakes. The 18 GS transmit these loads to the pedestal ring, which is an integral part of the cryostat structure. In a design change implemented in 2015, the base of the TFGS is keyed to the cryostat ring to prevent toroidal sliding.

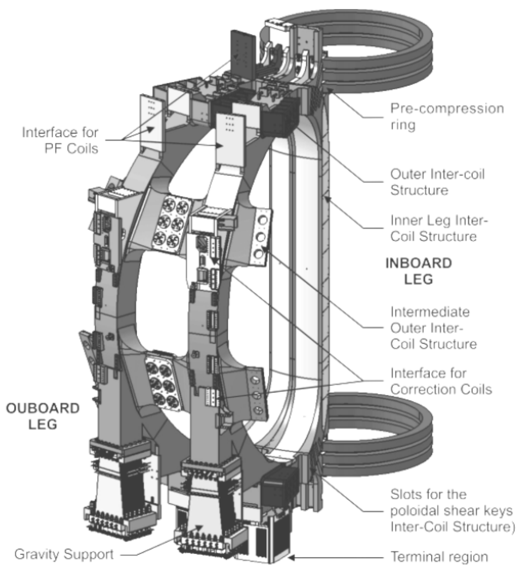

Fig. 6.1-4: The TF Coil Subsystem (2 coils)

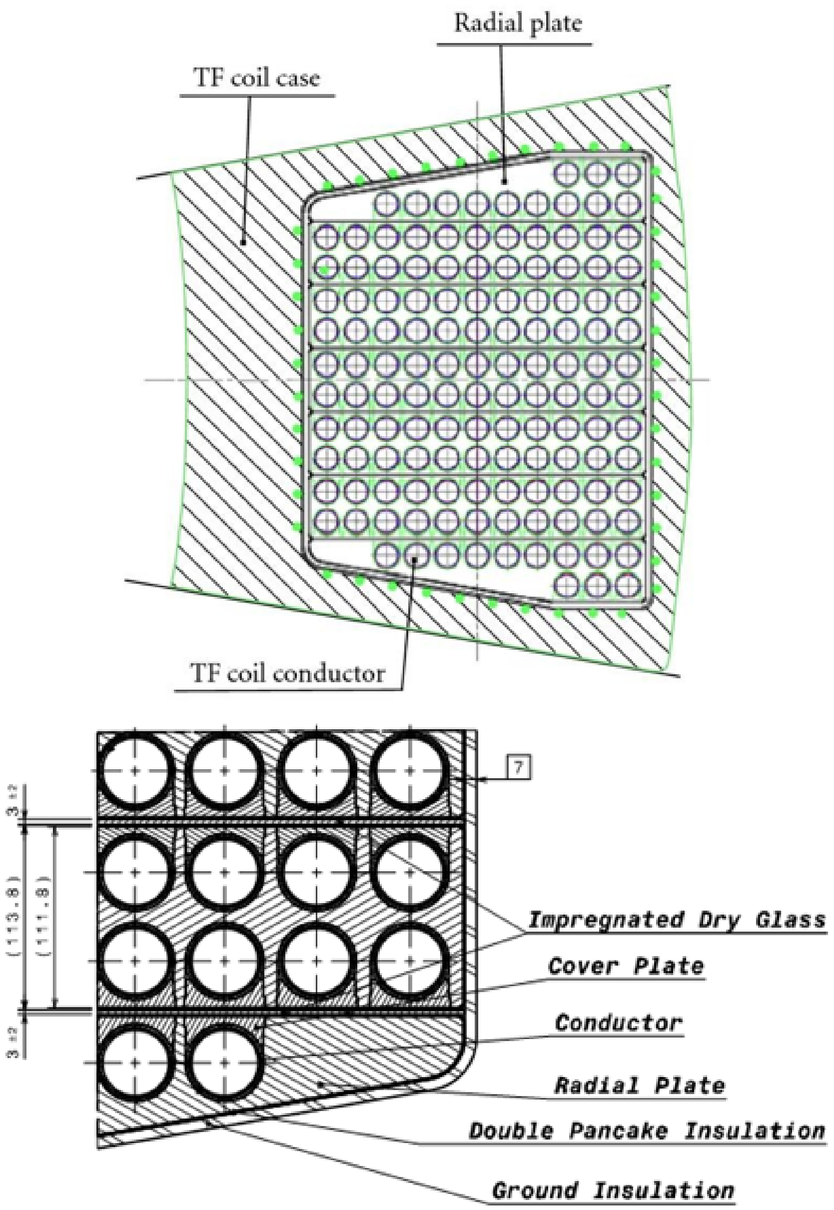

Fig. 6.1-5: TF Coil Cross Section

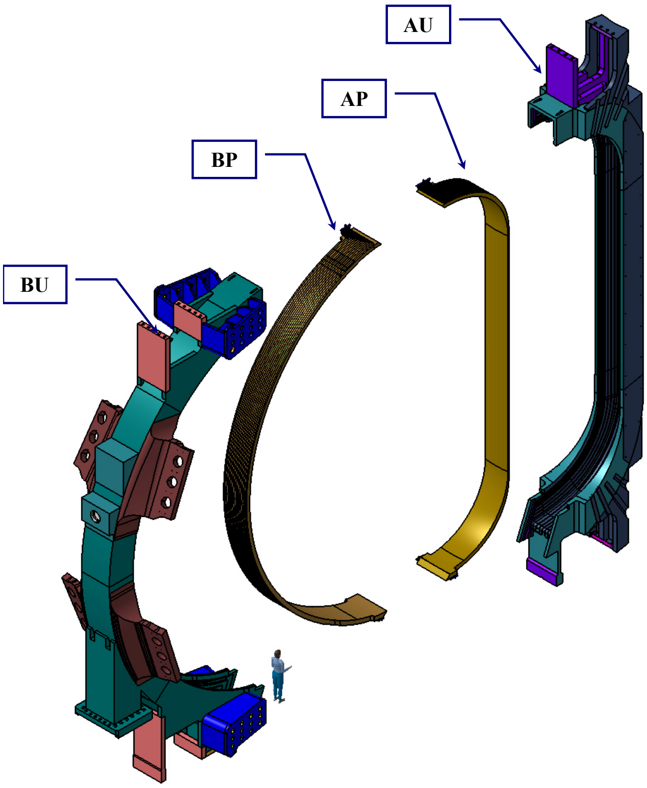

Fig. 6.1-6: The 4 Sub-Assemblies of the TF Coil Case

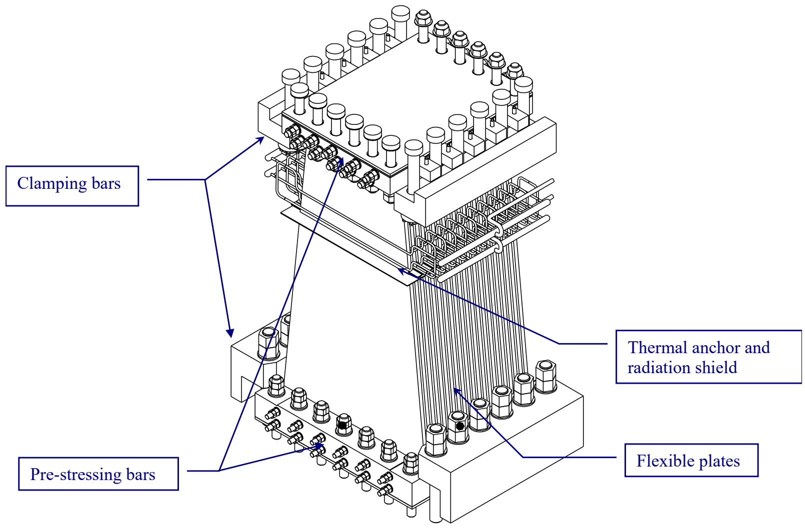

Fig. 6.1-7: TF coil gravity support

6.1.2.3 PF Coils

6.1.2.3.1 PF Windings

The PF system consists of 6 coils, PF1 through PF6 that serve to shape and stabilize the position of the plasma in the tokamak, Figure 6.1-8. All coils are built by stacking 6 to 9 double-pancake (DP) windings wound with two-in-hand NbTi superconducting CICCs (cable-in-conduit conductors). The outer diameters of the coils vary between ~8m and ~ 24m.

The PF coils are wound in a "two-in-hand" configuration, Figure 6.1-9. Two conductors are wound together from the outer diameter in to form the lower pancake. At the inner-most turn, an upward vertical joggle is formed in each conductor. This is followed by two-in-hand winding of the upper pancake from the inner diameter. There is an external joint between the two 'hands.'

To avoid major disassembly of the tokamak to extract a PF coil and repair a failed DP, all PF coils are designed to allow a DP to be bypassed with a superconducting jumper in the event of failure. As the failure is anticipated to be an electrical short, not only does the failed DP have to be bypassed but the closed-circuit loop created by the short has to be opened, either at the internal DP joint or by cutting the conductors, depending on its location, to prevent large eddy currents. The loss of Ampere-turn in the repaired coil is recovered by increasing the operating current. The joints are, therefore, placed 'outside' the line of the winding pack so that they can (in principle) be accessed to allow the jumpers to be connected.

The coils have particularly thick turn and pancake insulation. This partly results from the early (2001) design of the insulation where each conductor was wrapped with a metal grounded foil (to allow insulation fault detection) which was eliminated by 2007 (due to the huge capacitance that such an arrangement causes in the coil, with many possible resonance effects with fast voltage transients, due to the much higher internal voltages between the screen and the conductor, and the restrictions the foil creates on the resin flow in the impregnation process). The space occupied by the foil was replaced by a thicker insulation to keep the same current density in the coil and avoid increasing the peak field. The peak field levels can be an issue for the NbTi conductors.

6.1.2.3.2 PF Supports

At each PF coil support, the winding pack is clamped between a pair of plates linked by tie-rods. The clamping plates and tie rods can be used for lifting/handling purposes during PF coil fabrication and installation. They are also used in some of the PF coils to support the coil terminals, outer protection cases and insulating breaks in the cooling lines. The PF coils are self-supporting as regards the radial magnetic loads which are reacted by hoop tensile stresses in the conductor jacket.

The supports for PF Coils 1 and 6 have 9 clamps to allow space for the joints, the others have 18. Load transmission is through sliding supports for the PF1 and PF6 coils where space is limited, with flexible suspension plates to allow radial expansion of the PF coils which are then connected to the TF coil cases. These are two flexible plates on each side of the coil which are welded at one end to one of the clamping plates and at the other to flanges which are bolted to the support plate. The support plates are placed on the side of the coil nearest the machine equatorial plane so that the vertical forces, in almost all load cases directed towards the equatorial plane, create tension in the flexible plates and avoid a risk of buckling.

The PF3 and PF4 coils are linked to each other by a strut connecting the support posts of each coil. Each strut is linked to the adjacent TF coil just below the PF3 coil by a circular dowel. This supports the resultant vertical loads and allows free out of plane rotation of the TF coils.

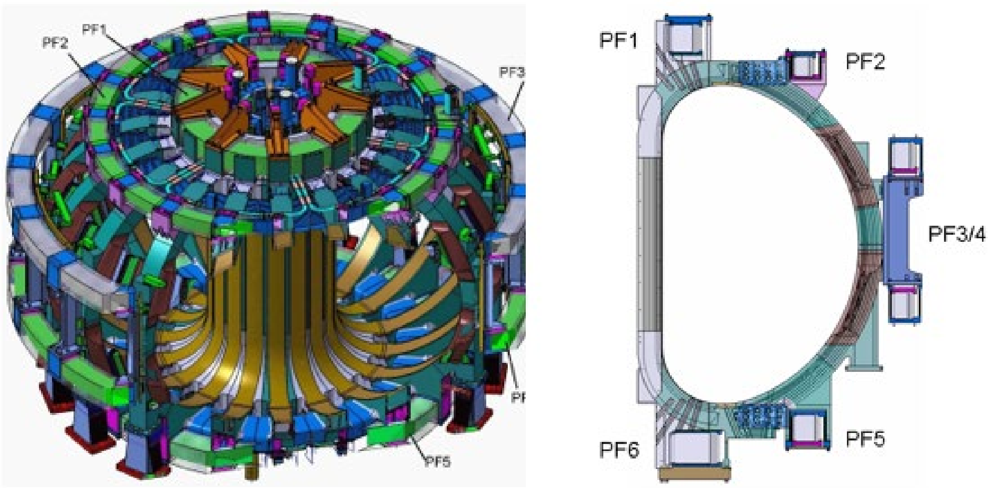

(a) 6 PF coils supported by 18 TF coil cases.

(b) Poloidal positions of PF coil supports on the TF coil case.

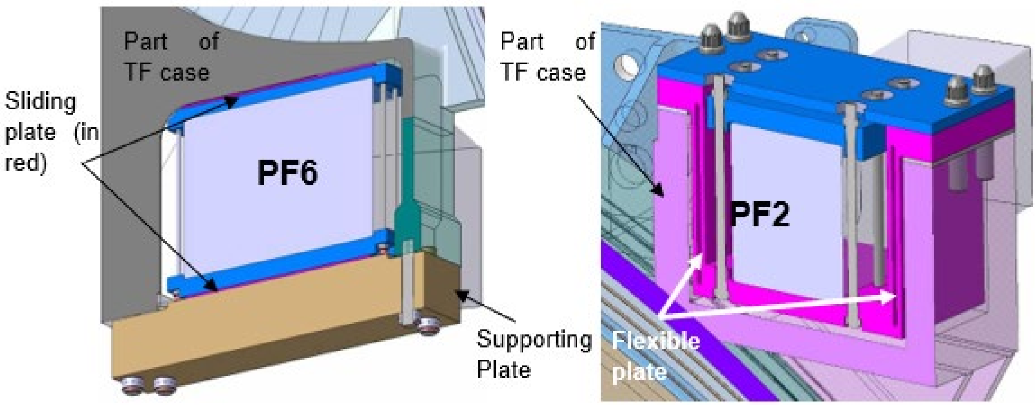

(c) PF1 and PF6 coil support using top and bottom sliding plates in the coil housing.

(d) PF2 – PF5 coil support using vertical flexible plate in the coil housing.

Fig. 6.1-8: PF Coil System, Coils and Supports.

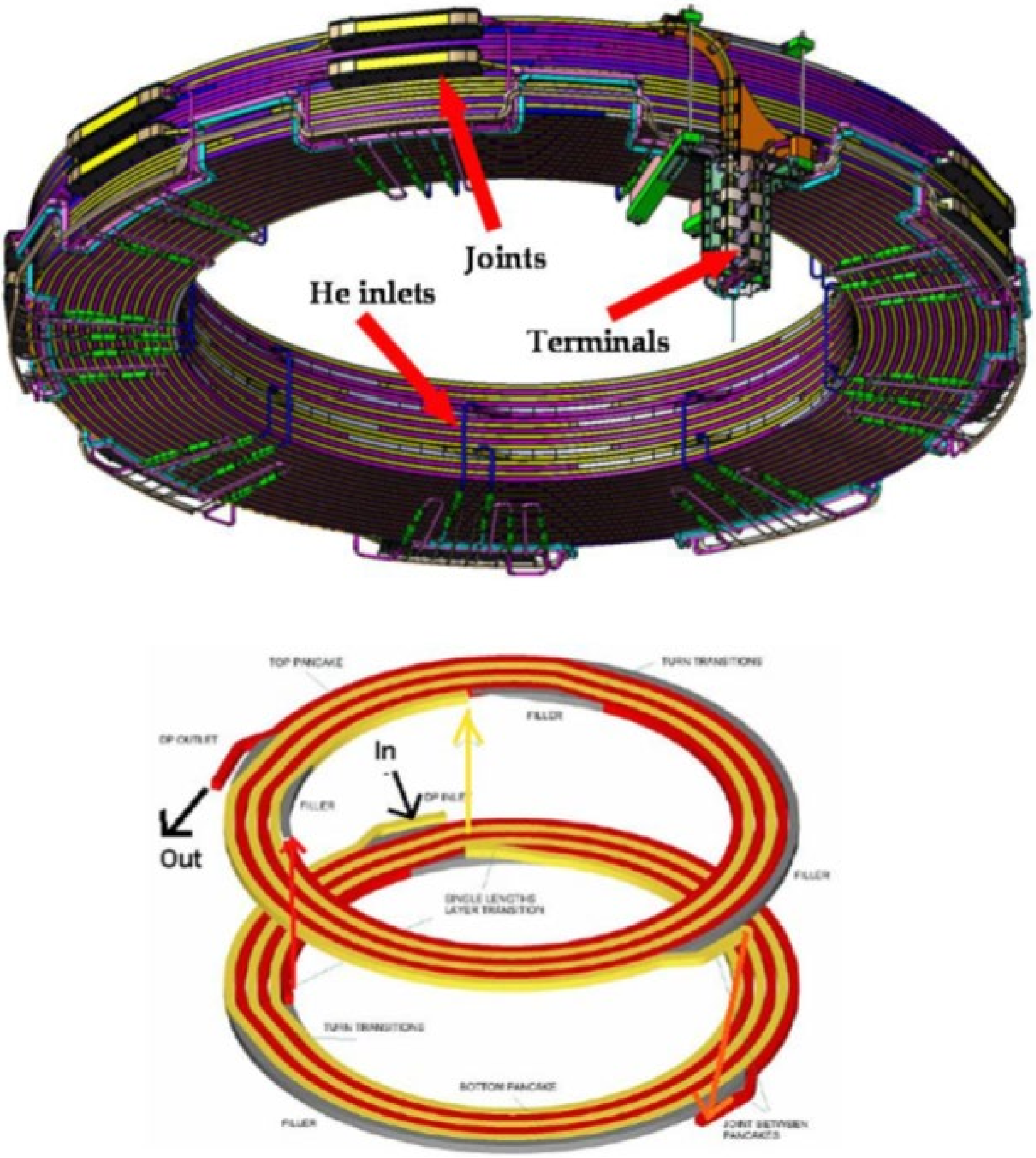

Fig. 6.1-9: PF6 Winding Pack Layout (typical for all PFs) and two in hand double pancake scheme.

6.1.2.4 CS Coils

6.1.2.4.1 CS Modules

The modules are pancake wound, each with 40 pancakes or layers and 14 turns per layer. The module is not fabricated as a continuous winding but is made from seven separate windings requiring six joints, Figure 6.1-10. The 40 layers are constructed from six hexapancakes (HPs) and one quadpancake (QP). The modules are fully identical (and therefore interchangeable) as regards the winding layout. As compared with the more conventional double pancake winding arrangement, the HP and QP winding arrangements minimize the number of joints at the outer diameter and therefore reduce the complication associated with the joint configuration. The total number of turns is 554 (instead of 560) because of the radial transitions and the finite lead separation. The total conductor length in the finished coil is 5894 m.

The conductor is wound at a constant radius with a turn-to-turn transition region over a toroidal angle of 31° within each pancake. The pancake-to-pancake transitions at the inner and outer bores are similarly confined to a 28° and 16° region, respectively. The location of the transition region is rotated for each pancake so that the modules have uniformly toroidal mechanical properties.

The HPs and QP are linked using a six-petal splice joint. The splice joint is made in the outer turns where the stresses are lower. The terminals break out radially at the outside diameter of the module at the top and bottom turns where leads extend vertically to the feeder system. The structural element (winding lock and tail) that carries the conductor hoop load around the conductor terminal joggle is also installed with the module terminals (see section 3.3.3).

6.1.2.4.2 CS Structures

The CS pre-compression structure is split into a set of nine identical independent subunits, each one consisting of an inner tie plate, two outer tie plates, load distribution and isolation plates, a lower key block, an upper key block and connecting bolts, Figures 6.1-10, 6.1-11 and 6.1-12. The tie plate region has sufficient open space in the toroidal direction for the joints, current leads, and helium pipe arrangement which run vertically up and down the modules on inside and outside.

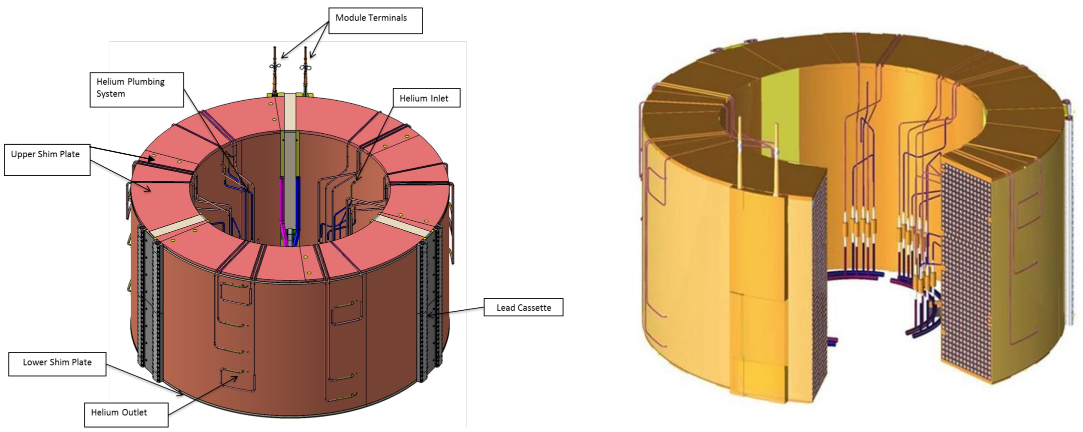

Fig. 6.1-10: Two views of a CS module.

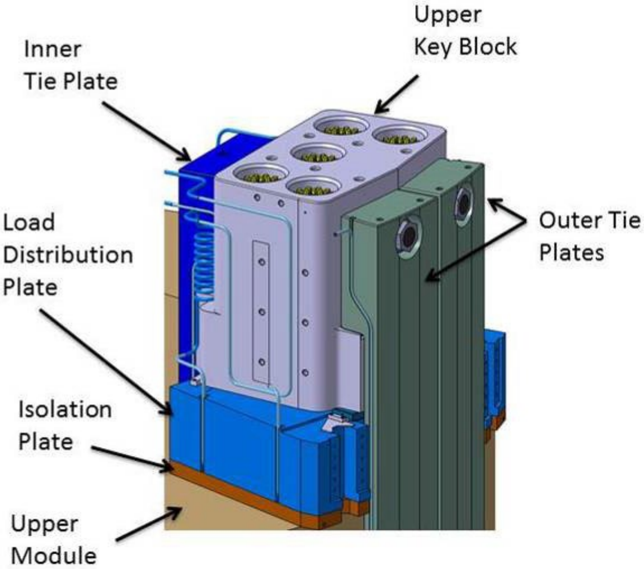

Fig. 6.1-11: CS Upper Pre-compression Structure 1/9 Unit.

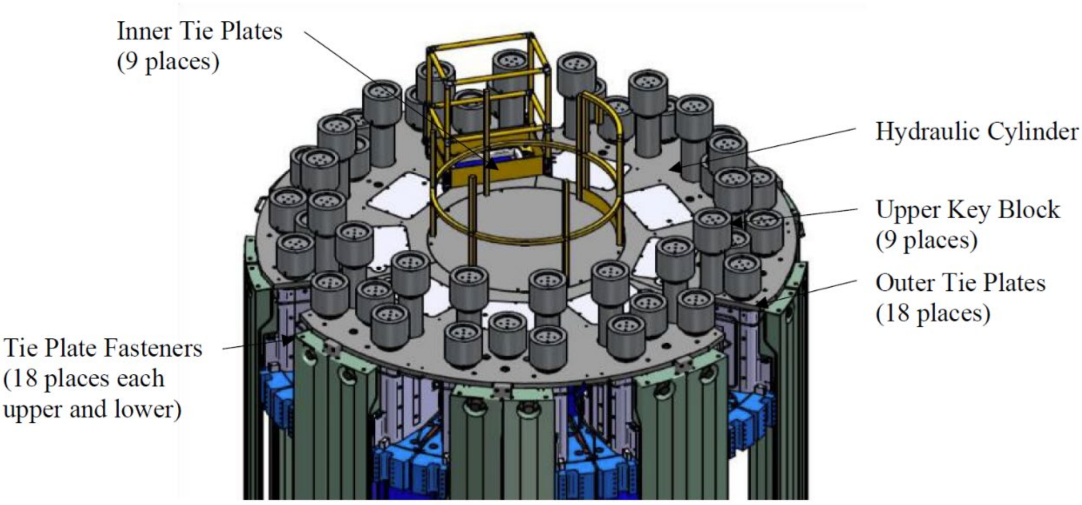

Fig. 6.1-12: Upper end of CS stack with precompression hydraulic cylinder in position.

The CS stack is pre-loaded using sets of hydraulic cylinders which replaced an earlier system using multi jack bolt tensioners (which could not achieve the required load levels). Once the load is achieved, shims are inserted at the ledges where the tie plates link to the key blocks, to maintain it.

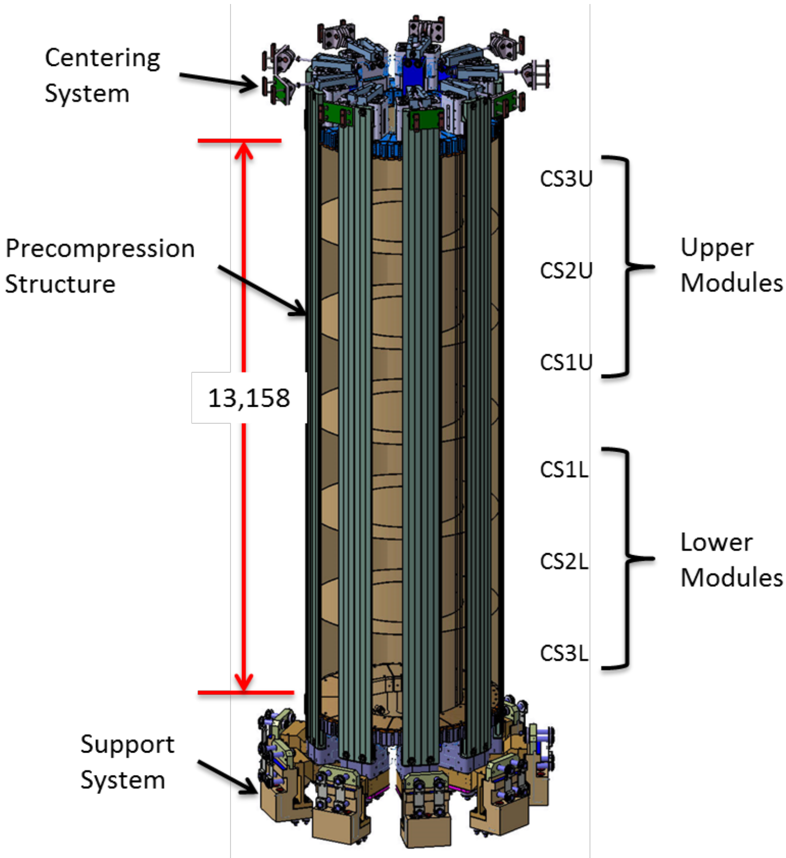

Fig. 6.1-13: CS System Structures and Supports.

6.1.2.4.3 CS Stack

The central solenoid (CS) consists of six electrically independent modules, arranged in a vertical stack as shown in Figure 6.1-13. The stack is free standing and supports all the magnetic loads through structural material (the conductor jacket) within the winding. The main loads are the magnetic hoop force, which creates hoop tension in the structural material (i.e., the conductor jacket and the winding lock), and the vertical inward pressure from the outer modules which is highest at IM and creates vertical compression. The resultant vertical force component is reacted through the lower support structure.

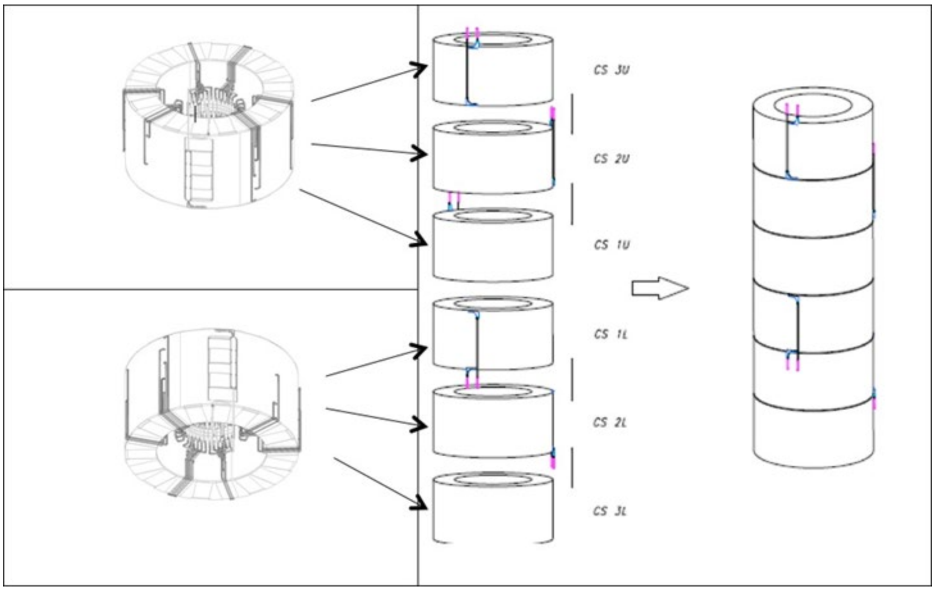

Fig. 6.1-14: Arrangement of modules and busbars in CS stack.

Each upper module is placed in the stack so that it is rotated by 120° about the vertical axis relative to the module below it. The lower three modules are similarly rotated but are placed upside down relative to the upper three. The terminal leads, running outside the modules (up for the top three modules and down for the lower three) are therefore distributed uniformly around the outer perimeter (between the vertical tie plates). The helium supplies to the modules run in the inner bore of the stack, as there is insufficient space to keep them outside). The outlets from each cooling path are located at the outer diameter. They are collected together and run across to the inner bore through six sets of grooves cut in the interface plates. These outlets connect to the insulating breaks and manifolds located in the inner bore. Because of the vertical pressure on the module, the busbars with long vertical lengths on the outside of the module require sliding to allow flexing to prevent stress concentrations at the grooves or at helium outlets from the conductor but also require strong support against the toroidal magnetic forces (the module currents vary substantially through a plasma pulse). The busbars are potted with a debonding agent into cassettes embedded in the ground insulation outside each module, Figure 6.1-10. The modules are keyed together with radial keys inserted into holes drilled during the stacking process into the interface plates between them (as well as, of course, by the busbar cassettes on the outside).

6.1.2.5 Correction Coils

6.1.2.5.1 Correction Coil Windings and Cases

The correction coil (CC) system consists of three sets of six superconducting coils (top, side and bottom) distributed poloidally, each opposite coil pair being connected in anti-series, to produce a n=1, 2, 3 asymmetric correction component. The total CC current capacity based on the field correction requirements are 320kA for the top and bottom coils and 200kA for the side coils.

The cable-in-conduit conductor (CICC) of the correction coils contains 300 NbTi SC strands with a cable strand pattern wrapped with a 40% overlap stainless steel 0.08mm thick tape and swaged in a 19.2mm x 19.2mm square 316L stainless steel jacket (2.2mm thick). The configuration of the multi-stage cable layout is 3x4x5x5. The cable and jacket are assembled using a pull-through, forming circle shape tube to square section by compaction of conduit technique onto new cabling/jacketing facilities producing up to 600m lengths.

The 20-turn SCC Quad-pancake and the 32-turn BCC/TCC configuration require 594m and 555m of conductor respectively. The non-planar SCC winding has overall dimensions of 7.2m x 8.4m with a 11.287m out of plane radius of curvature. A continuous one-in-hand winding scheme without internal joints is used to reduce losses.

Each conductor is wrapped with a 1.2mm thickness of E glass-Kapton tapes. The ground insulation consists of 4mm glass fiber-polyimide interleaved layers impregnated into resin epoxy under vacuum/ pressure cycles. The impregnation is carried out using the coil case as a mold.

Each CC casing consists of two half parts, a U section and a closure lid, each produced by narrow gap TIG welding of oversized stainless steel AISI 316LN 30mm thick plates with subsequent machining to the nominal 20mm thickness. Each case has a low voltage insulating break in its perimeter, made with G10 and with forces supported by a bolted flange.

6.1.2.5.2 Correction Coil Supports

The support structure of TCCs, and BCCs, consist in 8 clamps per coil attached to Toroidal Field Coil cases (TFCs) with a total of three design types as shown on Figure 6.1-15 & 6.1-16. Three outer supports are provided along the outboard toroidal branch; three supports are provided along the inboard branch and there is one support on each radial branch of the B/TCC.

The SCCs supports are of two types. On the horizontal legs, there are 9 individual mechanical clamps connecting the SCC case and the supporting horizontal structural beams making bridges between TFCs as shown in Figure 6.1-16 & 17 to react the expected loads onto CCs. Those bridge structures are directly bolted onto TFC interface extensions and require adequate stiffness to accommodate the expected TF side plane maximum rotation of 0.3mrad during operation, the azimuthal displacement of 20mm and the maximum radial TF expansion of 0.8mm. On the vertical legs, there are 10 clamps connecting the SCC case to the structural case of the TF coils.

Because each SCC bridge beam is attached to three adjacent TF coils, the attachment of the SCCs must provide adjustment capability to accommodate all expected misalignments of the TF coils (radial, toroidal and vertical) due to manufacturing and assembly tolerances. The system of clamp supports accommodates the expected displacements of the TFCs during normal operation and exceptional load cases resulting from in plane and out of plane loads. Each individual support has some degree of mechanical shimming adjustment up to +/-2.5mm to compensate TFC assembly misalignment and the CCs manufacture tolerances.

Originally the CC cases included cooling channels to remove eddy current heating and conducted heat from the TF coil cases. This design was modified (due to the problem of making and integrating into the supports the cooling channels) through deviation requests so that each CC case includes an insulated break, and the CC supports include copper cooled plates acting as a thermal intercept.

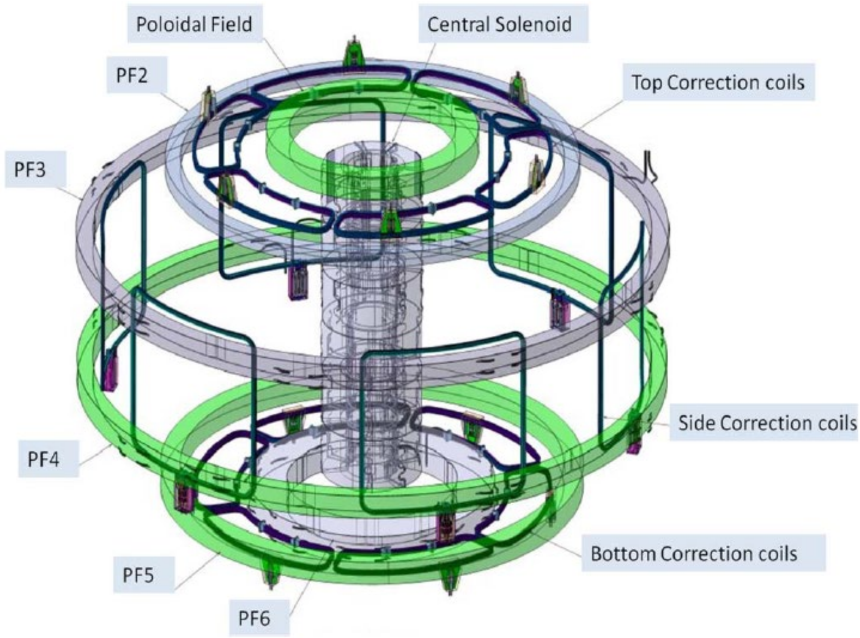

Fig. 6.1-15: Correction Coil System.

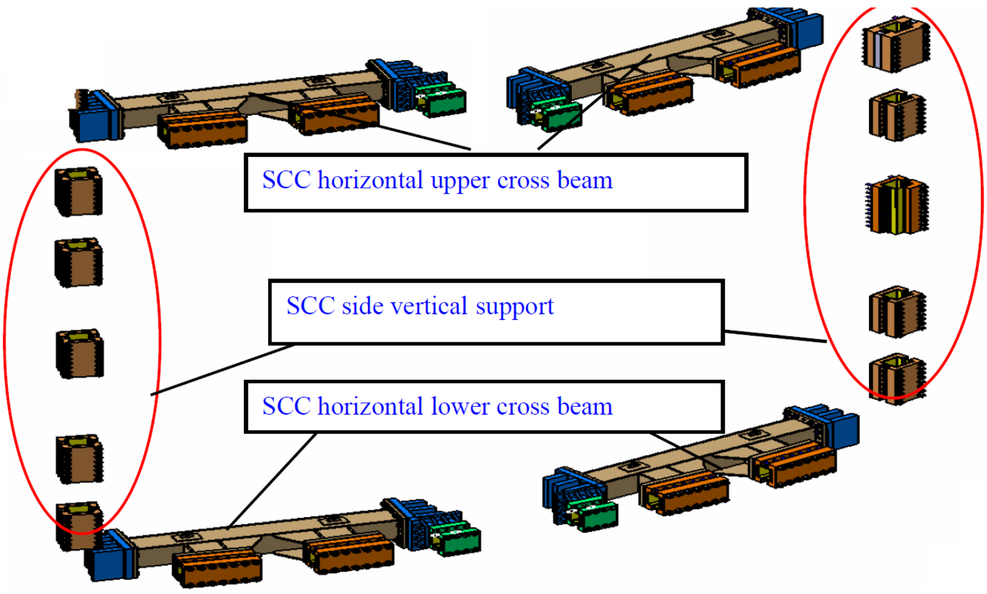

Fig. 6.1-16: Supports (to TF coil) for a Side Correction Coil.

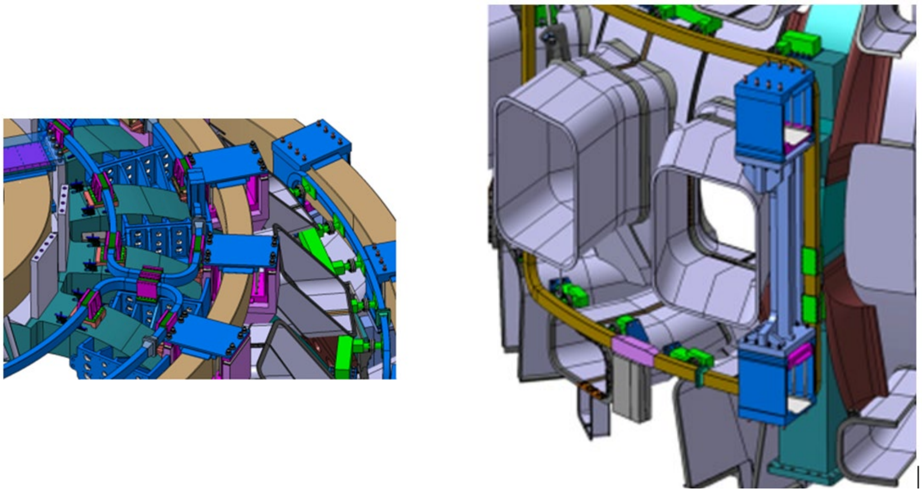

Fig. 6.1-17: Top and Side Correction Coils in place on the TF coils (TCC is between PF1 and PF2).

6.1.2.6 *Feeders and Instrumentation*

6.1.2.6.1 Feeders

The cryostat is surrounded by 21 feeders positioned in the lower Tokamak gallery (B2 level), Figure 6.1-18; they include 9 TF feeders supporting 18 TF coils (with each pair of adjacent coils connected in series), 3 PF feeders supplying the PF4 to PF6 coils, 3 CS feeders connected with the CS1L to CS3L lower modules, 3 CC feeders (each with 2 pairs of current leads in each unit) for 6 pairs of correction coils, 1 structure (STR) cooling feeder supplying cryogen to the magnet structure of all coils, and 2 instrumentation (INSTR) feeders that monitor the operation condition of the magnet structure. The upper level (L3 level) magnet system is connected by 10 feeders: 3 PF feeders for PF1 to PF3, 3 CS feeders for the CS1U to CS3U modules, 2 CC feeders for the 3 pairs of upper correction coils, and 2 STR feeders for conveying the returned flow from the structure cooling system.

At the other (warm) end, the feeders connect the cryogenic magnet system to the power supplies, the cryo-distribution lines, and the control/monitoring instrumentation.

As magnets cool down, the length of cryogenic busbars and coolant pipes must compensate for the differential contraction as compared with the RT (room-temperature) vacuum jacket length. The overall differential thermal contraction between the current lead and the centre of the Tokamak is on the order of 80mm. Inside the cryostat, the maximum vertical cooldown displacement of the coil is about 35mm. The maximum operational displacement is estimated at 25mm in the radial direction and can be up to 15mm in the out of plane (toroidal) direction due to the torsion of the TF magnets. The bulk (about two thirds) of the radial displacement can be taken by the 'S bends' included in the CTBs (for busbars and Helium supply lines) but the rest has to be absorbed by flexing within the cryostat. With the busbar connected rigidly to the coil terminal, the busbar support must provide sufficient flexibility to allow regulated deflection of the busbar Inside the cryostat, while still providing mechanical support (a busbar that carries currents up to 68kA is loaded by the background magnetic field of up to 4T). The paired busbars must be properly arranged to reduce the rotational moment in the feeder supports, and the busbar clamps must also be designed to support repulsive forces and shear loads, while providing flexibility for the coil flexing. The bellows at the cryostat feed through of the busbars and the cryogenic supply lines have also to absorb relative displacements of the order of 10mm.

Viewed from the outermost room-temperature component, a coil feeder consists of the following components, Figure 6.1-19: a Dry Box (DB), a combined Coil Terminal Box (CTB)/S-bend Box (SBB), a Cryostat Feedthrough (CFT) with a Vacuum Barrier (VB) and an In-Cryostat Feeder (ICF) including the terminal transition box structural support to the terminal joint connections.

Beyond this global arrangement, the feeder design in 2001 was far from complete and supporting analysis missing. Some improvements were made between 2001 and 2007 (the introduction of HTS Current Leads in particular) but all of the detailed design (and some of the conceptual) was done between 2007 and 2013: changes resulting from ongoing detailed analysis (missed earlier) and assembly problems are still on-going. It was not feasible to trace most of this design development through change requests due to a lack of resources, and the situation was further complicated by the complete redesign of the cryostat base in 2011 in response to safety measures introduced after the Fukushima earthquake.

The following sections describe the feeders largely as-built, in 2024.

Dry Box (DB) Figure 6.1-20

The DB is located at the outboard end of a coil feeder. It provides the interface between the feeder current leads (CLs) and the power supply RT busbars (water cooled) in a dry air environment. It is designed with a gravity support and is bolted on the back panel of the CTB for ease of maintenance. Nominally a simple component, it had to be modified to be airtight with forced circulation of dry air to avoid water condensation, at a late stage of the design. Heaters (with high voltage insulation) also had to be included in the ends of the CLs to avoid the risk of the cooling water freezing and gave rise to some qualification issues.

Combined Coil Terminal Box/S-Bend Box (CTB/SBB) Figure 6.1-20 *& PRVR Fig. 6.1 19.*

The CTB contains the piping and valves for the supply and return of supercritical helium for the coil and feeder; the supply of 50K helium for CLs; the supply and return of thermal shield helium (80K, 1.8 MPa); the rapid discharge of Supercritical He from the coil and busbars via pressure-limiting valves into the vacuum jacketed quench line; the discharge of Gaseous He from the feeder's thermal shield and CLs via pressure-relief valves into the low-pressure recovery line.

The other main components in the CTB are a pair of Current Leads (CLs with normally one pair per CTB but 2 pairs in the CC CTB), SC busbars, a 10mm thick separator plate and gravity supports between the CLs and busbars at opposite polarities, HV cables, actively cooled aluminium thermal shield (TS) panels/pipes wrapped with MLI (Multi Layer Insulation).

Next to the CTB there is a Pressure Relief Valve Rack (PRVR) which provides a mounting locating for some of the valves (due to insufficient space on the CTB itself)

The busbar and supply pipes are continued into the SBB volume with two wavelengths of S-shaped bends. During magnet cooldown and operation, the S-bends are stretched to compensate for the length required to relieve the cooldown stresses in the busbars in higher background magnetic fields. The S-bends do not provide all the flexibility required between CTBs and coils and relative movement is required between in-cryostat feeder components. In the 2001 feeder design, the CTB and S-bends were separate units (due to gallery assembly issues), but they were merged in 2008 (due to internal design and assembly issues) to a much longer single unit.

HV Cables and Satellites Figure 6.1-22

The HV cables are routed through the CFT and SBB to reach the HV satellites at RT. The satellites did not exist up to 2008 (and nor did any HV feedthroughs) and were the only solution to provide the surface area needed to install the feedthroughs. The HV cables in the cryostat are contained in ducts which originally (up to 2017) terminated at the VB (see below) and the cables exited the cryostat vacuum through plates containing plugs glued to the cable surface. These plugs (and the cables themselves) could not be made vacuum tight and in 2017 the cable ducts were extended from the VB through the CTB and into the satellites where the plugs could be installed at room temperature. The cryostat vacuum thus extends in the instrumentation ducts into the CTB.

Vacuum Barrier (VB) Figure 6.1-21

The VB, placed within the CFT, separates the cryostat main vacuum from the CTB vacuum, which allows the maintenance/repair of CTB components without breaking the cryostat vacuum and is also less restrictive for the use of materials within the CTB. Stainless steel bellows are used as an interface between the VB disc and busbars/coolant/instrumentation pipes with a radial insulating break around the busbars. The HV cable ducts penetrating the VB are directly welded to the bellows and the HV cables continue into the CTB in a local cryostat vacuum containment.

Cryostat Feedthrough (CFT) Figure 6.1-21

The CFT is located in the Tokamak gallery between the SBB and the cryostat. For all feeders, except PF4, the CFT is a common component that consists of a straight vacuum jacket, an actively cooled thermal shield, a bolted containment duct, a separator plate with thermal intercepts, busbars, coil and busbar cooling pipes, HV cable ducts, and cold mass supports. A similar strategy is used in the CC, STR, and INSTR feeders.

The CFT vacuum duct penetrates the cryostat with a 2-ply, 10-convolution bellows, which is used to isolate any seismic displacement of the CFT from the cryostat. The CFT's TS interfaces with the cryostat's TS with labyrinths that block the line-of-sight radiation heating to the cold mass. The cryostat end of the busbar is a half twin-box joint for connection to the busbar in the ICF.

The unique PF4 CFT vacuum duct penetrates the bioshield with a horizontal straight length, followed by a horizontal bend and a vertical upward bend to reach the feedthrough at the lower flange of the cryostat. Due to the concrete support of the crown ring (implemented in 2011), this feeder was embedded in concrete during the final completion of the building in 2019, before installation of the cryostat base.

In-Cryostat Feeder (ICF)

The In-Cryostat Feeder (ICF) is a subassembly that connects a coil or structure to the end of a CFT located near the inner wall of the cryostat TS. Like the CFT, it also includes a robust stainless steel containment duct which is, however, not a vacuum containment.

There are multiple forms of ICFs. The TF ICFs form a ring under the TF coil terminal regions, and the PF and CS ICFs have convoluted shapes (partly resulting from re-organisation in the 2011 cryostat redesign) to provide sufficient compliance to match the coil movement. The CC and structural feeder form half or one-third rings around the cryostat (Figure 6.1-18). To allow flexibility at the cryostat wall location (and the join to the CFT) the joint at the cryostat wall is housed in a short tube with two-axial gimbals at both ends.

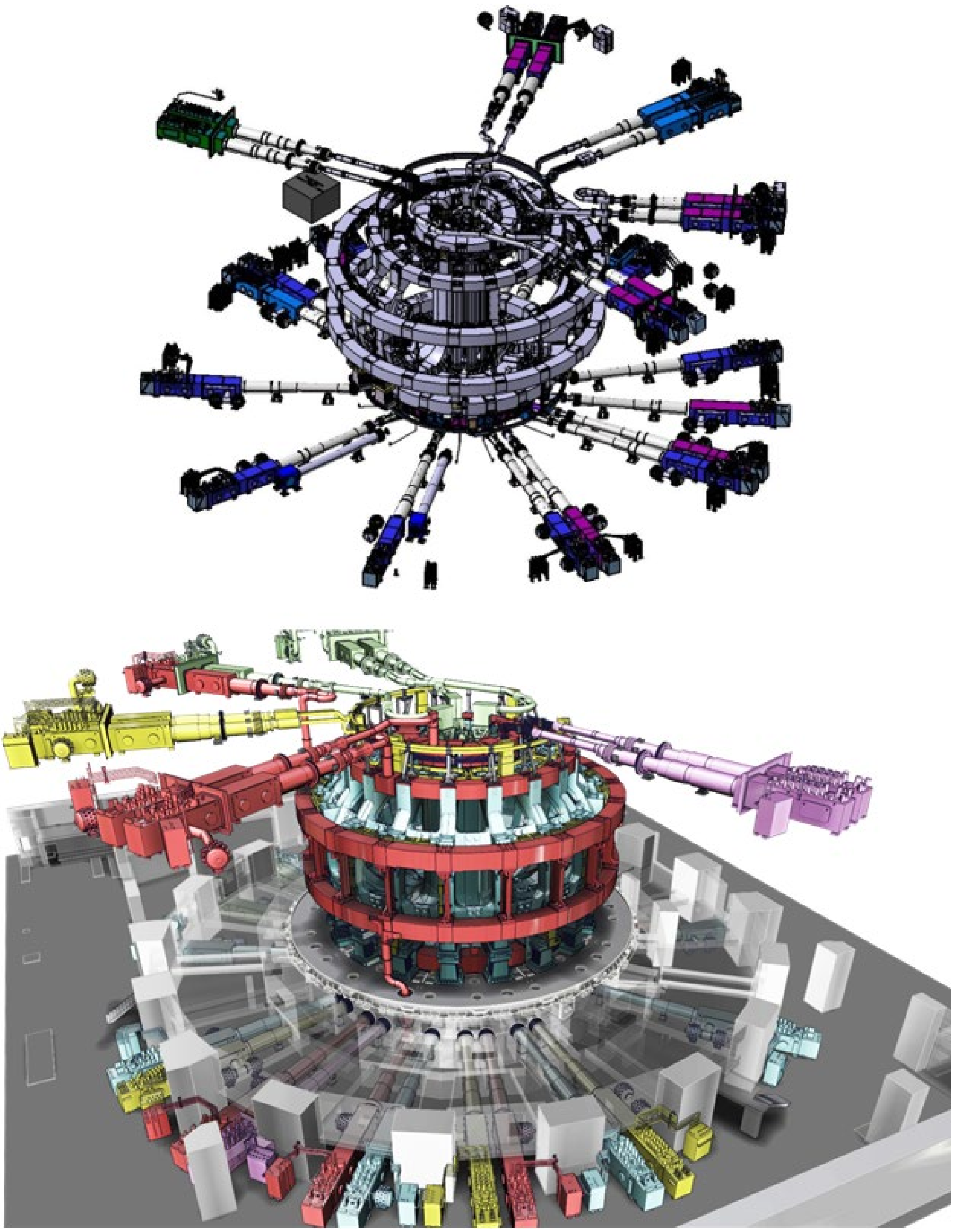

Fig. 6.1-18: Two Views of the Overall Feeder Layout (with and without parts of the building, but without cryostat).

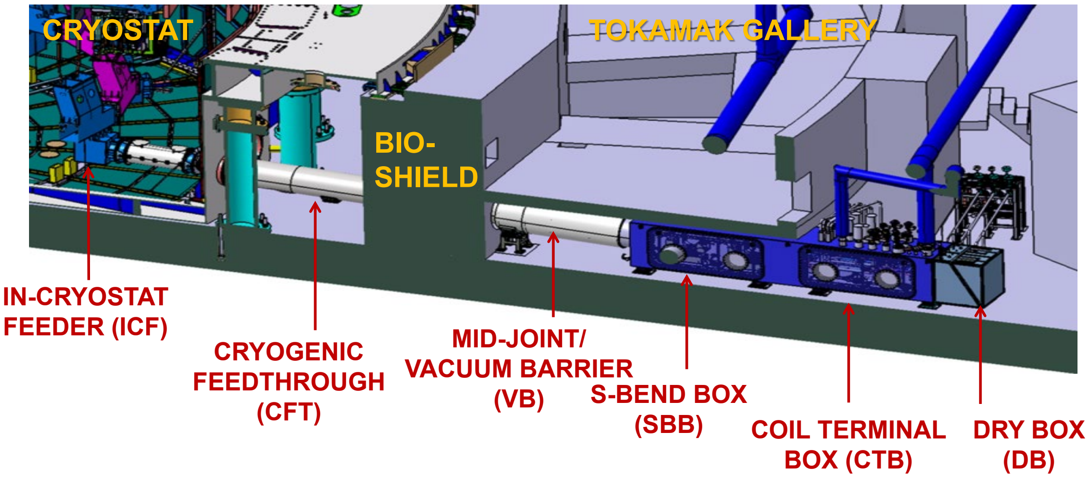

Fig. 6.1-19: Elements of a Typical (TF) Feeder. The PRVR is just above the Dry Box.

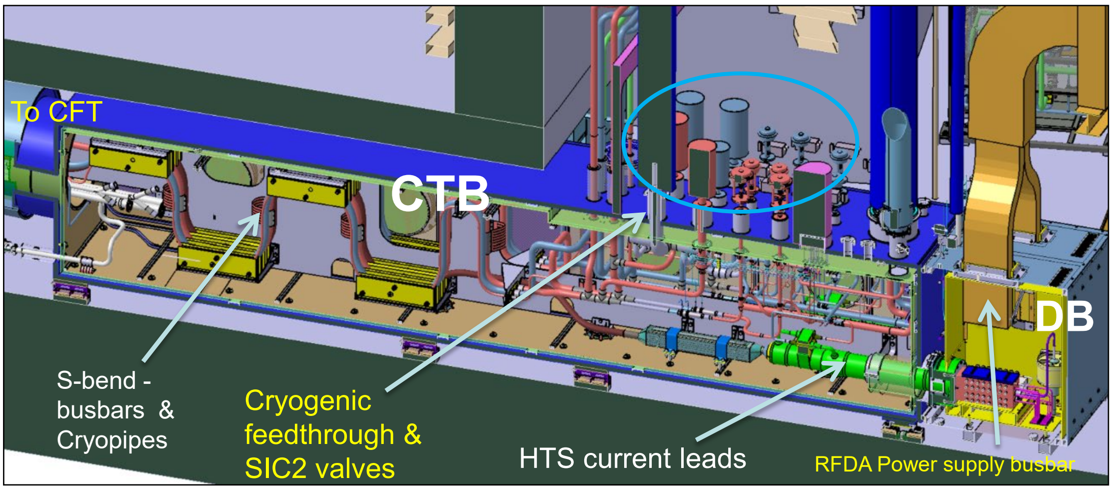

Fig. 6.1-20: Inside a CTB (~26 tons, ~10 m in length).

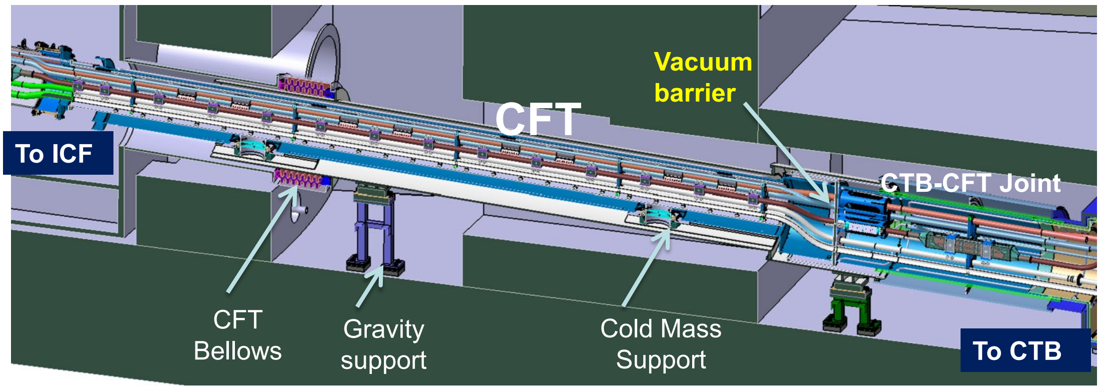

Fig. 6.1-21: Inside a CFT (each CFT weighs 5-10 tons, 7-10 m in length).

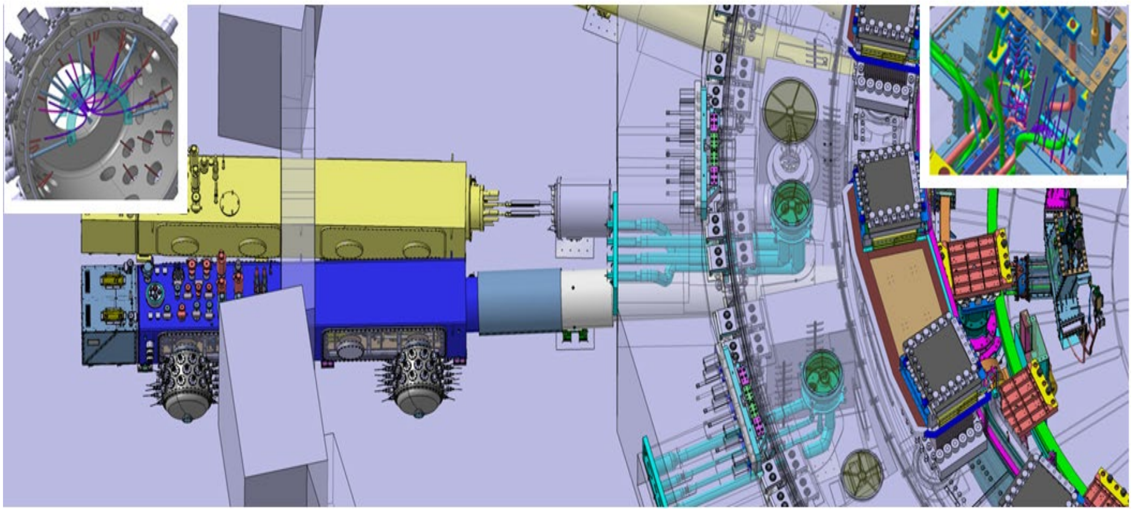

Fig. 6.1-22: Instrumentation satellites on the side of the CTBs, containing the HV cable feedthroughs to atmosphere.

The baseline design (up to 2001) of current leads for ITER utilized supercritical helium flowing along a long copper heat exchanger up to room temperature. This generates a high cryogenic load. A more efficient design (previously used on current leads up to 15kA) uses HTS material to bring the current up to 50-70K, followed by a copper heat exchanger and, after its selection into the baseline in 2004, was developed by ITER in the period 2009-12.

The most suitable HTS material available at the time, BSCCO 2223 tape, is used in the ITER current leads. The detail of the HTS material and the current lead design was not finalized until 2010 with successful prototype testing in 2012. Although a limited supply base existed for BSCCO, the choice was driven by a preference for a known HTS material, even if this were not at the forefront of HTS development. Nevertheless, an extensive development program was needed to scale up the technology from 15kA to the 70kA required for ITER, and the design underwent 3 major changes during this, in order to achieve workable manufacturing requirements. Assistance from CERN to the supplier (ASIPP) was critical, as the final HTS leads are scaled up from an original CERN design.

The change from conventional copper leads to HTS was formalised through two PCRs, PCR-044 for the current leads (Figure 6.1-23) and PCR-045 for the cryoplant. The gain in electric power of 2.45MW is equivalent to 10kW of cooling power at 4.5K. The required cryoplant capacity during plasma operation then dropped by about 15% (10 kW of cooling power at 4.5K out of a total of about 70kW).

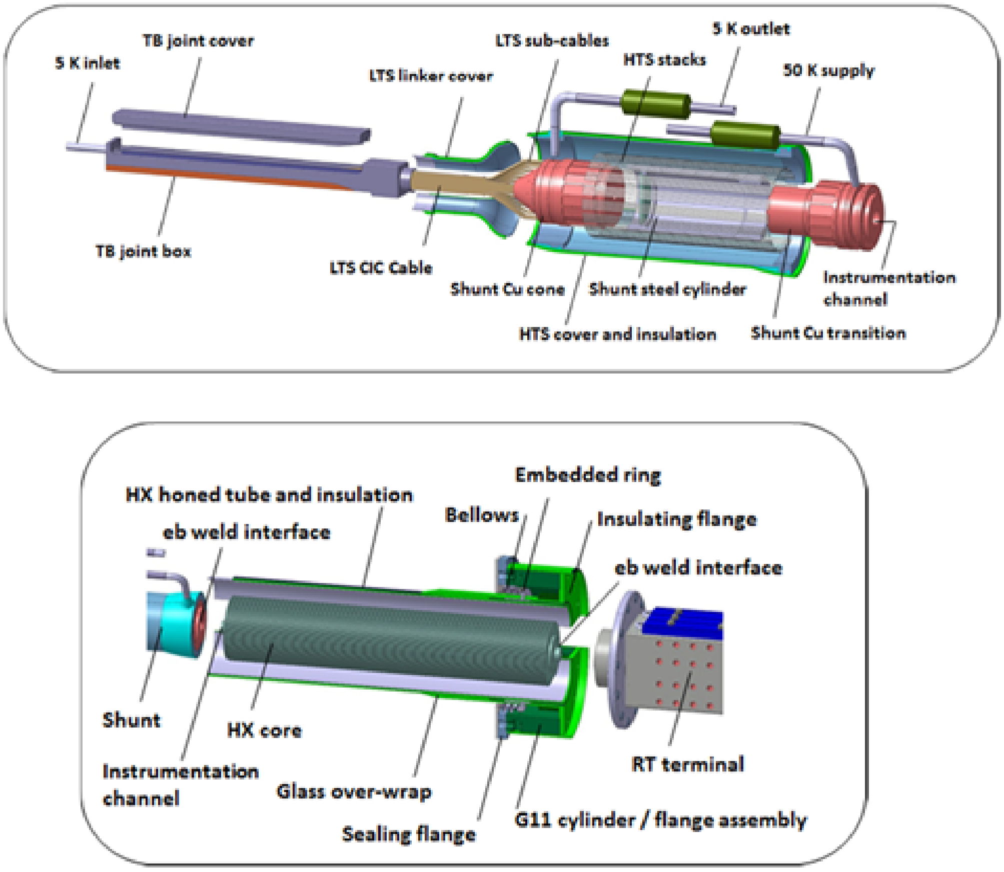

Fig. 6.1-23: HTS Current Lead (shown in two sections).
Top is the left low temperature end, bottom is the right high temperature end.

6.1.2.6.2 Instrumentation

The magnet instrumentation has also undergone substantial but largely invisible changes since 2001 (and after 2007), as illustrated in Tables 6.1-1 and 6.1-2. The nature of the instrumentation is self-explanatory in the Tables.

Table 6.1-1: Quantities of Sensors, Low Voltage, 2001-2020

Sensor	Type	Number 2001	Number 2020
Temperature	Platinum (1 kΩ)	60	785
Temperature	Carbon-glass (≈1 kΩ)	96	1408
Temperature	A set of Platinum (20- 300 K) and Carbon-glass (4 - 20 K), or Ceramic Thermometer	323	
Pressure	Strain gauge type transducer	176	515
Mass Flow	Orifice Plate & Strain gauge type transducer	96	138
Mass Flow Differential Pressure	Orifice Plate & Capillary Strain gauge type transducer	231	277
Displacement	Strain gauge type transducer or Laser type transducer	160	

Table 6.1-2: Quantities of Instrumentation Wires & Fibres, 2001 to 2020

	Length (m) 2001	Length (m) 2020
High Voltage Wire (single conductor)	35,000	57,800
High voltage cables (5-30kV)	0	22,500
Low voltage wire (4 conductors & shield)	45,000	8,000
Fibre optic bundles	0	9000-10000

There are multiple reasons for the changes:

- In 2001, ITER was seen as less of a research device and in-cryostat instrumentation was minimised, especially as the expected reliability/lifetime is much less than that of the machine. By 2024, extensive instrumentation was seen as part of the engineering commissioning (especially in the absence of coil cold tests), even if the instrumentation is only functional for the first 1-2 years of operation.
- The original critical instrumentation (HV wires and cables) did not provide redundancy. This is now included, up to the room temperature feedthroughs in the satellites.
- Optical fibres now substantially replace the LV wires for displacement sensors, strain gauges and temperature sensors.
- The full scope of the assembly of the instrumentation in the cryostat was not properly included in the original assembly CWPs.

6.1.2.7 In-Vessel Coils

The In-Vessel Coil system (IVC), shown in Figure 6.1-24, consists of two types of coils (VS and ELM), their related Feeders, Feedthroughs (FTs) and Insulating Breaks (IBs).

The in-vessel radiation and temperature environment is severe and conventional electrical insulation materials and insulating processes cannot be used in the fabrication of the IVCs. Mineral insulated conductor technology is the only viable choice, but it does not commercially exist in the large cross section (59 mm OD) required for the ELM and VS coils so that an R&D program was necessary to develop conductor fabrication and joining techniques. Thus the use of a “Stainless Steel Jacketed Mineral Insulated Conductor” (SSMIC) is a key feature of the design of both the ELM and VS coils, Figure 6.1-25.

The conductor was originally (in 2011 when the IVC were first officially adopted) made in short lengths of a few 10s of meters so that both VS and ELM coil had to include joints. The unit length was in 2017 extended to >80m which avoids such intermediate joints. The conductor is produced using a seamless extruded length of Cu tube with a central hole, with high accuracy on the outer diameter. Rings of compacted MgO are then slide along the copper, arranged in a straight line, and then the outer steel tube is pulled over the MgO. The whole assembly is then compacted and spooled, forming a high density MgO layer.

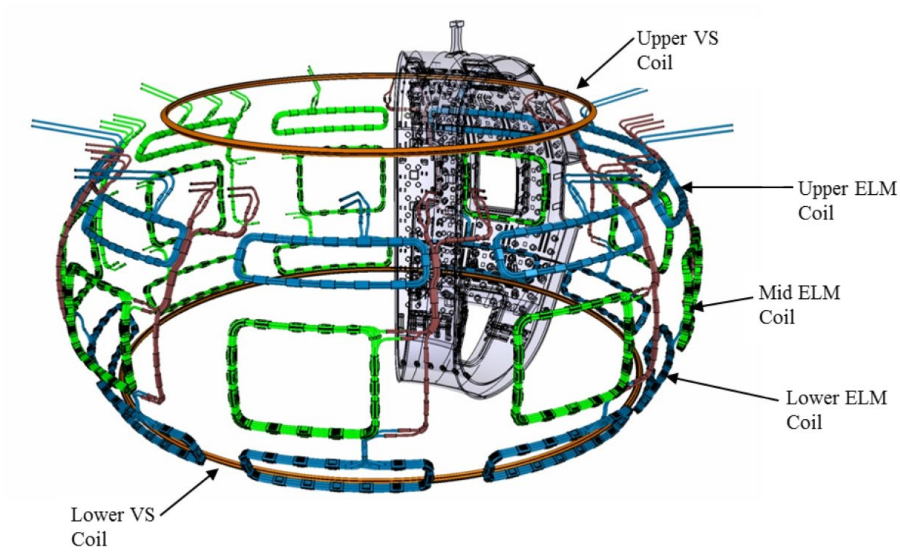

Fig. 6.1-24: ITER In-Vessel Coil System.

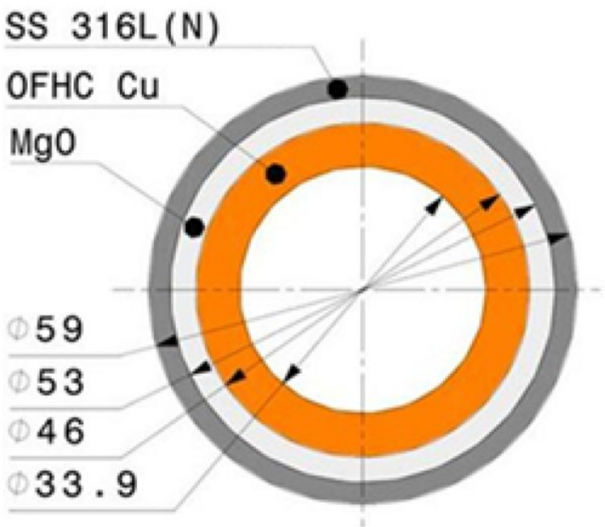

Fig. 6.1-25: IVC conductor cross-section dimensions (in mm). Thickness: SS Jacket (316LN) = 3.0 mm,

MgO = 3.5 mm, Cu = 6.05 mm.

The coils are wound from the conductor, the ELM in a 6-turn coil from a single unit length fabricated off-site, and the VS as individual turns which must be wound inside the vacuum vessel. The coils use a common bracket system to attach to the vessel and clamps to hold the conductors together which are not attached to the vessel, as shown in Figure 6.1-26 and Figure.6.1-27. One of the major design issues for the coils was the non-optimally distributed support brackets (rails) welded to the VV, which were fixed by 2015. At the time, repair/replacement of the rails was not permitted under nuclear quality regulations. The problem is compounded now by the inaccurate positioning of many of the rails on the VV inner surface. In some cases, it has been possible to compensate by extension of the IVC support brackets, but of course negative tolerances cannot be so compensated, and the clearance to the blanket also limits the flexibility. Some 10% of the ELM coil VV rails are likely to be repositioned (with over 50% having a significant position error (the rework is small compared to that needed for the VV bevel repairs). For the VS coils, the rail alignment is more critical since the coils bridge VV segments, and the alignment is affected by the VV closure welding alignments. Rail adjustment may be needed after completion of the VV welds.

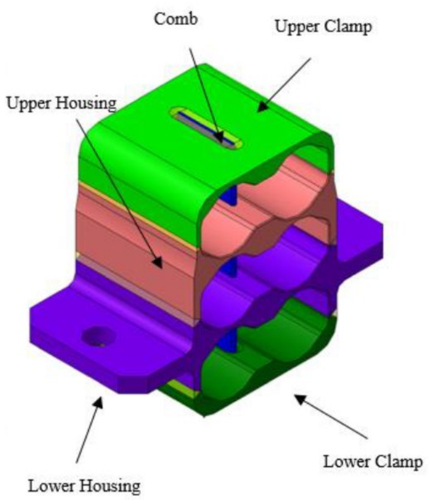

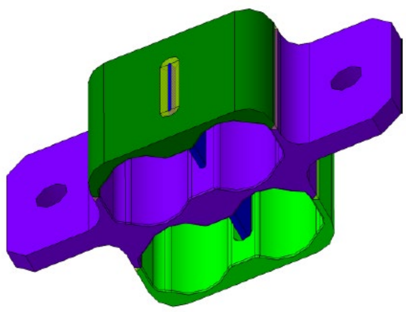

Fig. 6.1-26: Details of the ELM brackets Details of the VS brackets

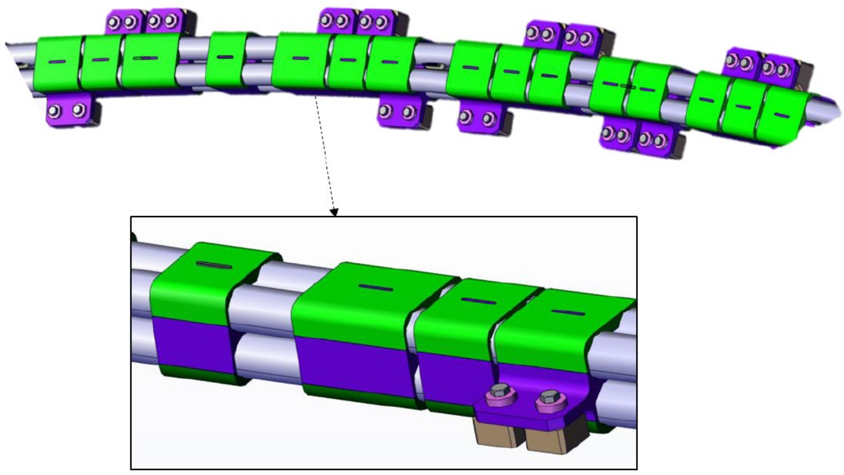

Fig. 6.1-27: Example of VS coil sector with bracket and clamp arrangement and the VV rails.

The final component of the VS and ELM coils are the feeders and the feeder feedthroughs, Figure 6.1-28. The feeder runs can be seen in Figure 6.1-29 & 30. The feedthroughs penetrate the main nuclear confinement barrier in the port walls and are there safety class. They are complex because of the combination of vacuum barriers, water containment within electrically active conductors and the need to seal the MgO insulation. The multiple vacuum areas must be monitored for leaks, Figure 6.1-28.

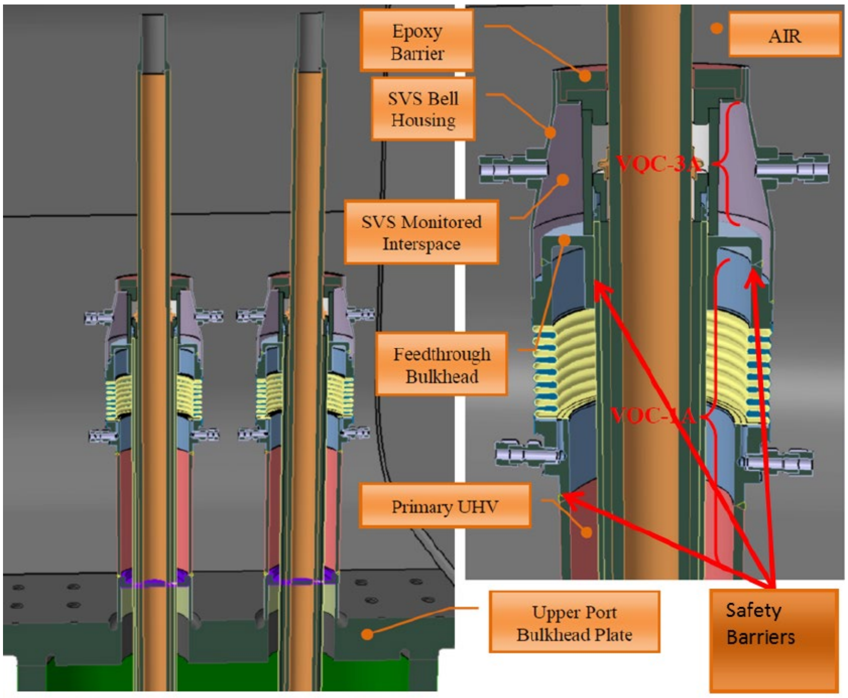

Fig. 6.1-28: The IVC feedthrough region in the ports. The primary vacuum boundaries are the welding of the Vacuum Tube to the Bulkhead plate, the welding of the FT Bulkhead to Bell housing and the brazing of the conductor jacket to the FT Bulkhead.

6.1.2.7.1 Vertical Stability Coils

The elongated plasma of ITER is inherently unstable and requires feedback control to maintain vertical position. Vertical stabilization is nominally provided by eddy current flow in first wall, banket and VV structures along with feedback control of the Poloidal Field (PF) coils. However, from 2001 on, analyses have indicated that the stabilisation capability, measured by the ability to recover from an initial displacement in plasma vertical position, is not robust because the low resistance of the VV screens the correction fields (see also section 3.6). A loss of vertical plasma position control in ITER will cause large loads on in vessel components from vertical displacement/ disruption events. A set of in-vessel coils to provide a robust stabilisation inside the VV was already in discussion in 2001 and was finally agreed for implementation in 2011, far after the design of the other in vessel components and requiring large modifications. Because of this, not all of the design is satisfactory (especially, VV supports, feeders in the port cells and the cooling system from the IBED loop providing significantly different temperatures in the IVC to the VV on which they are mounted, section 3.7) being obviously an 'add-on' with significant extra failure risks.

As shown in Figure 6.1-29, the VS coils consist of one upper and one lower 4-turn coil connected in an anti-series arrangement. The coils are mounted to the vacuum vessel and positioned behind the blanket shield modules. The conductors use Cu which is cooled by water provided by the diverter and blanket/first wall cooling system. The VS coils are rated for 2.4kV and 2.4kA rms per turn with a peak current of 60kA permitted during VDEs. All VS coils/turns are operated independently and therefore, can work with a turn or turns out of circuit and bypassed.

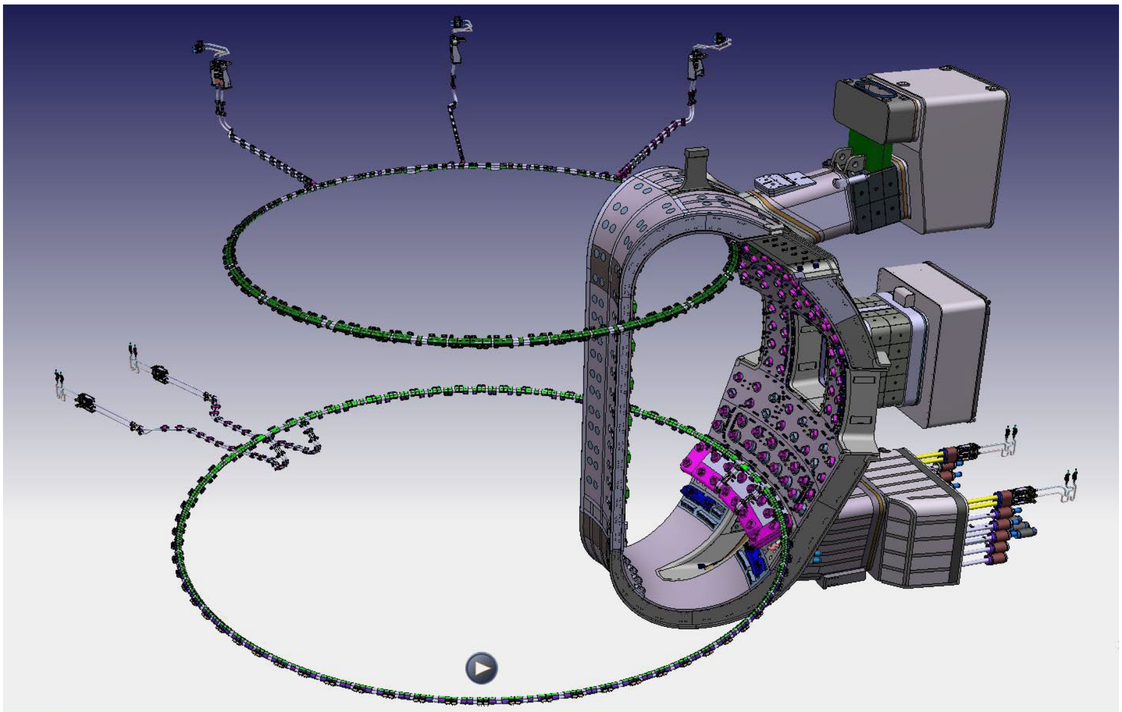

Fig. 6.1-29: VS coils, vacuum vessels and feeders.

6.1.2.7.2 ELM Coils

The ELM coils consist of nine toroidal sectors of three (upper, mid or equatorial, and lower) 6-turn rectangular “picture frame coils”, giving a total of 27 coils mounted to the vacuum vessel (VV) and positioned behind the blanket shield modules (BSM) as shown in Figure 6.1-30.

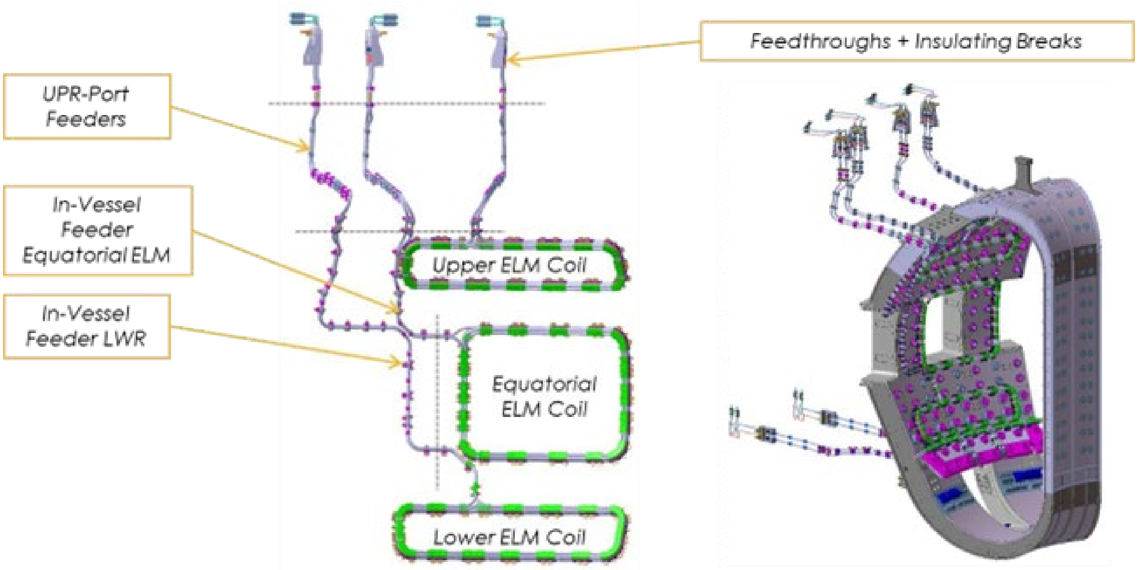

Fig. 6.1-30: ELM coils, feeders and VV.

6.1.3 Design Background and Remaining Issues

6.1.3.1 Basic design decisions

Although the ITER EDA FDR nominally took place in 2001, quite a number of design points were fixed or adjusted between 2001-2007. In particular the FDR did not produce detailed design drawings with important items like tolerances often missing, and manufacturing routes (normally defined and validated by the FDR stage) were in some cases not available. This led to changes imposed by manufacturing or performance problems, as late as 2018 in some cases in the magnets. In magnets, we tried to resolve these by staging of procurement arrangements as discussed in the section on industrial strategy, but this created an extra risk for the suppliers.

More significant changes were made in the period 2002-2007 and then 2011-12, as detailed below. Some of the basic decisions (for example bucking vs wedging) were addressed as black-white choices with highly simplified performance assessments which have proved to be more nuanced (and incomplete) in the subsequent 25 years of detailed design and manufacturing experience.

During the manufacturing phase (effectively from 2010 until 2020) many design changes had to be implemented in the individual components, mostly minor but also sometimes quite significant. These were rarely recorded as Project Change Requests, more often as Deviation Requests and via NCRs. A reasonably comprehensive list is being included in the 2024-25 updates of the PBS11 DDDs. There were also external changes imposed, for example in the repair possibilities for the magnets, that may have an impact in commissioning.

Also from 2015, the in-vessel coils were allocated to the magnets who were able to overcome the design and development issues and finalise a credible design: it is clear however that the complexity of in-vessel coils was significantly underestimated in the 2012 decision to implement them in ITER.

6.1.3.2 Bucking-wedging and Out-of-Plane Coil Support

There are two basic concepts available for supporting the centring forces of the TF coils. The first of these, known as "bucking", reacts the centring force on each coil directly on a structure which, for ITER, must be the CS itself in order to save space in the centre of the machine. The second, known as "wedging", reacts the centring force through a central vault formed by the inboard legs of the TF coils themselves, leaving a free-standing CS in the bore. Each concept comes with advantages and constraints.

Bucking was applied in a number of early copper tokamaks, in particular JET. It was proposed as a solution for ITER in the early 1990s but soon proved to be an unrealisable design in a superconducting environment, due to the difficulties of low friction sliding linked to those of thermal contraction, and the application of torsion from the TF coils to the central solenoid. It is noticeable since then that no superconducting machines (out of EAST, KSTAR, JT60SA, BEST and DTT) have been constructed using it. It re-appears now (2024) again in some compact nuclear tokamak designs, most notably SPARC but also some DEMO reactors. It is covered here since also in wedged machines, attempts to produce a compact solenoid design led to restrictions on independent modules within the CS stack and exotic solutions with layered designs and feeder connections in the high field central bore. It is possible that some of the lessons learned 25 years ago (as well as in production of the ITER CS coils) need to be re-examined for some of the new designs.

The bucked system means that the CS must be layer wound (to avoid joints in the high stress region where the TF coils make contact), but the CS hoop bursting forces are almost completely reacted by the TF centring forces, reducing the stresses in both the TF coils and the CS. The layer winding results in uniform current density over the whole height of the solenoid (restricting the plasma shaping capability). The "breathing" of the TF coils, as the CS cycles in the pulse, makes linking the TF coils to each other to support the magnetic out-of-plane forces from the poloidal field more difficult. The torsion of the CS by the TF coil out-of-plane tilting motion complicates its design.

In the first version of the ITER EDA machine (1994-95) a concept of TF coil winding pack design was developed consisting of layers of toroidal plates, with a circular insulated conductor embedded in them in a groove (layer wound). The toroidal plates in adjacent coils were keyed together (with insulated keys) to provide a continuous series of toroidal shells to resist the coil out of plane displacements. In a later version of this design, still bucked, the plates became radial plates (with now a pancake wound conductor) inside a case, with the out of plane forces now resisted by external structures and keys between the cases. In this configuration there is a limited value to the plates which contribute little to the reaction of the centring forces and are ineffective to resist the overturning moments. In the final iteration, to the ITER 2001 FDR design, a wedged system was adopted, maintaining the radial plates. In this, the radial plates have a role in protecting the conductor insulation from the wedging pressures.

The wedged system means that the CS must resist high cyclic tensile stresses due to the hoop bursting forces. The TF coils are subject to a large compressive hoop load at their inboard leg thus making the stress conditions in this region more critical. On the other hand, the wedged system allows a simpler TF coil structure (compared to bucking) that provides effective out-of-plane support of the TF coils.

A second demand on the self-supporting CS (as opposed to a bucked one which had to be layer wound) is that it contains modules that can be independently energised to provide adequate plasma shape control. This gives rise to large variations on the vertical forces which have to be reacted through the winding packs and a vertical support structure. The combination of vertical and hoop forces means that a conductor with an external square shape and an internal circular cable is favoured.

Increased shaping also results in more severe out-of-plane load distributions at the ends of the inboard leg of the TF coil. The wedged design can provide an effective support against these out-of-plane loads.

Wedging offers in addition the following conceptual advantages which however can be complex to realise, with sub-problems that detract from the apparent gains:

- i) the CS can be manufactured in repairable, or replaceable, sub-modules (issue: feeder supply lines and module vertical repulsive forces);
- ii) it simplifies component performance prediction in the TF coil inboard leg region by avoiding many of the sliding interfaces (and associated uncertainty of the friction behaviour) inherent in a bucked design. (issue: wedging also involves sliding interfaces);
- iii) it allows the use of keys in the TF coil inboard leg curved region, which provide effective out-of-plane support. (issue: key insertion and maintaining contact as TF coils are energised)

Although ITER has been a wedged machine since about 1999, details of the wedging were not finally fixed until 2018. Wedging the noses of the TF coils to form a circular vault sounds a simple-to-achieve design. However, the coils have to be accurately manufactured and aligned to achieve the toroidal arch, and the larger the coils, the more difficult this becomes. Tolerances are required, ~0.5-2.5mm per coil, which accumulate to 9-45mm over 18 coils. Gaps are required (or there is a risk that the coil noses do not fit) and these have to be filled and distributed…. a single 18mm gap is obviously not acceptable from a structural or error field viewpoint. Figure 6.1-31 shows the multiple interfaces which have to be aligned during the assembly of the 18 TF coils.

This was recognised in 2001 and the TF coils are assembled with an average 2mm gap between each of them, although in 2001 without any definition of how such a gap could be practically implemented (and even measured). It was not until 2017-18 that the TF inner leg tolerances were finally demonstrated, and 2022 before a full 1/9 sector (including 2 TF coils) was aligned and put into the cryostat, demonstrating that the TF assembly alignments could be achieved. In 2017-19 the shimming of the inner leg and the attachment of the insulated interface surfaces was established. Over the top and bottom regions of the TF inner leg, where the centring forces drop off, there is sliding between the coils which requires low friction, whereas in the central region, there is no slip and high friction is needed. The Pre-compression rings, which assist to maintain compression in the inner intercoil structures (the shear keys) had also to go through 3 basic design iterations before being manufactured after 2017, and the pre-loading system had to be completely redesigned in 2021 (a change from superbolts to a hydraulic system), see also section 9.2. The vertical pre-load system of the central solenoid was also redesigned in 2020 (changing again from the use of superbolts, which cannot function as intended, to a hydraulic system).

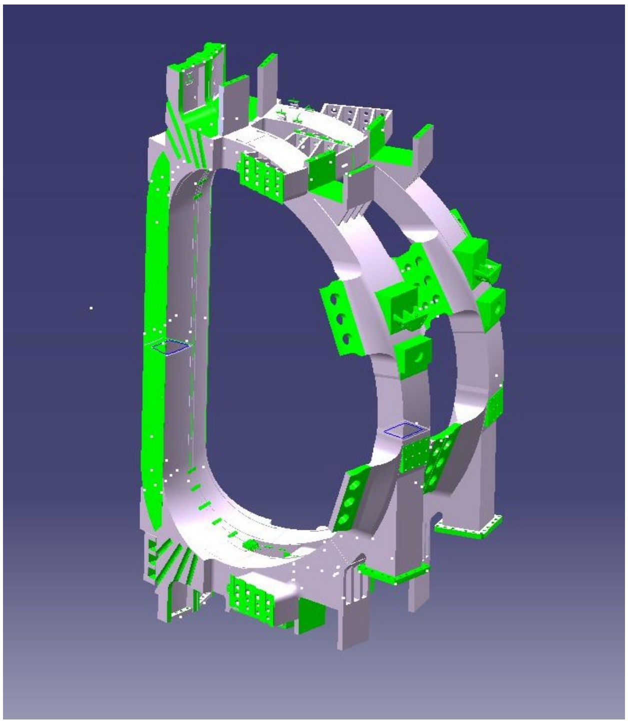

Fig. 6.1-31: TF interfaces (coloured green)

6.1.3.3 Conductors

An overview of the timeline for the events reported in section 3.3 is summarised in Figure 6.1-32.

ITER Conductor Programme Timeline

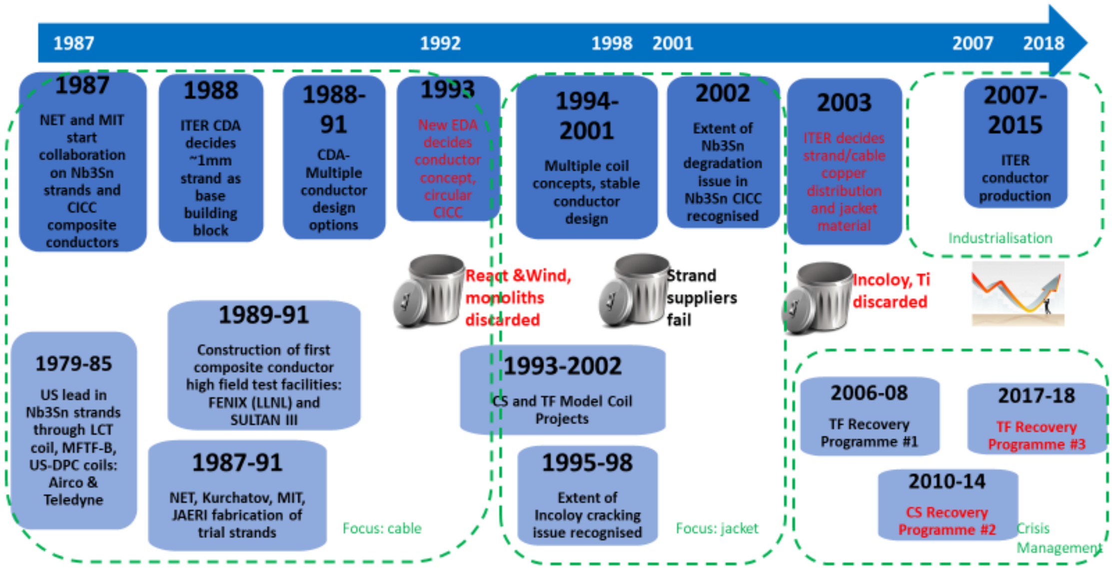

Fig. 6.1-32: ITER Nb_3Sn Conductor Development Timeline.

6.1.3.3.1 Strands and Cables

During the 1980s, a range of Nb_3Sn conductors were developed and a range appeared as options in the 1991 CDA magnet report. At this time, the main candidates were Nb_3Sn but divided between React, Wind and Insulate (R&W&I) and W&R&I. Eventually need for Kapton insulation-imposed W&R&I and at this point CICC became the obvious choice. It allows the full cross-section to be exploited for the superconducting material which in turn allows much higher conductor current which directly reduces the voltage. Other advantages are a relatively cheap manufacturing process and an ability to carry out quality controls on components like cable and jacket + welds before assembling the final conductor. Although CICC cables can be rectangular (several were developed in the early 1990s) ITER chose a circular configuration in 1993 and this has remained the baseline ever since, Figure 6.1-32 and 6-33. The overall conductor development iterations are summarised in the diagram above.

The use of the CICC concept allowed major cost savings to be achieved in 2003. The very large quantity of Nb_3Sn required for the ITER magnets and the associated cost implied that an economic strategy for the magnet design was essential – in other superconducting tokamaks, large temperature margins were used to address the lack of knowledge of Nb_3Sn CICC behaviour, an approach not affordable for ITER. The Cu to non-Cu ratio in the superconducting strands was therefore fixed at 1.0 and the copper needed for thermal protection provided via separate pure copper strands. This required that one of the core design criteria passed on from NbTi conductors, the 'well cooled – ill cooled' criterion was abandoned. The ITER Nb_3Sn cables have such a slow transition between the normal and superconducting states (i.e. a low n value where n is the exponent on the growth of the electric field along the strand as current sharing starts) that dynamic stability is adequately defined by the overall heat removal capability and the local temperature, rather than by heat transfer from the strands. This adjustment of the cable design allowed the number of superconducting strands in the lowest cable stage (a triplet) to be reduced from 3 to 2, with the third member of the triplet a pure copper strand. This replaced the usual approach involving 3 superconducting strands with a Cu to non-Cu ratio of 2. Since Nb_3Sn strand costs are substantially driven by the processing, rather than by the input materials, the cost of strands with a Cu to non-Cu ratio of 1 or 2 is not much different, so that the change reduced the quantity of superconducting strand by 33%, thereby saving approximately 250t of strand, about €200 million. This change also had a negative impact on the susceptibility to degradation due to filament fracture, since the strand loads increased by 50% (see 3.3.2).

A further design decision taken in 2003 was the elimination of exotic jacket materials. These were developed with the intention of better matching the thermal contraction of Nb_3Sn and therefore reducing the loss of critical current due to the lattice distortion. However, the alloys (most notoriously Incoloy 908) introduced major manufacturing issues and the advantages in critical current have been found to be less than anticipated.

It is worth to note after the iterations in the 1990s and 2000s, that the most obviously direct ancestor of the ITER CICC cables is in fact the Westinghouse Airco conductor used in the LCT coil in the 1970s, together with a steel jacket, embedded in a radial plate (see section 3.3.3). The strand properties have been hugely improved, and the cable is modified but the similarities are clear.

The superconducting strands used in ITER (and other devices) are produced in long lengths with a current capability of around 100A at the field and temperature levels required (about 5K and 6T for NbTi and 12-13 T for Nb_3Sn). Around 500-1000 strands have therefore to be used in parallel to achieve the required cable current capacity.

The cable-in-conduit conductor concept was proposed by MIT in 1975 for use with NbTi superconductors, as a way of achieving good helium contact and therefore stability in an AC environment, but it existed in parallel with other conductor concepts during the 1980s and early 1990s. Improved understanding of the manufacturing and design issues, driven by ITER R&D on conductor samples, led to the selection of the concept for all of the ITER conductors: it is, in particular, from the manufacturing point-of-view, low cost and flexible. However, as regards performance, the reasons for choosing this concept for NbTi conductors are different from those important for Nb_3Sn.

For NbTi, the driver is a combination of current uniformity and cryogenic stability[1]. For the large ITER cables, in particular, the CICC concept provides not only good helium contact but also a controlled electrical contact – too low and AC losses drive instabilities, too high and the cable instability is driven by the strand with the highest current/field combination. Several high-profile failures occurred during the 1980s with NbTi coils that either could hardly be ramped up in current at all, or quenched at significantly less than the theoretical current sharing temperature based on strand currents, because the strands were insulated from each other and current could not redistribute between them. It took almost 10 years to establish the appropriate strand coating (Ni), a joint concept for testing short samples of large conductors (giving similar, but not identical, contact resistance to all strands) and cable compaction, and to qualify the final design concept in a PF insert test in 2008. The PF insert qualified the highest field PF conductor (for PF1 & 6). The results obtained from this coil[2] gave confidence to change the conductor and strand specification for the low field PF coils (through PCR-164) in 2008, reducing the copper to non-copper ratio from an extreme value of 6.9 to 2.3

Fig. 6.1-33: ITER TF cable in conduit conductors.

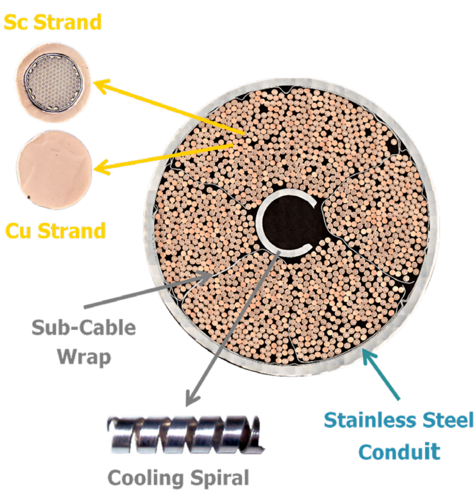

Fig. 6.1-34: Elements of the present ITER TF conductor.

For Nb_3Sn it was initially expected in the 1990s that cryogenic stability would be a similar issue as with the NbTi conductors. However, it was realised when large conductors began to be tested in environments where the n value could be measured, that Nb_3Sn conductors have a low n value (n is the exponent in the development of the electrical field in the transition region), well under 10, and that the strands themselves have lower n than NbTi (typically about one half). The more gradual development of an electric field as a strand approaches critical conditions allow current to transfer into adjacent strands, cryogenic stability is not needed. Strand coatings (resistant to the Nb_3Sn heat treatment) also required development (this time in the 1990s) before Cr was selected.

6.1.3.3.2 Nb3Sn Strand Degradation

A further feature of Nb_3Sn strands in CICC cables is a susceptibility to degradation. Despite the 2001 reports of excellent performance, the CSI, TFI (and the CSMC) showed significant degradation relative to the expected performance, the existence of which was not acknowledged until 2003. The TFMC did not allow sufficiently accurate performance measurements to be made to identify degradation but did not rule it out, either[3]. This report summarises the results of the coil tests and the accuracy limits of the assessments. It also provides a summary of the model coil publications 2001-2002. Although there was concern in the 1990s about the brittleness of Nb3Sn and the possibility of filament fracture in operation, this was not observed (or the mechanisms partially understood) until after 2010. In the above report there was still uncertainty about the role of manufacturing processes in causing conductor degradation, and whether it could be due to strand bending as well as filament fracture. The role of thermal cycles in triggering degradation was also not identified until 2010 in the above report, stabilisation of degradation was observed over several magnetic load cycles.

The two figures in Figure 6.1-35 show this degradation and stabilisation clearly. The right one from the CS insert is from 2003, the left, for the CS model coil itself, was produced in 2018 after about 100 charging cycles had been accumulated. As described in section 3.3.1, all the conductor designs were reworked 2006-2012 (as regards void fraction and twist pitch).

As a precursor to this rework, the Sultan test samples were redesigned to ensure that current uniformity and cable-jacket slip could not be causing an artificial interpretation of degradation. The use of voltage taps was extended after the recognition that significant voltage variation exists around the conductor jacket as well as along it.

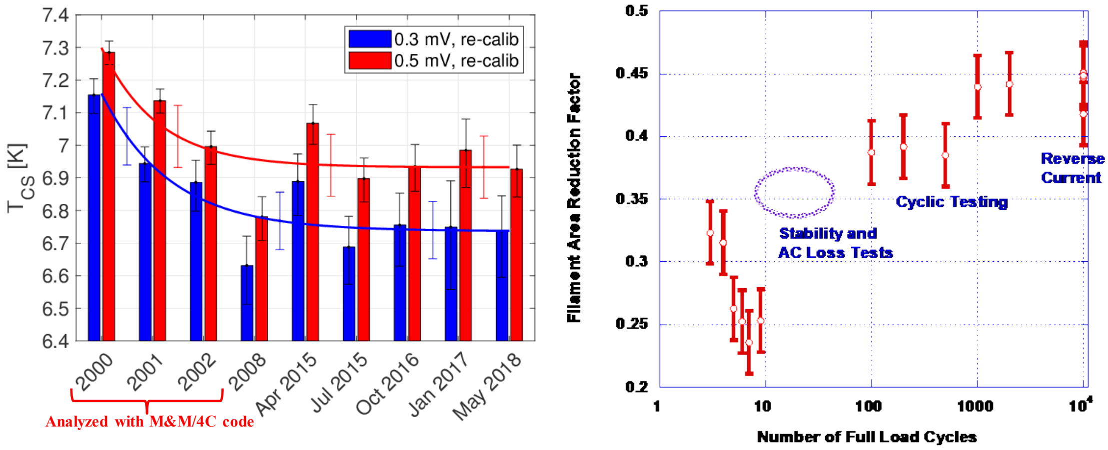

Fig. 6.1-35: Degradation in the original ITER conductor designs from 2001.

CS Model Coil Layer 1 CS Insert
(acknowledgement. R. Zanino, PolTorino N. Mitchell, ITER)

For the CS conductors, where there was time for a final development iteration, the problem was completely solved by a further optimization of cable void fraction and twist pitch combinations in 2010-11[4]. This program was also verified by a test of a second CS insert in 2016[5].

There was only partial success in the case of the TF. Insufficient attention was paid to TF conductor degradation with load cycling, after initial warnings in 2003, until it was clearly identified in conductor samples in 2007, too late to allow a proper mitigation program to be implemented in the manufacturing which started in 2009. As a result of this, efforts have been made to minimise the number of ITER thermal cycles (i.e. warm up and cool down) which trigger degradation 'steps', as well as (less severely) the number of magnetic load cycles. The specific scientific literature is dedicated to these steps[6].

6.1.3.3.3 Conductors and Plates

A basic conceptual decision with superconducting magnets is the integration of the structural material within the coil. Early magnets were often based on essentially putting the superconductor in static liquid helium, the so-called pool boiling concept, for example in several of the coils in the LCT project[7]. This was brought to a further stage of refinement in Tore Supra in the early 80s, using 1.8K superfluid helium as the 'pool' so that heat removal was improved by the extreme thermal conductivity of the helium rather than the flow or boiling heat transfer. However, such concepts required (1) a very low voltage since any insulation greatly reduced the conductor cooling (and helium itself is not a good insulator in the event of a loss of pressure), (2) an external case since structural material cannot be included as part of the conductor. The 3 LCT coils using force flowing cooling pointed the way to the future and this technology was used in all variants of ITER from 1988. With increasing coil size, and stored energy, discharge voltage increased (to over 10kV from about 2kV) and multiple overlapped layers of polyimide (Kapton) were included in all ITER insulation systems from the mid-1990s, glass-epoxy alone not being robust enough due to voids and cracks. This was well known from copper magnet systems but was a novelty for superconductors at the time.

This still left open the route to include the structural material and, as a side-effect of the increasing magnetic fields and the push to develop Nb_3Sn, how (and when in the manufacturing process) to carry out the Nb_3Sn reaction heat treatment to form the (brittle) Nb_3Sn compound from the malleable Nb and Sn metals in the strands as manufactured. Multiple processes were proposed (react, wind and insulate, for example) before ITER settled on wind-react-insulate as a basic process.

Generally, for pulse coils, closed toroidal loops have to be avoided because of eddy currents and there is a preference to avoid the complication of cases-with-joints, so a thick conductor jacket is placed around the cable, for ITER, square in form around the circular cable. A symmetric cross section (i.e. square) allows the jacket sections to be produced by hot extrusion, rectangular sections being much more difficult.

For the TF coils there are more options. One of the earliest was a 'radial plate' made of Aluminium, used in the fabrication of the Westinghouse LCT coil[8]. The Westinghouse cable was a 15kA cable in conduit, Nb_3Sn strand, square cross-section with rounded corners and was wound using a 'react, wind and insulate' process (so experienced some degradation of the Nb_3Sn although the coil still fully achieved its objectives while showing low resistive behaviour), wound into grooves in the plate, with the plates subsequently placed in a case. In many respects this coil can be considered a prototype of the ITER TF coils, although ITER conductor is much larger and was made with the 'wind, react and insulate' process.

In ITER, during the early 90s, a bucked design was proposed with layer wound TF coils (to allow conductor grading for cost reasons, the coil being divided into 3 grades). This resulted in layer wound coils and to provide the necessary out of plane stiffness, a winding of nested toroidal plates was adopted with each conductor layer contained in one plate. The plates were then connected by shear keys (insulated) between each coil. This design was dropped after 1996, after which the TF coils, still bucked, used radial plates and a case, like that used in the present design. The plate design was found to be effective in protecting the TF conductor insulation, especially in the nose region of the TF coil when a wedged design was adopted after 1998. The plate design has advantages but also significant disadvantages and issues which had to be resolved once the ITER construction activity started after 2005. Among these are (or were):

- A fast discharge of the TF coils results in large eddy currents and heating of the plates, and a very large expulsion of the helium (expulsion rates reaching 100kg/s). Re-cooling the TF coils after such an event requires a minimum of 4 days. This event is a significant safety and operational consideration.
- The high cost of manufacturing such plates. The 2001 TFMC was no help in this respect (the manufacturing route was not scalable) and there were many investigations (for

example, by welding of shaped extruded sections) up to 2012 before the present route (forging and machining of subsections) was derived by EUDA.

- The high plate-to-conductor voltage (each conductor turn insulation has to resist the pancake voltage).
- Closure of the conductor groove by welding. This was also efficiently solved by EUDA without damaging the insulation or distorting the double pancakes.

Overall, the plate concept has proved effective and is being adopted in the future concept proposals for fusion power plants by CFS (SPARC) and UKAEA (STEP).

The square conductor in a winding has an issue when the conductor has to transition from one pancake to the next, where also ITER had to develop specific solutions. The winding is a spiral and the conductor must exit from a (flat) pancake and transition up or down to the next. This transition creates a discontinuity in the structural reaction of the magnetic hoop forces, especially at the coil terminals. The need for a particular termination at this transition was the subject of much discussion. Finally, in PF and CS coils, the internal pancake to pancake transitions are made without reinforcement but with G10 inserts or putty mouldings to avoid resin rich areas of insulation. Only at the coil terminals are (steel) reinforcements provided, in both CS and PF coils. Figure 6.1-36 shows the links for a CS module terminal, involving welded plates and insulated bolts. These represent an insulation weakness (one CS module having an insulation crack in this region after cold testing) due to the local insulation stress concentrations.

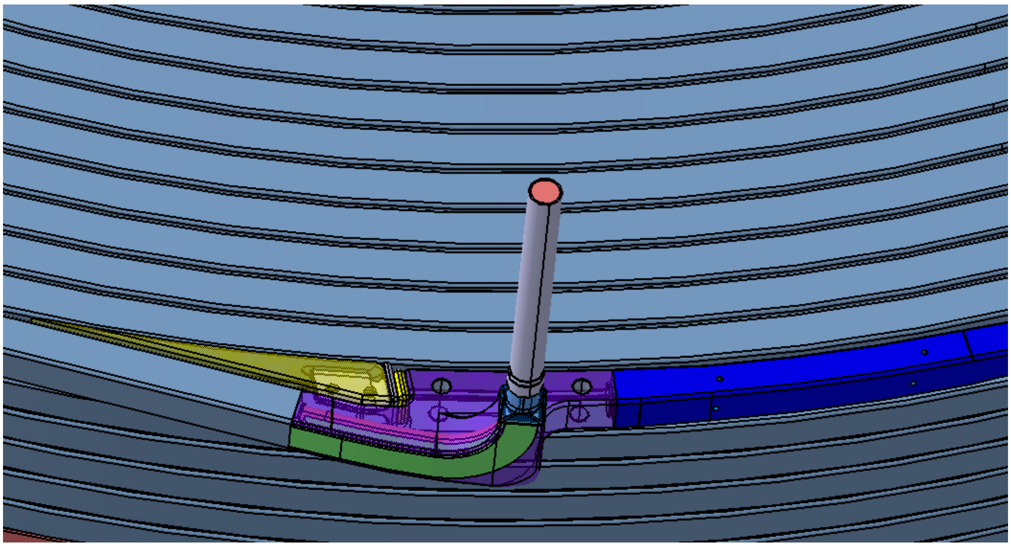

Fig. 6.1-36: CS module terminal break-out showing links (purple) to the next inner turn.

6.1.3.4 Feeders Layout and Assembly

6.1.3.4.1 Overall Layout

The feeder design was implemented as the last stage in the design process. The overall concept, shown below, was already in place in 1998 and does not seem to have been considered as something that could significantly impact assembly (contrasting with the problems now being found in 2024). During the CDA, the feeder design was placed underneath the tokamak rather than at the sides (although at this time the building was fully above ground). It is difficult to trace the evolution of the feeder design from this layout to that which appeared in 1998 with feeders in the side galleries at 2 levels, Figure 6.1-37, and then persisted through to 2001 and the present day.

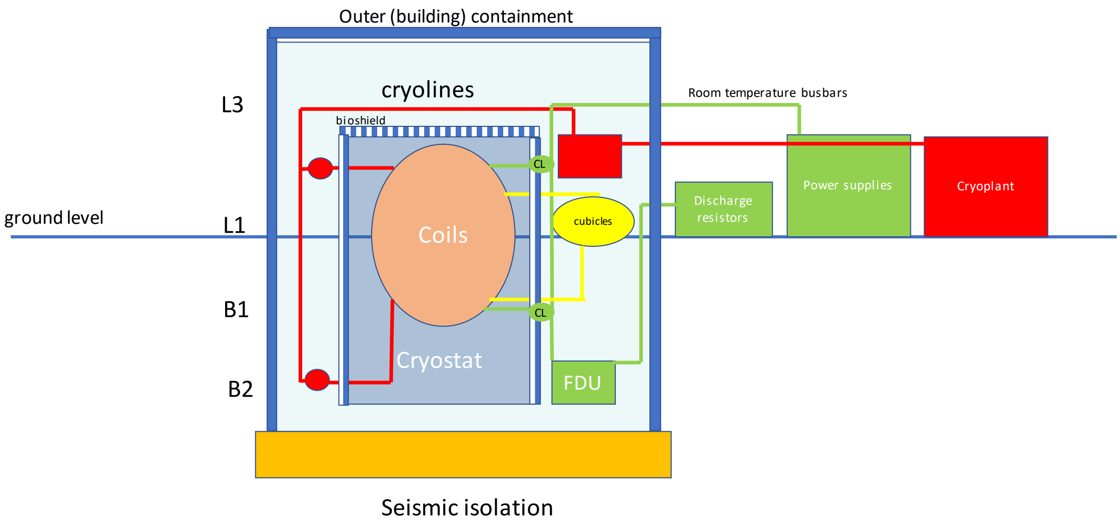

Fig. 6.1-37: Diagram of Coil Feeder Layout in ITER.

The real issue with the feeders is not the layout in the galleries surrounding the cryostat, but the layout in the cryostat itself going from the penetrations in the cryostat wall to the coil terminals. However, the decision (seemingly taken during the mid EDA in the 1990s and never really examined) to install the current leads horizontally created many issues in the configuration of the building galleries for the FDR 2001 design. It means that the feeder CTB have a long radial extension and extend well into the toroidal access space outside the bioshield. The cryogen and power supply connections within the galleries have also created a major set of piping and busbars running 360 degrees around the B2 and L3 galleries. More compact CTBs (and possible reduction in the number of cryostat penetrations) would have brought big benefits in installation time in the galleries.

6.1.3.4.2 In-Cryostat Layout

Within the cryostat most of the feeders access from below the device and then rise vertically to reach the coil terminals. The original concept was that each feeder was in 4 basic units, the CTB, the S-bend box, the CFT and the ICF (the S-bend box was later absorbed into the CTB). This means that 2 joints (CFT-ICF and ICF-coil) must be made in the restricted space inside the cryostat and that the ICF units (some very large and with irregular shape) have to be manoeuvred into position by lowering them inside the bore of the TF coils before the CS is inserted. This process has yet to be attempted but it appears inherently slow. One of the results of the present cryostat design is that there is very restricted access (essentially only person sized doors in the cryostat wall and low passages through the bioshield) to the lower cryostat regions and everything to connect the coils has to come from above, by crane (and is blocked by the presence of the TF coils and VV). Not enough attention was paid in ITER to the problems of in-cryostat assembly in the period 2006-2013, and the penalties are likely to appear during the feeder in cryostat assembly and in any repairs needed during commissioning.

Once complete, the major access to the internal components is through the cryostat lid. Originally, this had two removable sub-lids, one above the CS and one (as a ring surrounding it) above the PF1. These allowed the CS, and the CS upper ICFs, and the PF1, to be removed by removing the largest sub lid. There are some personal manholes to access the region above the outer PF coils but this (as well as the PF1 and CS access) is obstructed by the thermal shield which does not have easily removable panels.

6.1.3.5 Insulation and voltage

The working voltage range for the coils was fixed as not more than 20kV from the ITER EDA in 1991. The problem at this time was there was a very incomplete understanding of the steps required to produce high quality high voltage insulation. Superconducting magnets were operated at less than 2kV, one tenth of this value. It was expected that glass epoxy insulation systems could be adequate, and there was knowledge of the problems that Paschen breakdown would bring in imperfect vacuum systems which turned out to be typical of most cryostats. T15 provided the first evidence of the dangers of high voltage surfaces (even if insulators) exposed to such vacuums. High voltage testing and the experience of the ITER model coils in the 1990s made clear the necessity of including polyimide as an electrostatic barrier…glass on its own being far too prone to cracking in resin rich areas.

ITER implemented Paschen testing from the start of the ITER coil production in 2008 and imposed the implementation of robust ground planes on all surfaces exposed to the cryostat vacuum. There have still been substantial issues with instrumentation wire penetrations to the coil ground insulation and the discovery of Environmental Stress Corrosion between the resin used for the coil impregnation and the high voltage instrumentation wires (extruded polyimide). The problem here has been the great variety of resins used by suppliers and the lack of a single qualified design (each DA developed its own).

Clearly a reduction in the operational voltages would be helpful but the largest problem has come from the high voltages wires of the quench detection systems. Eliminating these (or greatly reducing their number or even imposing a single unified reliable design) would have reduced future operational risks. Figure 6.1-38 shows the range of resin suppliers involved in each of the coil and feeder sets…in this, it is obvious that ITER has no chance to ensure proper investigation of resin-wire interaction.

System	Resin mix
Mix TF A1 (MHI)	jER 807 / Baxxodur EC 302 (D 400) / Acc 399
Mix TF A2 (TS)	jER 807 / D230
Mix TF B	Araldite GY 282 / Jeffamine D 400 / Acc 399
Mix PF A	Araldite DBF / HY 951
Mix PF B / CC	SINOPEC CYD 128 / GY 051
Mix CS	EpoPro 275 A + B
Mix feeder	Gurit SE 84 LV
Mix instrumentation	EE 4215 / HD 3561
Mix repair	Stycast 2850 FT / 24 LV

Fig. 6.1-38: Individual resin types used in the coils (suppliers name).

6.1.3.6 Plasma Shaping and Control

The ITER Single Null has been the plasma basic shape since the start of the CDA. There were changes to the elongation during the EDA, but the present plasma surface has remained unchanged since the 2001 FDR.

There have however been significant changes to the method of vertical stabilisation. In-vessel coils (copper coils with magnesium oxide insulation) appeared in the ITER CDA in 1991, in the form of two loops above and below the plasma on the outside, more or less in the location of the present ITER in-vessel vertical stability coils. There are no details on their connection to services or installation, although such conductors were the subject of development within the EU NET team in the 1980s.

Although the vertical stability control remained a topic of concern in the ITER physics community, in-vessel coils were not implemented until about 2008 together with 27 sets of ELM coils, within the vacuum vessel PBS15.

Behind these changes there were a series of changes to the vacuum vessel configuration, in particular a reduction in the toroidal resistance (due to the inclusion of fully welded double shells) which made the plasma stabilisation with the main PF coils problematic, and an inability to include passive copper stabilising shells in the blanket (due to the disruption loads) as intended in 1998 and 2001:

- CDA report: Plasma elongation (K95) 1.9-2.0, I(plasma) 22-18MA, VV toroidal resistance 40µΩ.
- EDA 1998 FDR: K95 1.6-1.75. I 21MA, VV toroidal resistance 5µΩ.
- EDA 2001 FDR: K95 1.7. I 15MA, VV toroidal resistance 8µΩ.

As well as the in-vessel coils, the gain of the vertical stability controller for the VS1 circuit (which uses the PF2-5 coils) was increased in 2009. This increases the voltages and AC losses in these coils but improves their capability to stabilise excursions. The target for a maximum off-axis plasma excursion that can be stabilised was set at 0.2m (itself somewhat arbitrary).

The requirements for the accuracy of the plasma shape control were also tightened in 2009, to restrict the movement of the diverter strike points.

The avoidance of major vertical disruptions (VDE) has also been an increasing issue since 2015. Improved modelling of asymmetric disruptions show the potential for damage of VV and in-vessel components and a higher priority has been given to the Disruption Mitigation System (DMS) and the avoidance of rapid technical failures in the coils or their auxiliaries since such a loss of all means of plasma control will inevitably lead to a violent VDE, unless the DMS can be relied on.

6.1.3.7 In-Vessel Coils

ITER had in-vessel coils for vertical stabilisation (VS) in the CDA, up to 1991. These were eliminated in the 1990s variants (partly by a reduction in the plasma elongation). ELM control coils started to appear in tokamaks in the early 2000s. Neither VS nor ELM coils were included in the 2001 ITER FDR. The physics aspects of these two decisions were discussed in the period 2001-2007 with significant support among the DAs. It became clear that ITER vertical stability control by the ex-vessel coils would be marginal (due to the low resistance vacuum vessel of ITER) and the correction coils would not be able to substitute for in-vessel ELM coils (which could also provide Resistive Wall Mode control if needed).

The In-vessel coils (VS and ELM) were approved by PCR-166 in 2011 (it was submitted in 2008). The layout at this time was highly conceptual and many interface and assembly issues were not considered, even less the design functionality of the coils. The left figure below shows an example, Figure 6.1-39, shows the conceptual layout in 2011, the right the final layout in 2020.

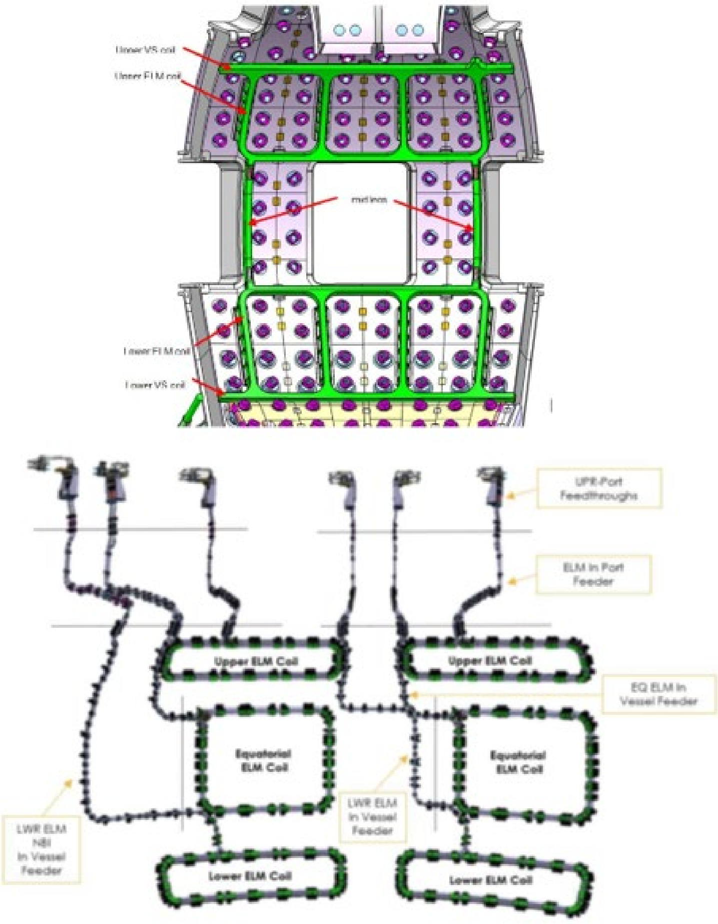

Fig. 6.1-39: ELM coils in 2011 and in 2020.

The IVC development continued under the VV supervision until 2015, when it was transferred to PBS11, magnets, following failure of a prototype ELM coil during manufacturing. A series of major reviews were held and proper load specifications written. The conductor and coil design was redone and staged development contracts for the conductor and then the coils were launched. The interfaces to the VV caused major problems, partly because of the (safety class) penetrations but also because the vacuum vessel support points had been fixed in 2013, see section 2.7 and up to 2023 repair was not permitted, on safety grounds, even though there were substantial errors in the positioning on the VV. The VV supports ('rails') were finally partly corrected in 2023-25 as part of the multiple VV repairs.

A further major issue was created by the water-cooling system. The Primary Heat Transfer System (PHTS) is composed of three subsystems: IBED-PHTS, VV-PHTS and NBI-PHTS. A well-known issue regarding ITER cooling water is that the IBED PHTS water is activated with N16/N17 when it passes through water channels of FW/BLK, Divertor and ELM/VS coils during plasma operation. This activated water emits gamma radiation and high energy neutrons when it decays and created problems with the radiation shielding provided by the building. This was resolved through a series of PCRs in 2015-16.

The VS and ELM coils were fixed by these PCRs as part of the IBED cooling loop and it was not practical (for safety reasons within the TCSWS and costs/space associated with heat exchangers) to separate them from the Diverter and FW cooling. However, the diverter and FW have to be baked at 240°C. The VS and ELM coils are firmly mounted on the VV inner surface which has a maximum temperature during bake-out of 190-200°C. This creates a large thermal stress at the coil supports, which is a design driver. Since the positions of the supports were fixed (as well as the cut-out spaces in the blanket), it was difficult to build in measures to mitigate the loads caused by the different temperatures (for example, support flexibility).

6.1.3.8 Design Criteria & Codes/Standards

The magnet structural design criteria were first set out in the 1991 magnet ITER CDR report which is within the ITER Magnets section[9]. This included the basic criteria that have evolved into the present set: defect-based design for structures with fatigue crack growth rate rules, limited by fast fracture as well as yielding. This methodology defines an allowable operating life based on the inspection levels set for manufacturing. By the FDR in 2001, there was a full version of the structural design criteria available which focused on fatigue and fracture and expanding the concept of a defect-based design, based on the Fitness for Service assessment method set out in API 579, later (in 2007) adopted into ASME as ASME FFS-1. This had important consequences for manufacturing since allowable weld defects can be set according to the total stress levels, making for less stringent NDT and fewer repairs. The 2001 criteria were revised 3 times from 2001 to 2012, improving the clarity, adding explanations and adding some new methodologies to address specific problems (for example, mean stress impact on fatigue crack growth, multi-axial fatigue and magneto-elastic stability).

The Superconducting and Electrical design criteria were first produced (in 2001), although the main elements of the superconducting part are included in the CDA Magnet report. The superconducting part was significantly updated in 2007-2009, the use (or not) of cryogenic stability (well-cooled and ill-cooled regimes) to determine the ratio of Cu to non-Cu, the reduction of temperature margin in Nb_3Sn and the recognition of a very low n (power factor of the superconducting transition) in Nb_3Sn cables. Due to the lack of a recent update, there are several critical electrical criteria missing from the electrical criteria (in particular, on Paschen breakdown and on tracking distances).

There are many codes and standards applicable to the manufacturing. These are taken from ASTM, EN, IEC and ISO standards where applicable ones could be found. In some cases (leak testing is an example), the full procedure is given as an Appendix to the Procurement Arrangement Annex B (the Technical Specification). The existence of these codes and standards in the

Procurement Arrangements is not a full definition of what was actually applied. In many cases, companies applied to use equivalent or near equivalent national standards and this was generally approved. This can often be found in the travellers provided on delivery.

Two other codes were identified as applicable in 2009 and had a significant impact on the manufacturing and assembly

- European Pressure Equipment Directive. Essentially the magnets themselves are not subject to the directive, but external helium piping is, also in the cryostat. The pressures and pipe diameters were chosen to ensure that the pipes were within Category 0 or Category 1 (self-assessment but CE marking required).
- European Machinery Directive: This Directive applies to machinery, interchangeable equipment, safety components, lifting accessories, chains, ropes and webbing, removable mechanical transmission devices and partly completed machinery. It is relevant for the magnets when tooling (or lifting frames) is supplied from outside the EU. This created some issues in the CS where the PA requires also lifting tooling for stacking the 6 modules to be supplied. The DA (US) has solved this by subcontracting to an EU company.

6.1.4 Load Specification Summary

This section gives a very brief summary of the load specifications for the superconducting coils, covering magnetic, electrical, thermal, nuclear and covering historical developments where changes had a significant impact. Unusually (for a load specification), it includes tolerances and error fields. These would more normally be considered as requirements but because of the dynamic changes experienced over the long period of ITER construction and assembly, they can better be considered as a type of load. The changes of load specifications give some idea of the background to the ITER delays. In a project where the design of most systems was not mature and interfaces not initially well defined, load changes resulting from other systems have had to be absorbed by design changes which easily lead to manufacturing delays.

6.1.4.1 Mechanical

The mechanical loads on the magnets are dominated by the magnetic forces. The global values are large, and have not significantly changed since 2001, Figure 6.1-40.

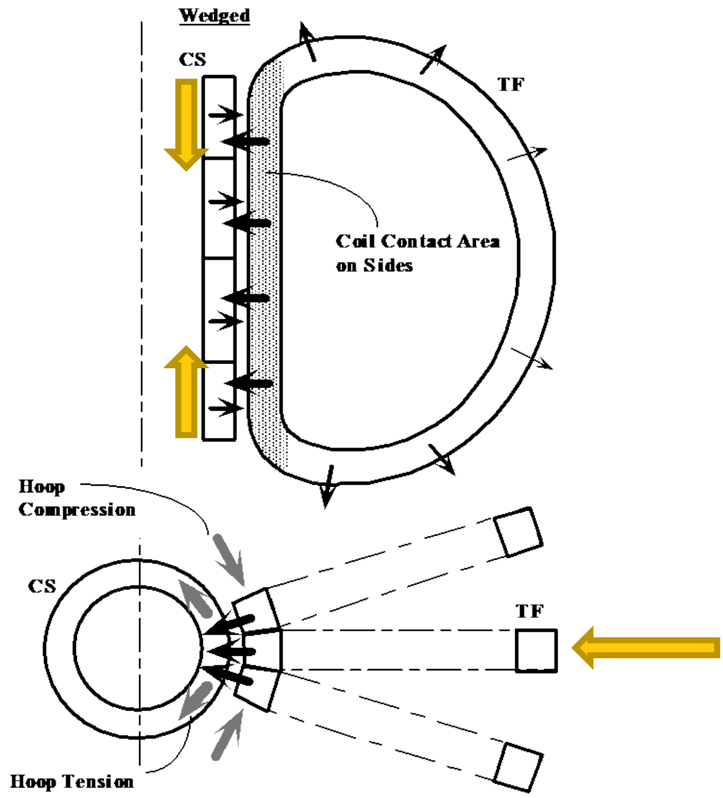

Fig. 6.1-40: CS and TF self-loads.

The interaction between CS and PF, and the TF, produces the classic out of plane forces on the TF coils.

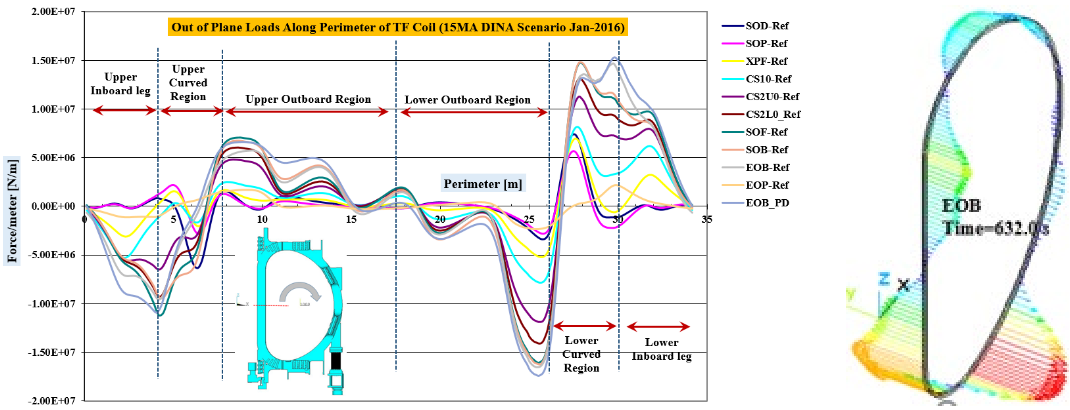

Fig. 6.1-41: Out of plane loads on TF due to CS & PF.

6.1.4.2 Electrical

The electrical conditions in 2001 were not assessed by an electrical model and do not consider possible single fault (to ground) conditions. New calculations from 2019 are below. These are different (but not largely) to the operational values from 2009 which were used as input to the manufacturing specifications. The addition of single fault conditions is a substantial change from 2001 expectations and acts as a design driver.

Table 6.1-3: Coil Voltage Levels.

<u>PF coils</u>

	Between terminals	Terminal-to-ground
In normal operation (kV) (including fast discharge)	14 13 for PF1 and PF6 19 for PF2, PF3, PF4, PF5	7 7 for PF1 and PF6 13 for PF2, PF3, PF4, PF5
During fault conditions (kV)	28 27 for PF2, PF3, PF4 26 for PF5 20 for PF1 21 for PF6	23 27 for PF2, PF3, PF4 and PF5 20 for PF1 21 for PF6

<u>CS coils</u>

	Between terminals	Terminal-to-ground
In normal operation (kV) (including fast discharge)	14 10 for CS1U and CS1L 22 for CS2U and CS2L 13 for CS3U and CS3L	7 18 for CS2U and CS2L

During fault conditions (kV)	30 18 for CS1U and CS1L 29 for CS2U and CS2L 20 for CS3U and CS3L	18 21 for CS1U and CS1L 29 for CS2U and CS2L 20 for CS3U and CS3L

<u>Correction Coils</u>

	Between terminals	Terminal-to-ground
In normal operation (kV) (including fast discharge)	0.6	0.3
During fault conditions (kV)	0.6	0.6

<u>TF coils</u>

	Between terminals (2 coils in series)	Terminal-to-ground
Normal operation (kV) (including fast discharge)	10	6
Fault conditions (kV)	20	16

6.1.4.3 Heat Loads

The heat loads are dominantly at 4K and have 7 components:

1. Conduction (from gravity supports and thermal shield supports)
2. Thermal Radiation (from the 80K thermal shields) and Conduction
3. Pump work (from the primary cooling circuit)
4. AC losses
5. Eddy currents

6. Nuclear
7. Resistance in the superconductor (joints)

The cryogenic heat load breakdown was not available in 2001. The first full estimate was in 2009. Since 2009, the heat loads have increased by 60% as seen in Table 6.1-4. In 2001, the cryoplant was sized based on a very approximate total estimate based on scaled (down) estimates from earlier larger ITER variants in the 1990s. Although not recorded, the introduction of HTS current leads in 2005 (see section 2.6.1) largely reduced the cryoplant heat loads but did not result in any size reduction of the cryoplant, with the extra cryoplant margin being introduced 'through the back door'.

Table 6.1-4: Total Cryogenic Heat Loads 2009 and 2024.

Original 2009									
MJ									
Coil	AC Loss	Eddy Curr	Thermal Radiation and Conducti on	Nuclear (b	Pump	Joints	Total MJ in 1800s		Average power W
TF	1.94	0.00	0.00	2.53		2.25	11.32		6288.89
CS	6.75	0.00	0.00	0.00		0.13	12.43		6905.56
PF+CC	1.77	0.00	0.00	0.00		0.34	12.26		6811.11
Structures	0.00	14.49	4.60	3.23		0.00	17.72		9844.44
Feeders	0.00	0.00	5.55	0.00		0.00	5.55		3083.33
Totals	10.46	14.49	10.15	5.76		2.72	59.28		32933.33

New 2024									
Coil	AC Loss	Eddy Curr	Thermal Radiation and Conducti on	Nuclear (b	Pump	Joints	Total MJ in 1800s		Average power W
TF	1.77	0.00	0.00	5.20		4.20	17.48		9711.92
CS	10.12	0.00	0.00	0.01		0.20	16.09		8938.89
PF+CC	5.04	0.00	0.00	1.17		0.55	18.83		10459.97
Structures	0.00	23.80	6.31	11.46		0.00	35.26		19588.89
Feeders	0.00	0.00	5.76	0.66		0.00	6.42		3565.83
Totals	16.93	23.80	12.07	18.50		4.95	94.08		52265.50

The largest proportional change is as expected the nuclear heating, but AC losses and eddy currents (due to control and faster plasma current ramp) also increase by about 60%. The pump power is about 12kW and has not changed much between 2009 and 2024.

There is an overall reduced heat load from the current lead redesign (with HTS leads) since 2005, but this was already present in 2009.

6.1.4.4 Nuclear Radiation

6.1.4.4.1 Nuclear Heating

The nuclear heating to the magnets is well known to have increased substantially (by a factor of close to 3) between 2001 (up to 2008) and then to 2023.

The main design changes which contribute to the increases are as follows:

- Reduced upper port top shield coverage
- Removal upper port manifold shields
- Decreased blanket mass, increase blanket tolerances (i.e. gaps)

In a number of cases design changes were implemented (for example, removal of the upper port shielding to allow space for the RF heating antennae) with a promise to re-instate the shielding within the thermal shields and then 3 years later rejecting this addition on the grounds of feasibility. The overall history is summarised in Figure 6.1-42 & 4-4.

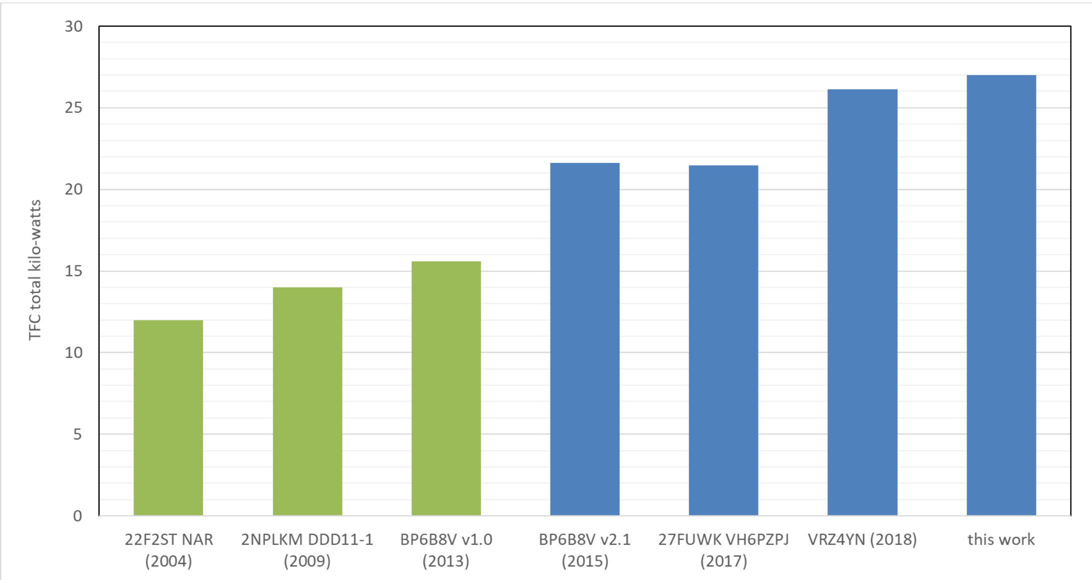

Fig. 6.1-42: Summary of historical TFC total integral heating results (green = best estimates, blue = upper estimates). The assessment of systematic errors and conservative estimates is complex and depends on the models being used.

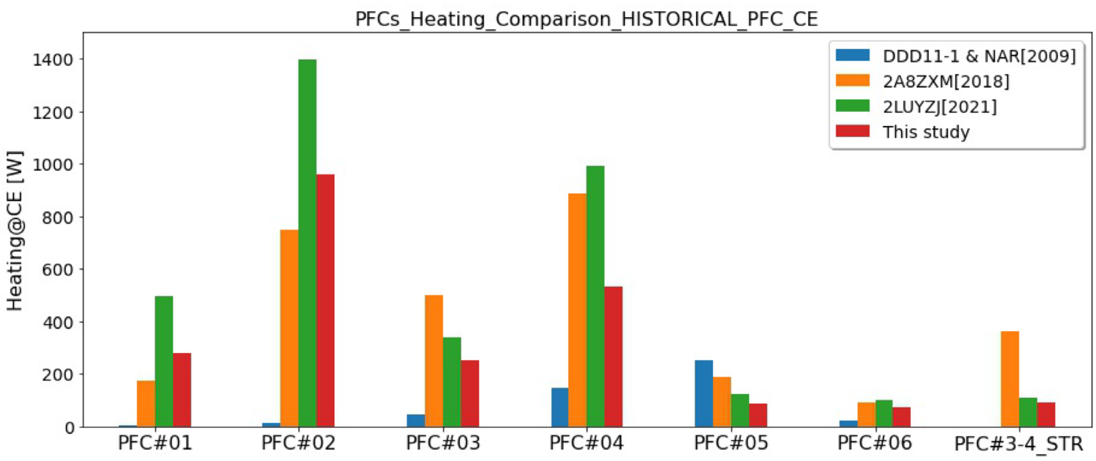

Fig. 6.1-43: Summary of historical PF Coil integrated heating development ('this study'=2023).

6.1.4.4.2 Nuclear Radiation Dose

The latest results (2023) on the TF coil radiation levels are shown below. These are the most comprehensive available, and responses are available with and without the uncertainty factors. These results match the 33.6kW of total nuclear heating (compared to 14kW in 2011 and 15kW in 2012) and indicate a neutron fluence of about $1.2\text{x}10^{22}\text{n/m}^2$ on the front insulation and absorbed dose of 4.5MGy which are computed with a total irradiation of 4700h at 500MW DT plasma neutron source.

Examining the development of radiation responses since the original ITER Nuclear Analysis Report of 2004, we observe that the neutron fluence scales roughly with nuclear heating (a factor of 3), as expected while the absorbed dose to the insulator has also almost doubled. The reasons behind these increases are mainly due to (a) the removal of shielding in critical areas (e.g., additional neutron shield from the thermal shield, cigar racks in the upper port), (b) the port plug design effect (e.g., upper launcher heating systems), and (c) the increased model accuracy (e.g., unaccounted effects of the NBI), which was not accounted for in the NAR (Nuclear Analysis Report) analysis.

The ITER insulation design fluence in 2001 was $1.0\text{x}10^{22}\text{n/m}^2$ and despite the x3 increase in nuclear heating, the TF coils are (just) within this limit, Figure 6.1-44 & 4-6.

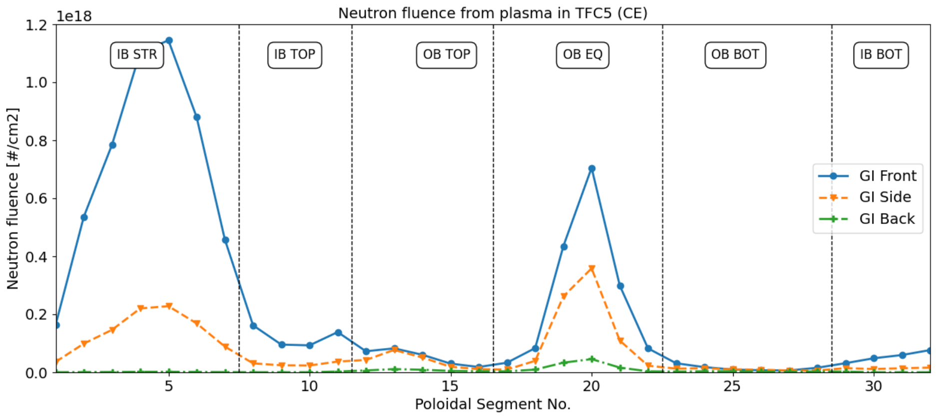

Fig. 6.1-44: Poloidal profiles of neutron fluence to different insulator areas in TFC5 [plasma source, conservative estimate].

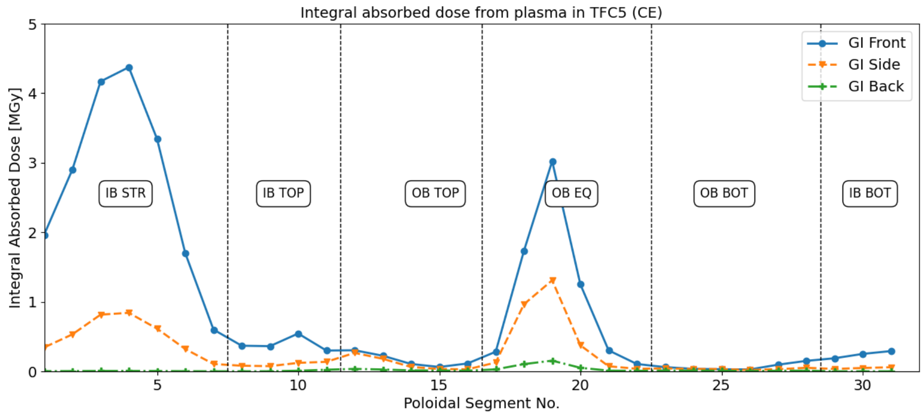

Fig. 6.1-45: Poloidal profiles of dose to different insulator areas in TFC5 [plasma source, conservative estimate].

The original radiation levels for the TF coils are given in the 2004 Nuclear Analysis Report and (after correction for the simplified 1D models used at this time) are:

- TF front insulator: $2.5 \times 10^{21} n/m^2$ neutron fluence

So, the increase by 2024 is somewhat more than the ratio of the nuclear heating increase.

6.1.4.5 Plasma Scenarios and Error Fields

The original ITER 'plasma scenarios' were produced before the EDA in the late 1990s and were at this time a series of axisymmetric plasma equilibria with an estimate of the current profile shape and the poloidal flux needed to ramp up the plasma current and drive it. These continued as the basis for the CS and PF coil/field current requirement definition until after the FDR in 2001.

It was not until 2007 that the first plasma simulations using the DINA code appeared. These were imperfect and did not include plasma breakdown or shutdown but produced self-consistent current profiles. The pre-bias and early plasma current formation had to be grafted onto the DINA scenarios from a separate code. The first true baseline scenarios for the ITER magnets, defined in 2009, therefore used a mixture of DINA and snapshots, matched by interpolation and poloidal flux alignment. The code timesteps at this time were too coarse to allow simulations of vertical stability control (frequency up to 100Hz) and these were done separately and superimposed on the scenario currents (time scale 10s).

It was not until 2016 that DINA advanced to the point that full plasma pulses could be simulated, including vertical stability control (simulated by injection of a white noise component into the model of the vertical stability controller). At this point a new set of scenarios were produced as a baseline. These also eliminated some of the 2009 'flexibility scenarios' as unachievable (especially those at low li) and changed the time of formation of the diverter and the rate of plasma current ramp up. As a result, the CS and PF current/field/force requirements have reduced and the plasma burn length appears potentially to be longer. The PF6 operation at fields above 6T also seems not to be required. Since manufacturing of most of the magnet system is complete, these changes will only result in increased margins.

The impact of the change in the electromagnetic environment since 2009 can be seen in the change of the AC loss and eddy current heat loads in the Heat Load section 4.3.

One area where progress has been limited is in disruption modelling of severe asymmetric vertical disruptions (AVDEs). There is no fully self-consistent plasma model (that can also include halo currents) and without electromagnetic self-consistency, exceptional magnetic loads can be generated or can be underestimated. The load specifications may be non-conservative for AVDEs and an approach based on experimental validation during the ITER start-up phase will be followed, using extra instrumentation installed on VV and TF gravity supports and starting with low current AVDEs.

One area of magnet current control that has yet to be investigated is the actions taken when a disruption is detected and attempts to control it are dropped in favour of mitigation of the event. Almost all models assume that the coil power supplies behave as if a zero voltage zero resistance element in the circuit, but without defining when this state is achieved. There is some potential for disruption consequence mitigation if active control is used.

The assessment of the impact of field errors has also advanced substantially since the 2001 FDR. The original correction coil capacity was derived purely by consideration of field asymmetries and their correction. The sources of the error fields were not linked to coil dimensional errors, and the criteria was based on the '3-mode' criterion, considering the lowest error field harmonics [(1,1); (2,1); (3,1)]. This was linked to combinations of coil centre line errors in the period 2003-2007 and it allowed a coherent set of coil tolerances to be produced.

However, a new method for correcting magnetic field errors in the ITER tokamak was developed using the Ideal Perturbed Equilibrium Code (IPEC). So-called "overlap" error field criteria were derived. In April 2017, based on the analysis performed by the ITPA MHD Topical Group (MDC-19), the "3-mode" criterion was excluded and only the "overlap" error field criterion was recommended for ITER. Assessments of the range of coil position errors is still on-going, but it appears that the CC current capacities are still adequate.

In the last 5 years, the issue of toroidal field perturbations creating localised heating on the first wall has arisen. This was to be compensated in ITER by measuring the error fields (using the plasma diagnostics) since the blanket and first wall were only installed in a second operation phase, after the magnets have been energised (and the real alignment can be measured). With the blanket now being installed before the coils are energised, alignment will depend on predictions of the final coil positions based on the assembly gaps and analysis of coil movements. In these assessments, individual coil location or shape errors have an impact.

6.1.4.6 Field

The magnetic field levels on the various coils have remained at the same values since the 2001 FDR.The TF coils have a peak field (including components from the CS and PF coils which add 0.2-0.3T) of 11.8T. This is weakly affected by the different plasma scenarios and also by the ripple in the toroidal field (the side pancakes have a slightly lower field than the centre ones, up to 0.5T).

The CS and PF coil field values are determined by the plasma scenarios (see section above).

The CS conductor has a peak field of 13.1T at 40kA, and 12.7T at 45kA, with the two limits corresponding to pre-bias (when all the modules are energised to nearly the same current) and end of burn, when the central modules of the six dominate. These values assume a coil operating temperature of 4.5K. Margin exists to increase the field levels by sub-cooling the coil but the coil limits come from the stresses in the conductor jacket, not the superconductor.

The PF coil design field levels are shown in the Table 6.1-5.

Table 6.1-5:

Coil	Field, B_{ref}
PF1 & 6	6.5 T
PF2, 3 & 4	5.0 T
PF5	6.0 T

There was discussion in 2001 before the FDR and again in 2006-7 about the need to make PF6 in Nb_3Sn instead of NbTi to include the ITER operating range. This was rejected in view of the cost, since subcooling (to 3.8K) is equally possible, and the scenario implications at the time were not fully investigated. Seen now, such a change would have been largely wasted as changes in the way the plasma is ramped up have off-loaded the PF6 and the limits come from the CS module vertical forces.

6.1.4.7 Thermo-Mechanical

The thermal loads in the magnets arise (quite conventionally) from two sources, differential contraction and different temperatures.

Different temperatures occur between the cryostat wall (at room temperature) and cryostat support ring which provides the support to the individual TF and VV gravity supports and is also at room temperature, and the overall magnet system, generally at 4-5K but with some parts up to 15-20K in operation. The main cases are:

- The TF coil gravity supports, which provide flexibility in the radial direction to adapt to the thermal contractor of the magnet system (the relative displacement of the top of the TF GS relative to the bottom is of the order of 30mm).
- The in-cryostat feeders, which are linked to the CTBs (bolted to the building floor) at one end and the magnets at the other, with a bellows connection also to the cryostat wall.

Differential contraction also occurs between many of the magnet components and materials and must be considered specifically in the design to avoid failures. The main cases are:

- Between insulation/resin-based materials and metals.
- Between Nb_3Sn strands and the conductor jacket.

Since 2001, a number of changes have been implemented to account for differential temperatures. The S-bend boxes in the feeders were originally intended to provide a flexible loop in the conductor and supply pipes to allow movements of 20-30mm. However, the feeder design changes, including complex curves in the ICFs, mean that the S bend flexibility cannot be properly transmitted to the full feeder lengths. Flexibility has to be built into the conductors and cooling pipes by allowing sliding within feeder units. This is a major change which is still being analysed in 2024. It will only be tested in operation. More detail is given in section 2.6.1.

6.1.4.8 Pre-Loading

Pre-loading is applied in several areas, essentially to keep surfaces in contact and either (1) avoid high cyclic loads that then result on keys, pins and bolts joining them or (2) to prevent gross movement of the two components relative to each other. Within the ITER magnets there are five of these, four of which have undergone a complete design since the 2001 FDR (and one of which did not exist in 2001). There was a lack of detail on the mechanism of pre-compression in 2001, often an oversimplified global solution such as tightening a bolt was proposed, with in some cases a bolt assisted by jackbolts to achieve the required preloads (this is also a proprietary technology known as 'Superbolts' which is now quite widely available in several variants). The problem with this is that the jackbolts require torsion and in general are unable to achieve high loads before frictional shear in the threads causes jamming and then failure. Most of the magnet superbolts have eventually been replace by hydraulic pre-load systems, often with some redesign to achieve the required accessibility.

Pre-compression Rings: The purpose is to preload the IIS keys between the coils to avoid gaps opening in operation. The original system involved tightening superbolts that pushed on 36 flanges to extend the rings outwards and pull the upper and lower flanges of the TF coils inwards through studs passing through the flanges and between the rings. The problem is that all superbolts have to move together, or the jackbolts overload. This means tightening thousands of jackbolts simultaneously. Multihead spanners could perhaps have been developed but many are required. The system was replaced by hydraulic stud tensioners which push on the flanges and pull on the studs, allowing the bolts to be tightened lightly without the use of jackbolts. Structural assessments found that a limited set of stud tensioners could be used and moved in steps as the PCRs can accept the non-uniform stresses.

Central Solenoid Vertical Pre-Load Structure: The purpose is to maintain a degree of surface contact between the 6 modules in the stack during all operational conditions. There are several cases where the CS modules vertically repel each other, and others where there is a strong compression of the top and bottom 3 modules towards the tokamak axis. The surface contact conditions have evolved since 2001 by being relaxed to allow gaps to open and a minimum contact area of about 20%. Originally, the CS was preloaded (at the top) by using Superbolts to push a pressure plate down onto the top surface of the top module while stretching the inner and outer tieplates, followed by a shimming of the gap. Trials in 2017-18 found that the Superbolts could not provide sufficient load, with the jackbolts seizing under the loads. A system of hydraulic preloading units was designed and purchase started in 2019.

TF gravity support plates: The TF gravity supports consist of a stack of plates that bend to allow the magnet system to move flexibly radially but are stiff to bending and sideways movement. Originally the plates were welded to a top and bottom plate that then interfaced to the coils and to the cryostat base. The welding was difficult and CNDA and their contractor SWIP proposed to form a stack of plates clamped together at top and bottom by studs, so that the plates are prevented from sliding by friction. The studs are tensioned by hydraulic stud tensioners at the supplier (HTXL in China) and the supports delivered as a complete unit.

TF Gravity supports to cryostat ring attachments: The bottom support of the TFGS is bolted to the top plate of the cryostat rings with studs set in holes in the ring (with some clearance to allow the TFGS to be positioned independently of the holes in the ring). There was no detailed design for this in 2001. After a detailed re-assessment in 2015 of the expected loads to be transmitted through the TFGS to the cryostat ring (especially due to vertical disruptions) the design was modified to change the number of studs and to add stoppers (fixed in groves machined in the cryostat ring and shimmed to match the base of the TFGS) to prevent gross slippage in the event of asymmetric VDEs. The studs were originally preloaded with Superbolts but these were replaced by hydraulic tensioners using the tokamak assembly contract TAC1. The TFGS are all now (2024) assembled onto the cryostat ring, with one major quality issue found in 2021, when delayed fracture of one of the Inconel studs occurred a few weeks after it was tightened. An inspection of the studs, in situ, found 2-3 where manufacturing quality mistakes appear to have allowed large defects to be included. These have been replaced.

PF Coil Support Clamps: These are clamps onto the PF coil windings that provide the interface to the supports onto the TF coils. The clamps are held in place by pre-loaded studs linking the top and bottom plates, loaded hydraulically. The system has not changed since 2001.

6.1.4.9 Hydraulic

The coil hydraulic loads cover the thermal, pressure and mass flow conditions in normal operation and quench. They are dependent on temperature (hence, AC losses, eddy currents, nuclear heating etc) and are highly variable with location. Inside coils, during quench, pressures can reach over 5MPa. In the feeders, pressures are under 2MPa even in transient conditions. The feeders are equipped with pressure relief burst disks that vent into the gallery, placed on the PRVR, that activate at 28bar.

6.1.4.10 Seismic

The seismic loads for the magnets have a complex history. They act as design drivers for the feeders and main TF gravity supports (which has led to design modifications in both systems during the period 2011-2024). In 2001 there was a generic seismic assessment using an SL-2 specification, for a building that did not have seismic isolators. For the magnets, no seismic analysis was done at this time (the most sensitive components, the feeders, were at a very basic design level). This seismic assessment was adapted to the Cadarache site, including the design of the tokamak building with isolators, by 2008. However, before any detailed magnet analysis was completed, the design of the machine supports was modified as a result of the Fukushima earthquake in 2011 and new requirements from the French regulator ASN. A further extreme seismic load was defined, known as SL-3. It was now required by the French Regulator to take into account certain phenomena, such as the "hard core" level earthquake (SL-3). The magnet hard core components are limited to the isolation valves which are in the galleries.

However, the magnets and feeders were defined as aggressors to the magnet HCC and all of the magnets are subject to the SL-3 stress test, for what appear to be rather arbitrary reasons. This creates the situation where the assessment of the entire magnet system is being carried out with factors of 1.5 x 1.25 on the out-of-date 2010 seismic spectrum and global tokamak support configuration.

6.1.5 Performance

It is not practical to include even a minor part of the ITER analyses produced as internal reports. Some of it is available as publications but due to limitations in paper length, such reports can only give global overviews. There is also a problem with the configuration to which such reports refer. Usually, structural analysis is performed and reported at an early stage of the design. Updates are made in internal reports, but such updates are rarely published. A set of the latest available publications of performance analyses is given here but these must be treated extremely cautiously as they are often several years out of date and often omit many details (and issues of concern).

6.1.5.1 References to the topic

- Structural Assessments
  - TF Coils and Structures
    - An Electromagnetic and Structural Finite Element Model of the ITER Toroidal Field Coils, Gabriele D'Amico, Alfredo Portone, Cornelis T. J. Jong, April 2018, Volume28 (Issue3) p.1- 5- IEEE Transactions on Applied Superconductivity
  - PF and Correction Coils

There are no adequate publications on the PFC or CC structural assessments. The three reports below give some summary values.

- B. Lim, F. Simon, Y. Ilyin, C. Y. Gung, J. Smith, Y. H. Hsu, C. Luongo, C. Jong, and N. Mitchell, Design of the ITER PF Coils, IEEE TRANSACTIONS ON APPLIED SUPERCONDUCTIVITY, VOL. 21, NO. 3, JUNE 2011
- B. Lim, F. Simon, Y. Ilyin, Q. Hua, C. Beemsterboer, N. Mitchell, P. Valente, K. Smith, N. P. Sabadi, A. Oustinov, R. Penco, A. Mednikov, E. Marushin, I. Rodin, Y. Song, G. Shen, W. Wu, Y. Chu, Approaching ITER PF Coil Manufacturing, IEEE Transactions on Applied Superconductivity, vol. 26, no. 4, pp. 1-4, June 2016, Art no. 4205204, doi: 10.1109/TASC.2015.2512705
- Foussat; P. Libeyre; N. Mitchell; Y. Gribov; C. T. J. Jong; D. Bessette et al., "Overview of the ITER Correction Coils Design," in IEEE Transactions on Applied Superconductivity, vol. 20, no. 3, pp. 402-406, June 2010, doi: 10.1109/TASC.2010.2041911

  - CS Coils

D. Everitt et al., "ITER Central Solenoid design," 2013 IEEE 25th Symposium on Fusion Engineering (SOFE), San Francisco, CA, USA, 2013, pp. 1-8, doi: 10.1109/SOFE.2013.6635515

- Kevin D Freudenberg, R. Myatt, ITER Central Solenoid support structure analysis, Fusion Engineering and Design, 24th Symposium on Fusion Engineering (SOFE), June 2011

- Conductor Assessments

- M Breschi, A Devred, M Casali, D Bessette, M C Jewell, N Mitchell, I Pong, A Vostner, P Bruzzone, B Stepanov, T Boutboul, N Martovetsky, K Kim, Y Takahashi, V Tronza and Wu Yu, Results of the TF conductor performance qualification samples for the ITER project, Superconductor Science and Technology, June 2012 Volume 25, Number 9
- D. Bessette, "Design of a Nb3Sn Cable-in-Conduit Conductor to Withstand the 60000 Electromagnetic Cycles of the ITER Central Solenoid," in IEEE Transactions on Applied Superconductivity, vol. 24, no. 3, pp. 1-5, June 2014, Art no. 4200505, doi: 10.1109/TASC.2013.2282399
- Yuri Ilyin, Denis Bessette, Elena Zapretilina, Cesar Luongo, Fabrice Simon, Byung Su Lim, and Neil Mitchell, Performance Analysis of the ITER Poloidal Field Coil Conductors, IEEE Transactions on Applied Superconductivity, Vol. 20, No. 3, JUNE 2010
- In Vessel Coil Assessments
- Alexander Vostner et al, The ITER In-Vessel Coils – design finalization and challenges, Fusion Engineering and Design Volume 146, Part B, September 2019, Pages 1490-1495

6.1.6 Safety

The magnets are an obvious concern for nuclear safety, as identified in the 1980s in the early NET reports. The concerns are always derivatives of (1) the stored magnetic energy (2) the very large magnetic forces which are equilibrated within the magnet system (3) the volume of cryogenic helium they contain. They are considered here since the operation of ITER is dependent on meeting the licencing conditions set by ASN, and in particular the conditions to release the successive hold points set through construction. At present (August 2024), ITER has still not achieved the release of the hold point for the start of the machine assembly (i.e. real irreversible installation of the sectors in the cryostat). It is certain that more hold points will be set as operation approaches and that these will increasingly impact magnets as the most 'active' component in the cryostat. Part of this will look at the magnet safety case (as outlined below) but also in the overall design basis and qualification, resolution of non-conformities from manufacturing and the predictability of magnet behaviour during commissioning.

In the 1998 version of the EDA FDR report, the magnets were identified as a 'safety important' system, meaning that incidents within the magnets could lead to the failure of one of the radiation confinement barriers. These barriers included the vacuum vessel, the building and occasionally the cryostat. In 1998, the first 'magnet safety' design document was produced, which assessed the various possible (and impossible) failure mechanisms and accident sequences. At this time, the stored magnetic energy in the magnet system was about 100GJ (1 GJ can melt about 1t of steel).

By 2001 for the EDA FDR, this safety document became the magnet safety design description document, being substantially updated for the reduced size ITER (now 40GJ of stored energy) and with many calculations giving quantification of electrical, structural and fluid incidents. Using this, we could show in 2002 that the magnets could not, by design, challenge any of the confinement barriers (except the cryostat which by this time was not a confinement barrier) to an extent that would result in the release of a significant amount of radiation, and it was agreed that the magnets could be dropped from the list of safety-important (SIC) systems. This categorisation (non-SIC) has been maintained throughout construction, although has had to be reinforced by SIC protection systems that can be placed within the feeders in the galleries, outside of the cryostat. It would be very difficult to construct a first-of-a-kind system as large and complex as the magnets under the supervision of an Authorised Notified Body such as was required for the VV, there were too many novel technical complexities on top of a difficult management environment.

The magnet design description document was updated in 2008. Magnet safety requirements are now set out in a set of defined requirements in the SRD and in a range of internal documents. The main points are as follows:

Structural

Structural analysis of failed (and shorted) TF coils shows that although the TF system can push the CS sideways, and the case can locally fracture, the combination of intercoil keys and ultimately the PF coils should prevent gross structural movements and impact to either the VV or the cryostat. This issue has been the subject of a question from the ASN Groupe Permanante, designated 24.3, in 2011, which is still (in 2024) being iterated with ASN. The analysis of the event is not complete and does not address all the conditions in the structural design criteria.

Fluid

The release of the entire helium inventory of the coils (20t) would eventually warm up and over pressurise first the cryostat and then the building. Vents would open which prevents containment uncontrolled failure but will release radioactive products. This is prevented by a set of (safety class) isolation valves that subdivide the helium circuits into units of less than 800kg. These are fired in the case of a helium leak in the cryostat or a TF fast discharge (which expels helium from the TF coils into collection tanks outside the building). The vent pipes leading from the CTBs through the building to the helium collection tanks are also safety class.

However, following the Fukushima earthquake in 2011, these isolation valves were designated as HCC (Hard Core Components) which had to be demonstrated as robust (both functionality and containment) in the event of an SL3 earthquake, taken as 1.5 times the magnitude of the standard SL2. Further, the entire magnet system was defined as 'Aggressors' to the isolation valves which mean that it also must be robust to an SL3 event. At present (2024), this verification (by analysis and some testing) is not complete.

Electrical

The electrical safety, which involves the containment or extraction of the magnet stored energy, is the most difficult part of the magnet safety case. It is further complicated because uncontrolled release of the magnetic energy can also create structural and/or fluid incidents. It can be separated into two parts:

- Energy release following a superconductor quench and a failure to discharge.
- Direct breakdown of high voltage insulation in an arc.

The energy release following a failure to discharge after a quench is addressed by making the fast discharge system safety class, and by a safety class quench detection system for the TF coils. It was shown in analyses up to 2016 that for individual TF coils, or PF or CS, a failure to discharge a quenching coil result in up to about 3GJ of magnetic energy being deposited in the coil. This causes extensive local melting (also to the extent of melted steel damaging but probably not penetrating the outer VV shell) and the coil is damaged beyond repair, but the containment stays intact. Of more concern is a TF coil quench when none of the TF coils are discharged, which allows up to 40GJ to be deposited in the coil, sufficient to locally melt both VV shells. To prevent this, a TF safety class detection system is installed in each of the 9 TF CTBs. This detects quench by net outflow of helium from the coils. However, to prevent many false positives from normal operational transients, the response time is close to 10s. In this time the coil is irreparably damaged by local melting, but the majority of the magnetic energy is still extracted by the discharge system.

Electrical arcing has proved to be a major problem and is still (2024) being resolved. The coil bulk insulation is robust and turn to turn shorts do not result in large energy deposition. The problem is coil (or feeder) to ground failures, including those started from the high voltage wiring. The original defences against this (up to 2019) were that an arc required a simultaneous double ground fault in order for current to circulate and that this was highly unlikely since the coils were designed against the voltages to ground resulting from a single ground fault, and such arcs would not involve or produce molten metal near the VV. Five factors have disrupted this.

- The JT60SA and CSM3 arcing incidents demonstrated the role of Paschen breakdown in enabling arc initiation from weak insulation, if the vacuum is weak, starting from a single ground fault. The incidents demonstrated arc cascades and arcs propagating through structural components.

1. The high voltage wiring, especially where it exits from the coil insulation, is prone to cracking (with many repairs during manufacturing tests), and possibly fatigue with thermal cycles.
2. There is a lack of operational high voltage testing foreseen so incipient weaknesses will not be detected.
3. A re-assessment of TF coil arc propagation suggest that arcs could jump to (and from) the VV and involve 2 TF coils via the in-cryostat feeders.
4. There is a logical weakness in defining the room temperature busbars and fast discharge system as safety class when their direct continuations through to the in-cryostat superconducting busbars are not.

Safety level mitigations for these factors are possible but are not (in 2024) implemented. One possibility is to redesign the ground current monitoring to intrinsically limit the current through the ground. This prevents the generation of the electrical fault and eventual creatin of a second electrical fault. Such a modification has been successfully implemented in JT60SA after the arc incident and is under consideration for ITER implementation

6.1.7 Investment Protection

Investment protection is an area that has received little systematic attention in the ITER design and manufacturing phases but will be a critical issue once commissioning and operation starts, and management becomes directly responsible for assessment and consequences of the risks involved. Investment protection is the protection against faults that may develop during operation (essentially fatigue related), or protection against off normal operating conditions that could potentially cause a major interruption to operations or even an unrecoverable damage to the machine. Investment protection is notionally separated from safety in ITER but events leading to damage will certainly involve the regulator and the operational license, even if radiation releases are not an issue.

The main events are:

1. Quench of a conductor
2. Insulation faults (in HV wires or in the main ground insulation) as a result of fatigue or aging

- Conductor degradation in Nb_3Sn TF coils due to magnetic and thermal cycling

3. Fatigue crack growth in mechanical structures
4. Ratcheting movement of coils with plasma cycles leading to changes of load paths and unanticipated mechanical loads

These are quite separate from safety related incidents where we can generally show (or expect to be able to show) that the magnets are not safety relevant (i.e. do not pose a risk to radiation confinement) when backed up by some safety class protection systems. This protects against radiation release but does not protect the coil systems against irrecoverable damage. Some of these lifetime limits are specifically embedded in the design criteria (for example, tolerance to initial defects present in structures based on crack growth predictions) and some have been the subject of extensive simulations (such as quench detection and conductor degradation) but a holistic approach to lifetime accounting and verification on the actual components of the models on which functionality and lifetime predictions are based is still under development.

6.1.7.1 Quench

Quench detection in ITER to prevent conductor damage from overheating is based on voltage detection. In TF and CS systems a co-wound tape is used to balance the inductive voltages associated with pulsed plasma operation and detect the very low resistive voltages (typically in the CS 0.1-0.5V with inductive voltages of 10kV) which are associated with the early stages of a quench. The TF coils have lower applied voltages but are still coupled to the plasma current. The quench detection thresholds have to be tuned, and the tuning must be conservative, because obviously any error will damage the conductor, possibly irrecoverably. The risk is that the initiating events for a quench are not known and probably cannot be simulated, so a real verification test of the quench protection system is not possible. More attention is likely to be needed for this kind of verification for ITER operation.

6.1.7.2 Insulation Faults

One of the main sources of insulation faults (and arc initiators) is the high voltage wiring associated with the primary quench detection systems. These unavoidably require voltage taps to the conductor, and connections to co-wound tapes, which have to penetrate the coil ground insulation and provide the compensation to separate inductive voltages (which are large) from resistive voltages (which are small). These wire exits present a mechanically weak point (due to differential thermal contraction), a region of high electric fields (due to the ground planes) and a compatibility issue between the coil resins and the wire insulation. Now that manufacturing is complete, mitigation will have to consist of in-service monitoring and evaluation (and improvement) of repair procedures and in-cryostat access to implement them.

6.1.7.3 Conductor Degradation

The TF conductors in ITER are known to suffer degradation during operation due to progressive fracture of the Nb_3Sn filaments. This problem was identified in time to change the CS conductor to use a shorter twist pitch in the first stage, which completely avoids the problem, but TF conductor production started before this solution was identified. The mechanism is not fully understood but seems to be related to both the thermal compression due to differential contraction with the steel jacket, and the magnetic loads on individual strands. Each thermal cycle initiates a further degradation cycle with the magnetic loads, which eventually stabilises until the next thermal cycle. This means that warm-ups of the coils (to 300K and to a lesser extent to 80K) have to be treated as a scarce resource. Magnetic load cycles are less critical but similarly need to be monitored. Exceptional load cases (such as in single coil tests before assembly) similarly needed to be treated very cautiously. More details on the degradation are given in section 3.3.

6.1.7.4 Structural Fatigue

After manufacturing, it is not practically possible to carry out further NDT (which is mostly carried out on subcomponents when access is possible). However, three protection steps are possible:

1. Structural verification (and, probably, modification). The fatigue predictions rely on stress analysis and complex structural models such as are required for the ITER magnets rarely give good simulations of the measured behaviour without tuning.
2. Lifetime accounting according to the structural history.

3. Monitoring with instrumentation to detect possible changes that might be caused by load path changes. This is difficult as the structural instrumentation is not located (and cannot be) at critical potential crack growth locations.

These require a significant effort in commissioning, especially in achieving correspondence between modelling and reality, and in setting up a database of load conditions that can be regularly reproduced throughout the operational life. A development program for these items is underway in frame of PBS 55-GT-Tokamak Systems Monitor activities[10].

6.1.7.5 Conclusion

The most basic means to mitigate investment risk is testing of components, and in particular final acceptance tests on the coils. The ITER 2001 FDR reports included a discussion on magnet cold testing including a cold test cost estimate, for the TF coils and the CS. However cold test costs were not specifically included in the 2001 cost estimate that was used as the basis for ITER construction, nor were they specified within the year 2000 'procurement packages' sent to the home teams for them to provide the input used in the final project cost estimate. They were actually included as an item in the 2001 R&D budget (a lump sum included in the project costing as a contingency for technical uncertainties) but this was not included in the subsequent use of the R&D fund.

From 2007 on, the cold test discussion restarted. Within the ITER team, the magnets division pushed for implementation of cold tests (at a minimum at 4K and a few kA of current). However, the costs were disputed by the DAs and at the magnets level the best that could be achieved was to specify a cold test in all the coil Procurement Arrangements as an option to be decided in the future by the ITER Council. It was clear that any global strategy for cold testing (possibly with coil energisation) would require new funding from the stakeholders, and this did not look promising, regardless of the risks involved.

There were assorted working groups to look at cold testing from 2008-2010. These generally pointed out the risks of not doing full cold tests, but it was not possible to reach any compromise. Eventually a proposal was made to the IC for only thermal cycles to 80K on the coils, and for the TF only the first 3 from each of the supplying DAs (EU and JA). The IC resolution was obscurely worded regarding the PF and CC coils and was clarified by a PCR (PCR-522). The EU agreed to test all its TF coils (but only to 80K).

Separately from this, US implemented a powered 4K test for all its CS modules, as a final acceptance test to confirm the completion of the work of the industrial supplier (in this case GA).

The 80K thermal cycles were implemented. However, experience from the US CS tests (where several modules have seen failures and one has had a major arcing accident) and some high voltage failures of wiring following 80K thermal cycles highlighted the risks of expecting full performance on the first commissioning, in particular for the 6 JA TF coils that have not been thermally cycled by ITER in 2023

The risks associated with inadequate component testing have been well demonstrated during the period of the ITER manufacture by incidents in JT60SA and LHC. Neither of these destroyed the devices but, in each case, some 4 years were required for recovery (and this is yet to be fully achieved in JT60SA in 2024). The two incidents had some commonality, occurring during commissioning because of inadequate testing during assembly, probably as a result of schedule pressure. ITER itself, in the full power testing of the CS modules at GA from 2019 to 2024 has experienced multiple faults in the coil operation, mostly within the facility but at the coil-facility interface. Some 75% of the module tests have been interrupted by unforeseen events (ie 5 tests out of 7) and one module has been more or less irreparably damaged.

The ITER project has eventually recognised the risks and is constructing a Magnet Coils Test Bench (MCTB) at the ITER site aiming to test as up to 4 TF coils at 4.5 K[11]. However, the assembly schedule (and the need to place TF coils in the cryostat) does not permit for full testing, except for the spare TF coil. STAC 25 (May 2025) has finally expressed some concern '*The STAC finds that although the schedule constraints are understood, the proposed test plan is suboptimal in terms of superconducting magnet performance risk reduction, in comparison to a more extensive program testing all coils at full current*'. The MCTB will, however, provide valuable design qualification if not a full manufacturing quality verification.

6.1.8 Manufacturing

The magnet PAs were divided into 6 separate packages, often with DA sharing (as agreed in the 2005 site negotiation):

1. Toroidal Field (TF) Coils
2. Structures (TF and CS)
3. Poloidal Field (PF) Coils and Correction Coils (CC)
4. Central Solenoid (CS)
5. Feeders
6. Conductor

Instrumentation was a direct ITER contract procurement.

The problem in the subdivision of the supply is that it took no notice of the technical needs of the project.

- Many technical interfaces were created without a technical specification being available (a good example is the TF structures to fit the TF windings) and changes had to be negotiated later, almost always at great length.

- Many unnecessary fabrication facilities and tooling were set up, often by inexperienced industries which had to be supported by IO staff and consultants (some descriptions of this are given in later sections).
- There was a tendency with a mix of experienced and inexperienced suppliers, especially initially, that we were pushed to the 'lowest common factor' in technical requirements and quality.

6.1.8.1 Conductor Manufacturing

6.1.8.1.1 Strategy

The Procurement Arrangements for the ITER TF Conductors were the first to be signed, starting in December 2007. The background at this time was:

- ITER had a small but experienced internal manufacturing team for the conductor, with experience from the TF and CS model coil projects summarised above.
- In the period 2002-2006 the IO team prepared detailed procurement technical specifications for the 3 parts of the conductor (Nb_3Sn strand, cabling and jacketing).
- The design changes during this time (primarily a reduction in the Nb_3Sn strand quantity by reduction in margins) were agreed with the Domestic Agencies. Initially these were the original 4 (US, RF, JA, EU) but CN and KO became involved from 2003, and the conductors were seen as an area of technical importance, with technical support from IO. They in turn involved their national suppliers in strand development.

So, by 2007, ITER had a reasonably well-informed distributed conductor technical team and a good range of potential suppliers.

In 2006, the ITER procurement distribution was agreed, and there were 6 DAs wanting to provide conductor (from 7% to 25% of the total supply). This pre-allocation of course prevented us from normal competitive tendering since every national supplier was guaranteed their national slice, at least in theory.

However, the multiple DAs involvement allowed us some 'levers' that we could exploit:

- For the conductor, where we were dealing with large scale standard production, we encouraged unofficial inter-DA cost sharing which allowed price competition and to assist this we asked DAs to place contracts in steps with new offers for each step. Even with one sole DA supplier, awareness of international prices pushed down national bids.
- Some examples of cross-DA procurements to save costs were KO contracted jacketing to EU, US jacketing failed so they contracted to KO who contracted to EU. Furthermore, part of the EU strand supply was produced in the US by subsidiaries of EU companies.

6.1.8.1.2 ITER Strand and Conductor Supply Implementation

The development of Nb_3Sn towards its application for fusion started in the 1980s, and the material was soon adopted as a core material for NET and, subsequently, ITER, TF and CS coils. The alternative, NbTi cooled to 1.8K, was discarded because of the limited nuclear heat removal capability and because of the problems of using solid high voltage insulation which requires a flow of superfluid helium.

The material went through 3 major development stages:

1. The ITER model coils provided the first real test of industrial capability in the 1990s, with the supply of ~30t of Nb_3Sn from some five suppliers. The supply was challenging, with several years of delay and one failure (Teledyne Wah Chang and the jelly-roll technique), although ultimately highly successful.
2. By 2002, there had been a marked improvement in Nb_3Sn performance since the model coil contracts were placed in 1993, and this improvement was included in the design. The baseline 'bronze route' critical current was taken as 700 Amm^{-2} (compared to 550 Amm^{-2} in 1993), and for 'internal tin' as 800 Amm^{-2} (compared to 650 A·mm^{-2} in 1993). These values could be achieved by a wide range of suppliers in EU, JA, RF and US. To ensure an adequate production rate and to maintain cost competition, the ITER conductor design kept the strand supply accessible to both internal tin and bronze route manufacturers (since, for the time being, the bronze route dominates the production capability). These requirements were kept although by 2012 Nb_3Sn critical currents of >2000Amm^{-2} were being achieved (now over 2500Amm^{-2}) by one supplier, Figure 6.1-46.

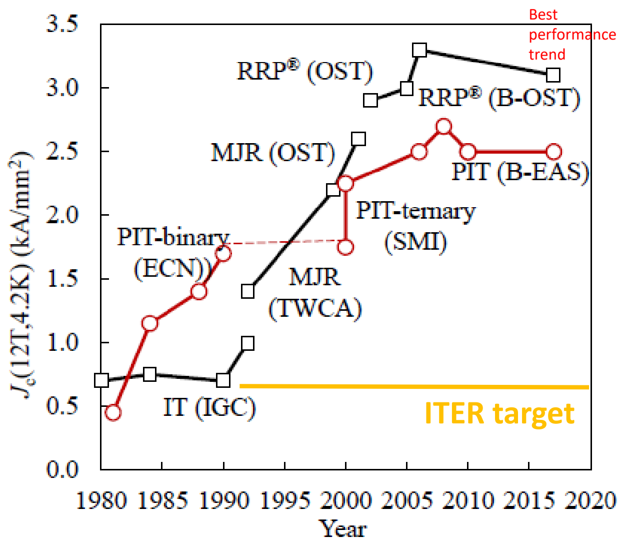

Fig. 6.1-46: Nb_3Sn Technology for High Field Accelerator Magnets (acknowledgement Alexander V Zlobin (Fermilab)).

3. Nb_3Sn was, nevertheless, essentially still a research material at the start of ITER construction in 2006, with a yearly global production of <20t and wide variability in the strand layouts and usage requirements (i.e. heat treatment of the tin/Nb elements to form the superconducting Nb_3Sn compound), as well as in manufacturing yield (unit lengths of more than a few hundred meters being a problem). A major achievement of the early part of the construction activity after 2008 was to establish convergence of the different strand layouts, to stabilize manufacturing and to improve quality controls, resulting in greatly improved yields and allowing a ramping up of the supply rate to ~100 t/year by 2011 as described below, Figure 6.1-48 and Figure 6.1-49.

In 2007, ITER wrote (and, more difficult, got agreement with them) a common procurement contract for all 6 DA suppliers. In this, the supply to ITER was at the level of completed (jacketed) conductor to minimise interface issues. The DAs chose to split the procurement variously as:

- Strand or strand plus cabling.
- Jacketing, or cabling plus jacketing and jacket material supply.

The strand was procured to a functional specification with tight requirements (diameter, jc, Cu to non-Cu ratio etc) but allowing different Nb_3Sn manufacturing methods to be used (especially bronze and internal tin routes), Figure 6.1-47. Broadly strand and cabling used existing plant (sometimes extra capacity was added), and the jacketing required a specially developed facility.

We used a review committee of eminent strand & conductor personages to supress DA argument about toughness of requirements (this worked well) and our assessments of the state of the art of industrial capabilities. We staged the work with strict QC and cross-checks, standardised measurements, strand performance, unit lengths, maximum rejection rates and so on. We could not control costs, but we could ensure that suppliers delivered value-for-money and the sanction of loss of contract if they could not perform, forcing DAs to turn to other non-national options.

6 procurement arrangements for the Nb_3Sn TF conductors were signed in 2008. The DAs then placed their contracts, exactly matching the IO procurement arrangement technical specification.

In the early stages (2009 & 10), IO provided much support to suppliers. Internal experience on cabling and jacketing was critical (some of the ITER team had experience of the CS and TF MC conductor production) and especially on cabling, achievement of low void fractions and different twist pitch combinations, Figure 6.1-51.

ITER ended up with some unnecessary duplication of the conductor jacketing lines (4, in Italy, Russia, China and Japan plus one in US that failed).

The TF Nb_3Sn jacketing lines were also used for the CS Nb_3Sn conductor (in Japan), for the PF NbTi conductor (Italy and China) and for the CC and feeder NbTi conductors (China).

The jacket itself was procured in lengths of seamless tube which were butt welded together. The Nb_3Sn tube required a very low carbon content to avoid embrittlement during the Nb_3Sn heat treatment. Suppliers included Jiuli in China, POSCO in Korea, and KST in Japan. The qualification of the material required a test program and several iterations on the tube composition and extent of compaction onto the cable (cold work increases the tendency to embrittlement).

The NbTi strands, used in the PF and CC coils and the feeders, were a much more standard industrial production. A typical strand is shown in Figure 6.1-50. There were variations in Cu to non-Cu ratio to match the application. The NbTi supply was ultimately provided by RF (ChMP) and CN (WST).

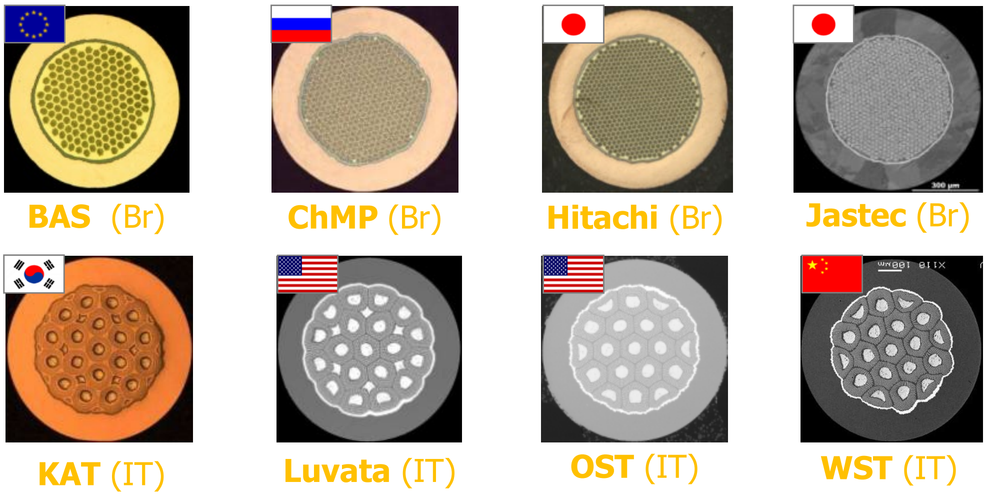

Fig. 6.1-47: Various Nb_3Sn strand types used in ITER.

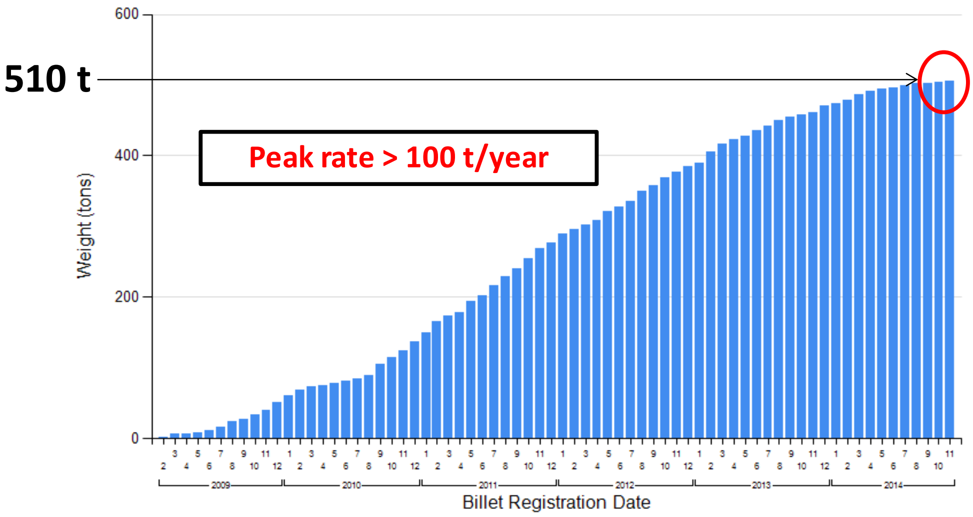

Fig. 6.1-48: ITER TF Conductor Strand Supply Rate.

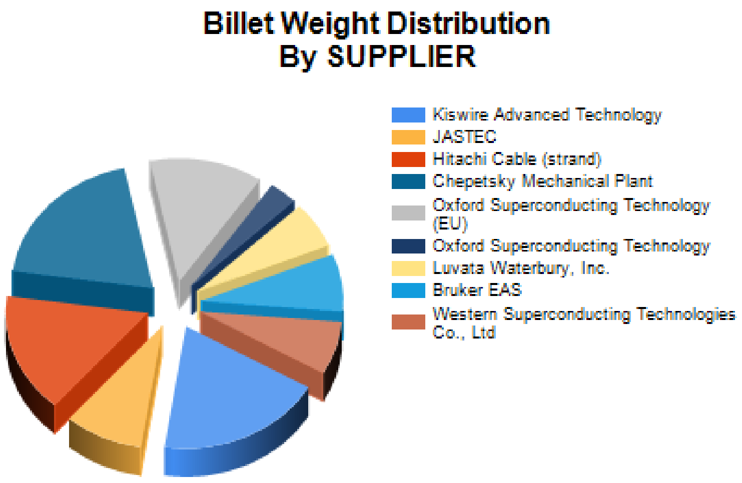

Fig. 6.1-49: Supplier Shares of Strand.

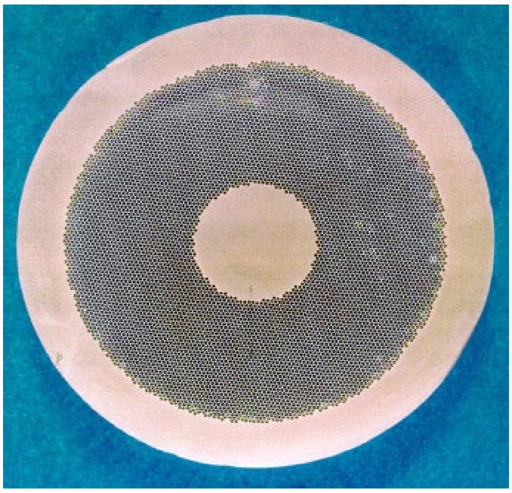

Fig. 6.1-50: NbTi Strand.

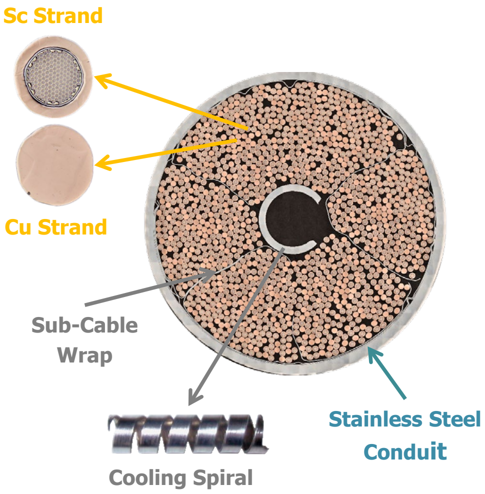

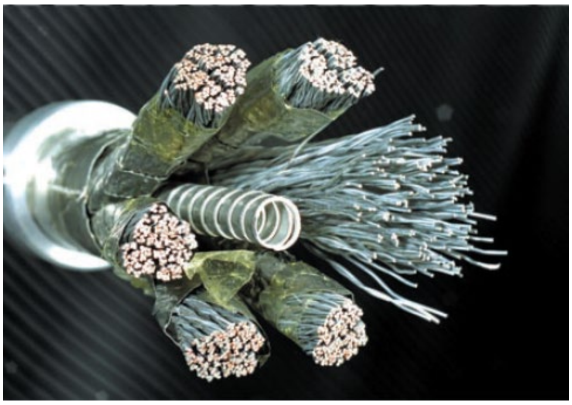

Fig. 6.1-51: ITER TF Conductor.

6.1.8.2 TF System Manufacturing

The TF Coils were supplied by Japan (9 coils) and Europe (10 coils, one of which was originally the spare). The TF structures (the cases) were provided by Japan but under an agreement that was part of the basis for the selection of Cadarache as the ITER construction site, EU agreed to pay for 9 of the cases in Japan. This agreement took several years to negotiate and delayed the start of the EU-funded part of the supply, although the impact was reduced since the JA-funded parts were supplied also to the first EU coils.

EU and JA both carried out tenders for the TF coil supply.

EU separated the supply of the coils into 3 packages:

1. Radial plates.
2. Winding pack (winding the conductor, heat treatment, insertion into the plates, stacking of double pancakes).
3. 80K thermal cycle on each winding pack and the casing operation.

The logic was that the radial plates could be defined quickly, and the delivery would be critical to the schedule. Manufacture went on in parallel with the preparation of the winding line buildings and tooling.

- The radial plates, Figure 6.1-52, were divided between CNIM and SIMIC. EUDA financed a gantry milling machine at SIMIC to guarantee the tolerances on the final plates.
- For the winding, after a call for an expression of interest, 4 suppliers were invited to tender and then after some negotiations and adjustment of the members, the winding

packs went to a consortium of Elytt Energy and ASG. ASG converted a special factory at La Spezia for the work (which took some 3 years, during which time radial plate and conductor manufacturing was ongoing). The site was close to La Spezia harbour to allow delivery by ship of radial plates and shipping out of complete TF winding packs, Figure 6.1-53 and Figure 6.1-54.

- The cold cycle test and casing operations went to SIMIC, at their site at Maghera (with sea access). This contract experienced long delays due to the late supply of the cases from Japan (or the sub-contractor in Korea), and a number of quality issues (non-conforming tolerances) were found on delivery of the KO/JA components, requiring repair.

Fig. 6.1-52: Radial Plate After Completion.

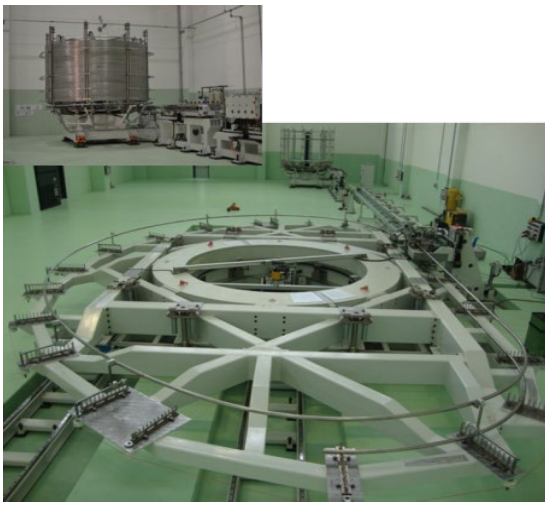

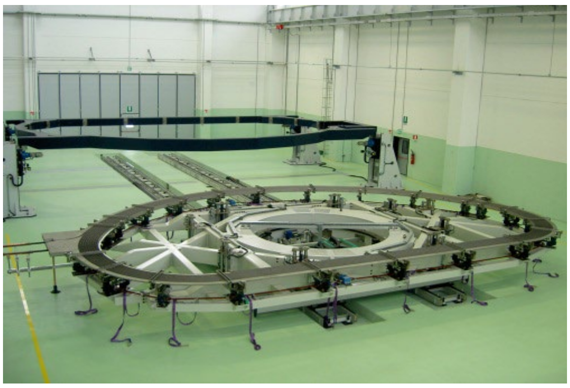

Fig. 6.1-53: TF Winding Underway at ASG.

Fig. 6.1-54: Completed TF Winding Pack.

JA-DA went through several iterations on the TF coil winding. An initial contract (for winding development) was tendered (between Toshiba and MHI) and was awarded exclusively to Toshiba. After development of a winding machine this contract was stopped as the winding machine had performance problems. In parallel, a contract for R&D into routes to make the radial plates was placed with IHI and stopped at an early stage. JA-DA then tendered the first full TF coil as a single element, and this was awarded to MHI (and Mitsubishi Electric). All know-how was transferred from Toshiba and IHI to MHI/ME. JADA then tendered successive coils individually and in the end 4 were awarded to Toshiba and 5 to MHI/ME. In manufacturing radial plates, the route pioneered by EU was followed (machining of sub sections from forged plates and then joining by welding) and several sub suppliers were involved including IHI. Later (in 2018) to recover delays in delivery dates to ITER, the spare TF coil was re-allocated to Japan who, therefore, provided 8 of the TF coils installed in ITER. The recovery attempt was inefficient because the VV had major technical issues both in the 1/9 sector supply and in the assembly procedure and will need some 10 years more than the TF coils for completion.

Regarding the fabrication procedure:

- ASG/Elytt set up the most sophisticated production line (Figure 6.1-53) with many operations done with advanced tooling and robotics. In terms of capacity and schedule, all 19 coils could have been made in the facility.
- MHI set up a partially automated line, for conductor winding and insertion into the radial plates. However, many operations were still by hand.
- Toshiba made the least investment in automated tooling and much of the winding manufacture was with hand tools.

In all 3 cases the winding was successful, with no major issues.

The structures (the TF coil cases) were complicated by the host site agreement, where EU agreed to pay for the 10 cases used by EU to be made in Japan. The initial PA for 9 sets of structures was placed in 2011, but it required 4 years of negotiations between JA-DA and EU-DA before the remaining 9 could be placed. The issue was as usual that the case sections cost far more than the notional ITER credit award for them, and EU-DA did not agree to pay the real price. Finally, EU-DA paid the ITER credit value but in return agreed to supply additional heating systems for JT60SA.

Once agreed, MHI subcontracted a significant part of the major assembly work to HHI in Korea (HHI were also manufacturing 3 of the VV sections, 2 of them re-assigned from EU-DA). Many sub suppliers were also engaged in Japan including IHI and KHI. A large fraction (>75% by weight) of the 316LN forgings for the case sections were subcontracted to Kind, in Germany. Pictures of the segments under fabrication are shown in section 10.

HHI had limited experience in high accuracy stainless steel structure manufacture and was already stretched by the VV manufacture for KO and EU. HHI also subcontracted to inexperienced local sub suppliers for machining work where there were further issues with tolerance control. ITER, EU-DA and JA-DA provided extensive support to HHI including purchase of a climate-controlled environment for final machining work. Under pressure from ITER, MHI received the 4 major structural units (from themselves or HHI) and did a fitting trial before shipping them.

Further issues on the structures (solved with ITER support) were the attachment of cooling pipes to the inside of the case sub-sections and the filling of the gap between the winding pack and the case once the case was welded closed. ITER developed a resin for the cooling pipe attachment, but JA-DA were reluctant to use it (especially as MHI did not at first properly mix it). After attempts to provide a metallic link to the pipes, JA-DA adopted the resin. The gap filling resin gave rise to concerns about crumbling with load cycles and EU-DA and JA-DA provided a glass wrap on the winding surface to reinforce it. The outer surface of the winding pack was coated with a debonding agent.

The supports (TF Gravity Supports, PF clamps and supports, CC supports) were supplied by CN-DA. The overall supply was allocated to SWIP who generally subcontracted to a range of industrial suppliers, HTXL, WHM and DFHM being the main ones. Figure 6.1-55 shows completed TFGS at HTXL.

Fig. 6.1-55: Completed TFGS Gravity Supports (right) and PF Supports (left)

The TFGS were qualified by a mock-up at SWIP and in advance of this, the design was modified from machined/welded plates to a stack compressed by tie rods. There were modifications to the cooling of the PF clamps. Apart from some industrial quality problems, there were no major issues. The most notable quality problem was the failure of one of the pre-loaded studs bolting the TFGS to the cryostat ring, about 1 month after installation. There had clearly been a manufacturing process failure (as well as an inspection failure), but the precise circumstances could not be established by ITER. As well as the failed bolt, a subsequent in situ inspection in the cryostat found 3 others of doubtful quality that were replaced.

The final part of the structures, the Pre-Compression Rings, were provided by EU-DA (although the flanges pulling on the inside of the ring were provided under the structures procurement by MHI). The original trials on the PCRs were carried out in 2004-7 by EU home team and ENEA as a voluntary activity, with construction of a test machine to test 1/5 scale rings made by winding uniaxial bundles of glass fibres.

However, the winding process for a 1/5 scale ring was slow, several months for a glass volume 1/800 of that of the final ring. No industrial offers could be found by EU-DA to manufacture the full-sized rings on this basis, especially with concerns about the stability of the ring shape and the effectiveness of the resin transfer process in a large cross-section (neither VPI nor wet winding seemed satisfactory for a large cross-section).

The next step by EU-DA was to try a process adapted from the aerospace industry, advance fibre placement. This achieved a reasonable rate of winding but the glass fibre (in the form of tape 'tows') was positionally unstable and the properties showed a severe degradation.

The final step was to move to a two-step process. A strip of glass fibres was extruded by a pultrusion process in a cured form and then wound into a ring, with bonding between the strips. This achieved a reasonable manufacturing time and quality and full-size tests confirmed the performance.

The original Procurement Arrangement with F4E was for 9 rings (6 installed, 3 spare stored below the machine). During final production, IO purchased a tenth ring through F4E to act as a spare for the top PCRs.

To confirm the performance of the rings, ITER constructed a full-scale test facility at CNIM (who were also winding the PCRs) and all 10 rings successfully went through a proof test, Figure 6.1-56.

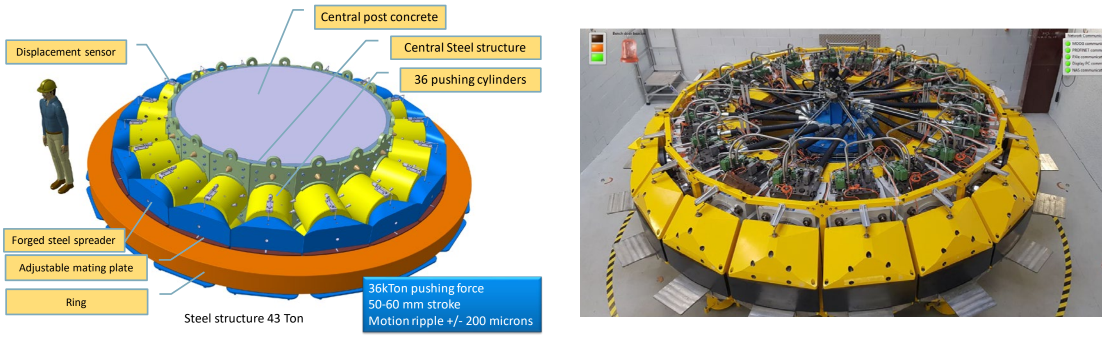

Fig. 6.1-56: Full Size Test Facility Concept Design and Final Configuration.

6.1.8.3 PF System Manufacturing

The 5 largest PF coils were (since 2001) intended to be wound on site and for this purpose a PF winding building was provided by the host and allocated to the DA undertaking the PF coil winding (EU-DA). The smallest PF coil PF1 was compatible with the road transport from Fos to the site and was allocated to RF-DA.

The original PF coil design was based on NbTi conductors, included a spare double pancake for the unreplaceable coils (P2-P6) together with a pre-installed jumper system and externally accessible double pancake to double pancake joints to allow a faulted double pancake to be bridged. In the 2001 design each conductor was surrounded by a metallic screen outside the turn insulation, mimicking the radial plates of the TF coils. This was dropped (via PCR-103) in 2007, see section 2.3.1. The space occupied by this metal screen was replaced by insulation to avoid a more compact winding pack since this would have increased the field.

A further modification occurred in 2019 (via a PCR) to eliminate the pre-installed jumpers on the coils for bridging failed double pancakes. These instead are delivered separately and stored in case of need, being then transported into the cryostat through a side port (see also section 2.3.1).

Some of the PF coil positions and number of turns were adjusted (via PCR-164) in 2008. There was discussion during the ITER design review of 2007 about the need to make PF6 a Nb3Sn coil. This was rejected and it was noted that subcooling PF6 to 3.9K would ensure the necessary margin.

The PF building on the ITER site was completed in 2011 but was not occupied by EU-DA until 2013. EU-DA initially tried to tender the entire PF fabrication as a single package. No financially acceptable offers were received. EU-DA then subdivided the package into 7 subpackages, one of them being an engineering coordinator, and asked for tenders separately. This resulted in an acceptable overall price. However, by this time the delay meant that it was no longer possible to make all the coils on schedule due to space limitations within the PF building (preventing in parallel working). EU-DA, therefore, subcontracted PF6 to ASIPP in China. This in turn meant that the road route from Fos to the ITER site had to be widened due to the size of PF6. The widening work included removal of a cliff bordering the road near St Paul-Lez-Durance in 2016-17. This widening also allowed the TF coils to be transported flat, rather than at an angle as was originally planned (vastly simplifying the transport frames). The main contractors for the on-site PF coils were initially ASG as engineering coordinator, CNIM for the winding execution and Sea Alp for the tooling. This arrangement (with its multiple interfaces) was not found satisfactory and ASG took over the full manufacturing in 2020.

The PF2-5 winding was carried out at the Cadarache site without major issues, Figure 6.1-57. The PF6 coil had major issues to pass the high voltage test at ASIPP in China after completion of the coil, with many Paschen breakdowns. These were solved by reworking some local insulation around interpancake joints and at helium inlets, repairing missing ground coatings on the outside of the coil and replacing some HV wire exits. No significant non-conformities were reported for the PF1 coil, fabricated by the Efremov Institute at St Petersburg.

Fig. 6.1-57: PF Coil Manufacturing Underway at ITER Site, PF5 (far left), PF2 (left middle), test cryostat (empty, right middle), PF6 (far right).

The clamps for the PF coils were supplied by CN-DA. The overall supply was allocated to SWIP who generally subcontracted to a range of industrial suppliers, HTXL, WHM and DFHM being the main ones. The large clamps for the sliding supports of the PF1 and 6 coils were forged plates with cooling channels in the plate made by gun drilling. The flexible supports for the P2-P5 coils were produced by water jet cutting of the flexible ligaments, avoiding the risk of welding in high stress regions.

Fig. 6.1-58: PF Structures (flexible supports) Under Manufacture at HTXL.

6.1.8.4 CS System Manufacture

The CS procurement was agreed with US-DA in 2005 but went through several iterations before a procurement arrangement could be signed. During this, the DA supervision was moved from MIT to the US-DA based at Oak Ridge, and the US decided to outsource the whole project to General Atomics in San Diego. GA insisted on design freedom within pre-defined and stable constraints and a functional PA was, therefore, agreed. This not only allowed design freedom but froze interfaces to the rest of the machine by creating an individual SRD that in effect could not be updated. US-DA also refused to participate in the ITER non-conformance management procedures and especially in standardisation attempts by ITER QA division. The object here was to decouple the supplier from the anticipated bureaucracy of the ITER project but it also meant that ITER had little control over the manufacturing processes and quality. To give a clear end point to the US deliveries, a powered cold test was required for each module.

GA at the start of the PA had little coil winding experience and recruited support from MIT and from the US suppliers (LM) and Institutes (LLNL) involved in the CS model coil production from 10 years before.

A number of interface issues had to be iterated:

- The CS hangs from the TF coils and the main support was shifted from the top of the TF coils to the bottom (the top support proved to be incompatible with the CS assembly from above into the bore of the TF), PCR-168, in 2009.
- The details of the connections of the busbar extensions (Nb_3Sn high field busbars that extend down the outside of the CS and are within the US supply) to the ITER NbTi busbars at top and bottom, especially the mechanical support.

A new factory (converted from existing building) was set up by GA. Development of the tooling and its qualification proceeded without major issues and the equipment for insulating the reacted Nb_3Sn hexapancakes was particularly impressive, Figure 6.1-59. Substantial problems were found with the dummy module and the HV tests of the quench detection wiring. Multiple faults developed, probably because of cascade breakdowns, and finally the wiring system was fully revised in agreement with ITER (the problem was an attempt to allow two options for a quench detection system to be implemented) reducing the number of HV wires by a factor of ~2.

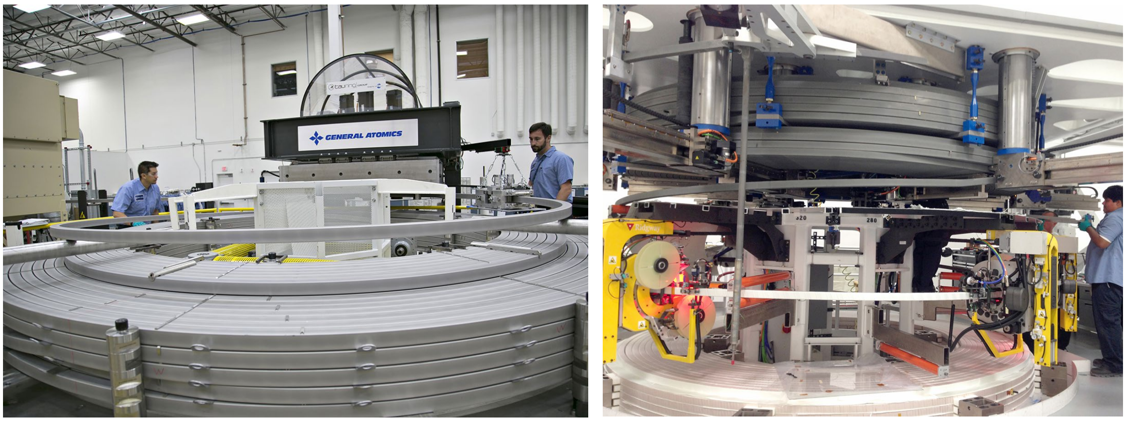

Fig. 6.1-59: Elements of the CS Winding Line (left), insulation after heat treatment (right)

The CS structures were produced through several GA subcontracts. The main elements are the inner and outer tie plates and the upper and lower key blocks, Fig 9-15.

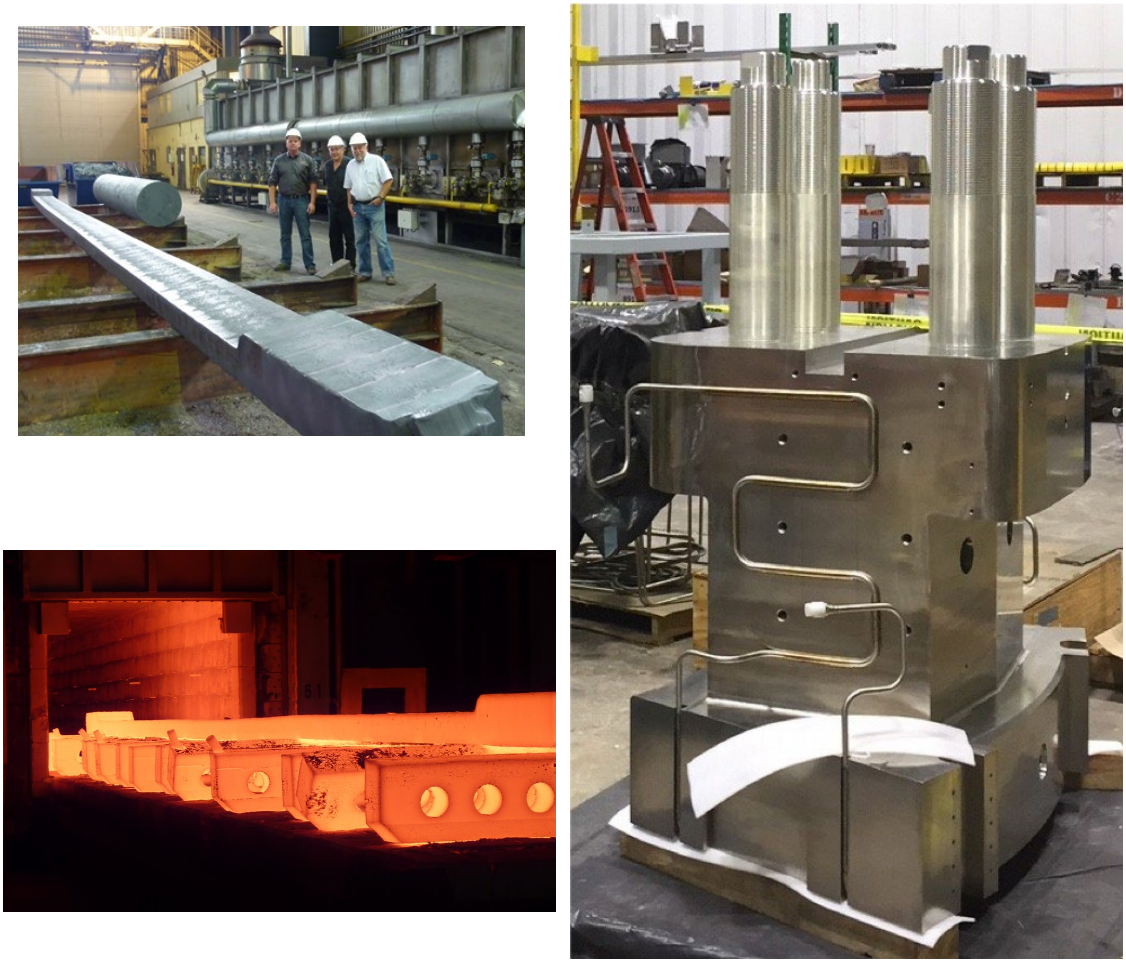

Fig. 6.1-60: CS Structures (Tie Rod, upper and Upper Keyblock lower).

The module testing created many issues, mostly linked to problems with the test facility. There have been 3 major issues:

- Collapse of the thermal shield due to eddy currents in fast discharge.
- Melting of a vacuum circuit breaker due to failure to open.
- Partial melting of a coil due to Paschen breakdown at the facility side of the supply busbar (Figure 6.1-61).

Overall, the CS module production itself included some major quality issues. This appears to be more than in any other PA except possibly the feeders, but this may result from the inclusion of a full power test in the factory acceptance tests which enabled measurements to be performed that have not yet been made on other coils.

- Several HV wire exit failures and rework after failure of a HV test. Some of these occurred after the final cold test and by 2024 there was a reluctance by US-DA and GA to investigate the root causes given the advanced manufacturing status. Such failures were repaired individually and passed the required acceptance test, but some appear linked to the manufacturing design and potentially exist elsewhere, possibly re-appearing in operation after more load cycles.
- Measurement of an unexpectedly low vertical elastic modulus of the modules (close to half the expected value). This is not a technical issue on its own but required a change in the pre-compression structure.

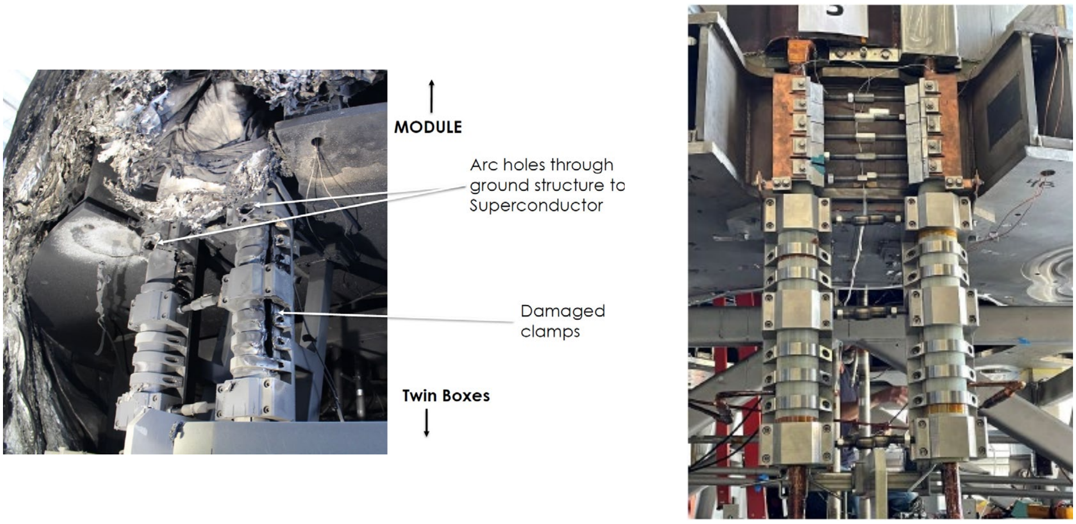

Fig. 6.1-61: Arc damage to a CS module (right, undamaged).

Overall, these quality problems which appeared at the final powered cold test do not appear to be a particular issue with the manufacturer but are perhaps related to the first-of-a-kind. This gives rise to some concerns about what can be expected during ITER commissioning when untested coils are operated in an untested facility.

6.1.8.5 Correction Coil System Manufacture

The correction coils appear in the 1998 version of the ITER design but as 16 coils (spanning 90° segments). This was increased to 18 coils in the 2001 FDR, spanning 60° segments. The correction coils since 2001 have undergone a series of minor adjustments in location, driven by their position between the PF and TF coils.

The main issues/changes since 2001 have been:

- Elimination of resistive wall mode control as a possible requirement (allowing a much-reduced AC specification for the conductor). This was linked to the inclusion (or not) of in-vessel coils.
- Linking the CC current capacity to a range of tolerances on the coil systems (from 2006 onwards).
- A major redesign of the side CC support system in 2014. The CC coils are largely loaded by the displacements of the TF coils, and a full analysis was not performed until 2013. The design (and manufacturing procedures) was reviewed in 2016 through a series of deviation requests.
- Repositioning of the insulated flange within the case.

The procurement arrangement was signed with CN-DA in 2010, and CN-DA contracted the work to ASIPP. ASIPP carried out the coil fabrication within the institute but set up a winding and casing facility near to the Institute. There were some development issues especially on forming the helium inlets to the conductor and on welding of the winding pack into the case, Figure 6.1-62, and some quality problems with the manufacture of the terminal service boxes. The lower coils are already parked at the bottom of the cryostat since 2021.

The CC supports were part of the overall magnet supports that were contracted to SWIP who in turn contracted them to a range of suppliers. The SCC supports had to be revised in 2013-14 since they provide bridges between TF coils and require careful control of compliances and gaps. Thermal intercepts are implemented at the supports to restrict heat transfer from the TF cases. These are copper plates with a brazed cooling pipe which have cause many manufacturing issues (due to the brazing technology).

Fig. 6.1-62: Bottom correction coil, case closure welding.

6.1.8.6 Feeder and Instrumentation System Manufacturing

The feeders and instrumentation in 2001 were the most immature of the ITER magnet components. There were only conceptual drawings, and almost no supporting analysis (other than hand calculations done for the original design). One exception was the current leads which were updated to use HTS superconductor as a design basis in 2005 (although without a baseline concept design), see section 2.6.1. There was little revision of the feeder design drawings between 2001 and 2007, and it was not possible to produce the first dedicated feeder DDD until late in 2009 and the first instrumentation DDD in late 2010. The feeder DDD has not been updated (along with the majority of the magnet DDDs) since this time, the Instrumentation has undergone regular updates almost yearly. A further problem now is that many feeder design changes have been implemented through deviation requests with ASIPP and it is now very difficult to get an overview.

In this situation, once ITER signed the Procurement Arrangement with CN-DA (and they had subcontracted it to ASIPP) in 2010, we had what was close to a functional specification and a major design work was started with ASIPP, some supported by CN-DA but much of it through ITER cash contracts. This resulted in the production of manufacturing drawings and basic analysis over the next 2-3 years from 2010. In parallel ASIPP engaged two suppliers spun out of ASIPP (Keye and Juneng) who constructed factories near ASIPP and started tooling procurement.

ITER provided technical support in some areas. The HTS current leads were designed by CERN (under the CERN-ITER collaboration) and ASIPP staff were trained in CERN workshops. The feeder conductors and joints were manufactured with extensive IO support at the workshop level. The feeder insulation (a prepreg interleaved with polyimide) was identified after a qualification program defined by ITER staff (of course, implemented successfully by ASIPP).

The rush to produce the detailed design led to many changes as the interior of the cryostat was designed in detail. Some of these are described below. It is a feature of the feeder PCRs that they bundled together several (or many) changes (sometimes retrospectively) and the situation is more fluid than appears at first sight.

Changes implemented by PCR-245 in 2010 were:

- The instrumentation satellites which were needed to provide space for the HV cable feedthroughs (this has proved to be a major complexity in implementing the HV cable electrical feedthroughs and the cable plugs which seal the cryostat vacuum).
- General position adjustments of the feeders.
- Location of CTB+S-Bend to Cryostat vacuum barrier re-located to CFT.

Changes not implemented in 2010 but later through DRs before 2013 were:

- TF-ICF delivered in basic plates, conductors and pipes to be build up inside the cryostat. This change is now (2024) being reversed as the tolerance requirement on alignment of the conductor supports is not achievable, and a pre-fabrication route will be implemented.
- The separate CTB and S-Bend boxes were joined.

PCR-315 introduced more feeder changes, inside the cryostat and including the feeder-cryostat wall bellows, in 2012.

A major PCR-445, for a new cryostat support system was introduced in 2013. This was a response to the review of nuclear reactor support systems following the Fukushima earthquake in 2011. As a result, the crown ring was re-designed. This had many impacts on the feeders (and of course on their assembly) with the largest being on the PF4 CFT, which then had to be embedded in the concrete of the crown ring.

In the original feeder concept, and up to 2015, the feeders at L3 formed part of a nuclear containment barrier to the upper pipe chase (containing the Tokamak Cooling Water Supply pipes, referred to as the pipe chase water barrier. This consisted of a barrier with bellows, sealing to the CFT through a circular penetration in the middle and a seal to the CFT bioshield port on the outside. The actual PCR that removed this requirement cannot be specifically identified (probably because the water containment barrier was improperly allocated to the feeders in 2010) but it could be PCR-662. ASIPP carried out the development and qualification of this barrier, completing it just as it was removed.

Changes (mostly through DRs) continued after 2015. One major one (done by DR) was the relocation of the cable feedthroughs and plugs (sealing the cryostat vacuum from the CTB vacuum) to the inside of the Satellites, with a long tube surrounding the cables in their path through the CTB. The reasons for this were (1) a need to provide access to install the plugs around the cables (2) a lack of functionality of the plugs at 4K (the satellites are at room temperature). This extends the cryostat vacuum to outside the bio shield, without apparently causing any safety concerns (the cryostat is anyway not a nuclear containment barrier).

A PCR was implemented in 2020, PCR-001020, to retrospectively approve a collection of changes to the In-Cryostat Feeder supports. A further one followed also in 2020 to segment the TCC circumferential in cryostat feeder to allow its installation. More regularisation of design changes is ongoing with PCR-001542 in 2024.

One major lesson from all this is not just that a more robust configuration management is needed, but that high technology non-nuclear but critical components should be placed in locations where they are more protected from interfaces with the nuclear ones, and should be more developed with the basic machine design (and not added as an afterthought). The side access of the feeders, and the distribution on 2 levels, projecting into the galleries, and their reliance on the (moving) coils for support, guarantees an impact every time the basic machine is adjusted. The structure of the feeders, with multiple subcomponents and much in-cryostat assembly, also seems likely to dominate some part of the assembly and is difficult to carry out in parallel with other work.

Despite the iterations the feeder manufacture is almost complete, and the components are mostly on site, Figure 6.1-63, 19 & 20.

Fig. 6.1-63: Feeder Component Manufacture Ongoing (left, S-bends, middle CTB internal pipes and current leads, right completed CTP.

Fig. 6.1-64: Left, vacuum barrier assembly in CFT, right FAT on PF4 CFT.

Fig. 6.1-65: Correction Coil in Cryostat Feeder.

The instrumentation is being procured directly by ITER. The original list of instrumentation is given in the 2001 magnets DDD (within the Magnet Procurement Packages, Annex 5), as shown above in the Tables 6.1-1 and 6.1-2 compared with 2020. The changes were partly authorised by PCR-567 in 2015 (at which point the resources for the instrumentation were doubled) but there is no scope control on the instrumentation and likely further increases have occurred. A further concern is that each individual sensor or cable has to be installed and then commissioned, and generally twice as many sensors require either twice the number of people, or twice the time. Assembly and commissioning were not considered as the sensor numbers were increased.

Many other HV related components are missing from the 2001 list, in particular the splicing devices (connecting wires to cables inside the cryostat), the current lead heaters and the HV feedthroughs from the satellites. For low voltage, fibre optics are now used extensively (which accounts for the reduction).

ITER purchased all the HV wires and cables from 2015 on (original installation was scheduled in 2022) but now they are not able to be installed in the cryostat until the early 2030s. A similar situation has occurred with low voltage instrumentation, such as temperature sensors and strain gauges. The consequences on the calibration of this equipment after storage at room temperature for 15 years, taking it well beyond any warranty period, is not known. Some defects have been found in high voltage cables during preservation inspections that were not present on delivery. This situation is still under investigation.

6.1.8.7 In-Vessel Coil System Manufacturing

After 2015, the IVC coil procurement was divided into packages and put out to tender by ITER. The contracts were staged, starting with the conductor in 2017, followed by the VS and ELM coils in 2020-2021 in two packages once the respective FDRs were completed, with the auxiliaries (feed throughs, insulating breaks, joints) in parallel with a further 3.

One of the main changes to the pre-2015 situation was to procure the conductor in unit lengths sufficient for the coils, eliminating internal joints. The procurement quantities are given in the Table 6.1-6 below and the conductor cross-section (copper and MgO insulation) in Figure 6.1-66.

Table 6.1-6: Conductors for the In Vessel Coils

Type of conductor	Length [m]	Reel Length [m]	No. of Reels
Spooled length,	2 600	70.0	26
		60.0	13
Spooled length,	2 050	100.0	10
		75.0	14
Straight lengths *	360 *	Unit length max 12m.)	

Initially two contracts were placed for Phase 1 development and qualification work, with ICAS (Italy) and ASIPP (China). Both successfully completed Phase 1 and on tendering for Phase 2, the production was awarded to ICAS. However, critical to the production was the extrusion of 80m lengths of copper tube (extending to 100m during the jacket & insulation compaction process). The ICAS sub-supplier for these lengths withdrew from the supply in 2019 (ICAS had not pre-ordered the full supply) and an alternative could not quickly be found (also not the ASIPP supplier). After about 2 years of negotiations a German copper supplier KME was persuaded to undertake the work (with extra financial support from ITER through ICAS for the tooling development and qualification).

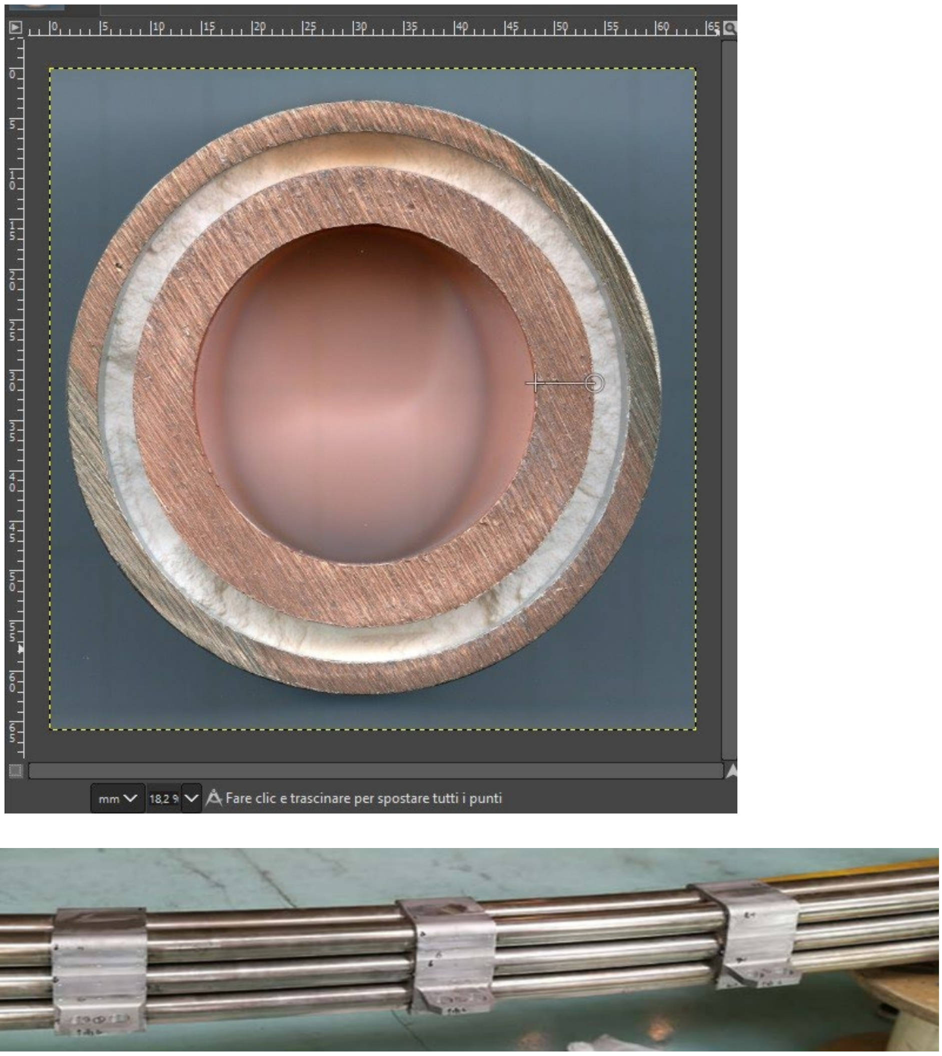

Fig. 6.1-66: Top, IVC Conductor, Bottom Supports welded to ELM coil conductors.

Procurement of In-Vessel Upper and Lower Vertical Stability Coils (UPR and LWR VS) includes the following activities:

- Finalization of all procedures and tooling for manufacturing;
- Production of full-size VS Coil prototype;
- Verification of In-Situ winding and Installation;
- Manufacturing, assembly and installation of both UPR and LWR VS Coils.

It does not include attachment of the feeders to the coils. The package was awarded to Vitzrotech, a Korean company. Significant technical problems have been encountered by the company. With the help of IO a new competent partner (Yujin) has been involved since 2024..

Procurement of all ELM coils, ELM Feeders and VS Feeders.

Phase 1 – Procedures for ELM Coils and Feeders production and Engineering design of tooling.

Phase 2 – Production of Tools and First of a Kinds according to phase 1.

Phase 3 – Production of ELM coils and Feeders.

The contract was awarded to two potential suppliers for Phase 1 & 2, ASG and ASIPP. This work is underway (2024). An example of the conductor and supports in an ELM coil are shown in Figure 6.1-66.

6.1.9 Assembly

At the time of writing magnet assembly is still on-going. Items that have been installed in the cryostat include:

- TF Gravity Supports
- Lower 3 Pre-compression rings (in parked position)
- 6 Bottom Correction Coils (parked)
- PF5 & 6 (parked)
- Most of the B2 level CTBs and CFTs and some of the L3 ones
- Sector 6 (2 TF coils) although this was later removed due to problems with the Thermal Shield
- Stacking (in the Assembly Hall) of 3 CS modules

In addition, for on-site preparation of the TF coils for assembly (covering Site Acceptance Tests, installation of the ILIS (Inner Leg Intercoil Structure), partial installation of the Correction Coil supports and some installation of surface cooling pipes) an on-site facility in a dedicated building was set up in 2018, operated by the TAC2 contractor, and all 18 of the TF coils are now ready for installation on the subsector assembly tools.

The assembly of two TF coils on Sector 6 in 2021-22 was outstandingly successful, with the coils being successfully aligned to a positional accuracy of about 0.5mm, Figure 6.1-67.

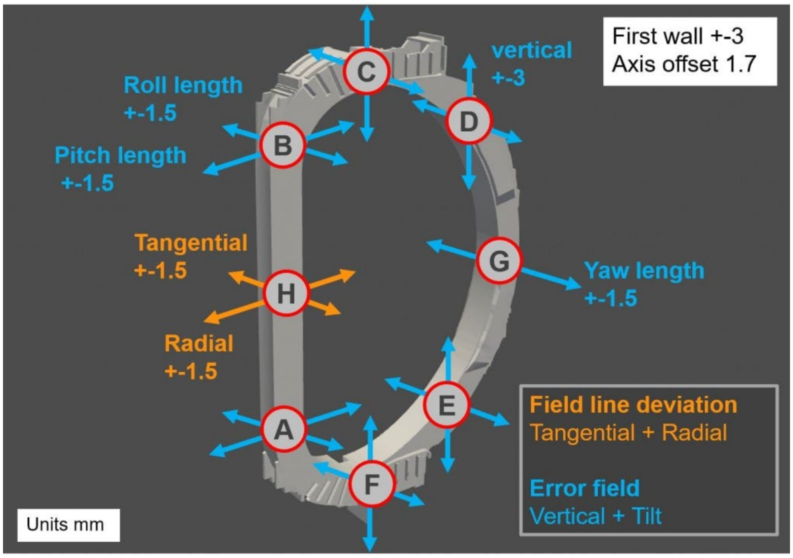

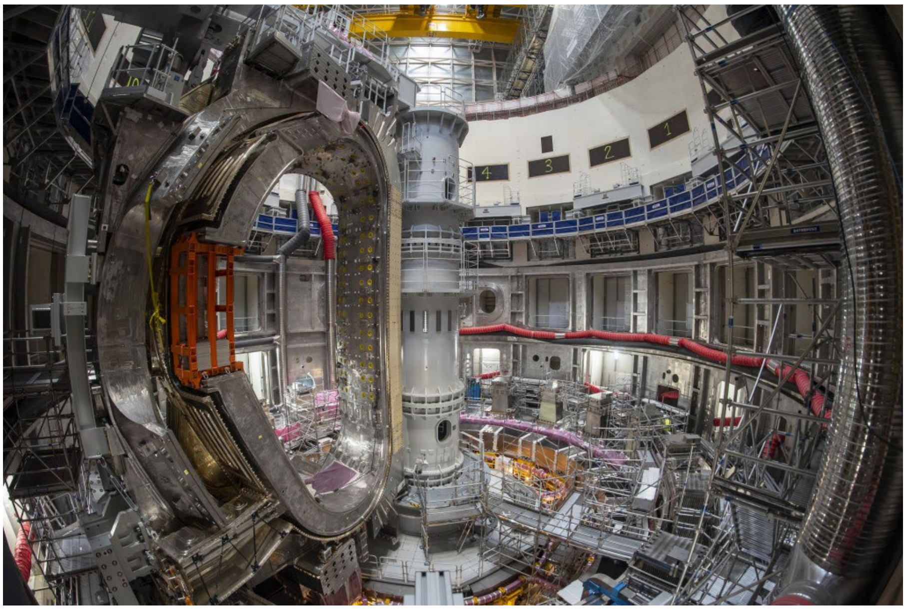

Fig. 6.1-67: Inside the Cryostat after installation of the first 1/9 subsector (2 TF coils, 1 VV sector). Above: tolerance requirements, met during the installation.

The main problems with assembly as it impacts the magnets have been a lack of preparation, identified in 2014-15. This has appeared in 4 areas:

- It became obvious that the Assembly Hall (B13) was by far too small to allow large components to be prepared before installation on the SSATs. For magnets this has partly been addressed by the construction of building B73.2 for TF preparation, and the use of B73.1, the re-purposing of the beryllium building (B22) as a workshop and the use of the cryostat building B56 for feeder preparation, plus the use of a feeder workshop on the other side of the Durance valley at Corbieres. However, the inefficiencies of such an adhoc solution have substantially contributed to the ITER delays. Proposals for an integrated on-site magnet assembly workshop were available from 2012 but were blocked by successive ITER directors on cost/necessity grounds. This has been partly compensating by installing a magnet workshop at CEA Cadarache in 2014.

- The assembly procedures had not been worked out in detail. This has become obvious in the work to assemble the feeders (CFT to CTB joints) in the galleries, but in-cryostat work is still far from being resolved. As an example, the TF feeders (the TF-ICF) are being redesigned with a new FDR in 2024 because the present assembly procedure (of the subcomponents as manufactured) cannot produce a functional component.
- For later work in the cryostat and vessel, the issue of congestion and parallel working has not been addressed, also not in 2024.
- The need for storage of components, since manufacturing after 2019 was obviously running ahead of assembly. The result has been a rushed and uncoordinated construction of extra buildings for storage (B55.1 & 2. B73.3 and use of B73.1 as regards the magnets) since 2017, often providing an unsuitable environment for storage times that will exceed 10 years.

6.1.10 Experiences and Lessons

The following sections give some specific examples of 'cases' from the ITER technical development activities.

6.1.10.1 Strand and conductor supply

The ITER Nb_3Sn strand production is a classic example of the successful industrialisation of a research product. At the start of ITER, in 1988, Nb_3Sn could be obtained from few suppliers in random lengths of a few hundred meters, with long (many months) delivery times for a few hundred kg. The step up in production to ~100t/year was driven by the fusion program, although commonality with NbTi production equipment (and suppliers) helped the scale up, since LHC in the 1990s provided a supplier stimulus which then carried suppliers over to the ITER work, while the early orders for the model coils allowed Nb_3Sn production techniques to be refined. There are similarities with the present advancing industrialisation of REBCO HTS tape.

A further and later lesson is the myth about establishing supply chains. The production of the ITER Nb_3Sn conductor required a supply chain to be established all the way from material suppliers to the strand and conductor production processes. However, supply chains develop according to need and cannot be 'created'. Within 3-4 years of completion of the ITER strand production (in 2016), most of the supply chains had disappeared as there were no follow-on orders. The teams were dispersed and much of the equipment was scrapped. Supply chains are 'nurtured', not created or established. This means that you must allow time, provide orders and demonstrate a future profitability to the parts of the supply chain. It must be coordinated with the progress of the rest of the device, as supply chains are very sensitive to interruptions in orders. The key points are the availability of skilled workers (training of someone who can set up an HTS or Nb_3Sn production line is >5 years), the raw material supply chain (specialised raw materials need to be reserved 12-24 months in advance…even something as basic as a special steel), and the tooling design and supply. Reserving materials will require penalty payments if orders are cancelled, and tooling supply companies will not start work without definite orders (and penalties for cancellation). A supply chain requires a long-term investment that can be minimised with good coordination and schedule control but cannot be avoided.

6.1.10.2 Insulation and High Voltage Engineering Development

6.1.10.2.1 Coil Internal Insulation

The concept of 'solid high voltage' cryogenic insulation systems was established very early in the development of large tokamaks, during the NET project at Garching in the 1980s, and is one of the major innovations brought to large superconducting systems by fusion.

The ITER insulation choice at the end of the CDA in 1991 was glass-epoxy. Quite striking was the absence of polyimide (Kapton). At this time, no one had really proposed the wind-react-insulate route which is what is now used for the ITER coils and there was passionate argument around wind-insulate-react (so the insulation has to go through the Nb_3Sn heat treatment which eliminates Kapton) and react-wind-insulate which means the Nb_3Sn has to be restricted to be close to the conductor neutral axis which limits the current. The history of the magnet insulation is a significant contribution to the present ITER design as it developed from 1991 to 2007, Figure 6.1-69. This argument (R&W&I and W&R&I) also had a major impact on the conductor jacket material and led to the Incoloy debacle of the late 90s (focused on the CS) and the lesser debacle of the JK2LB used in the present ITER CS.

The ITER magnets are typically designed for voltages in the range 20-30kV, almost an order of magnitude above the voltages typical of superconducting magnet systems used in high energy physics or in previous superconducting fusion devices. This requires very careful use of overlapped polyimide-based electrical barriers (rather than relying on glass and a physical separation) involving the identification of solutions to industrial problems with the polyimide wrapping, resin bonding to the polyimide surface and resin flow/gas evacuation through the labyrinth formed by the overlapping layers. The need for polyimide insulation systems was not widely recognized at first, and the lack of it caused several failures on superconducting fusion devices in the 1990s and early 2000s.

The role of the (imperfect) cryostat vacuum in allowing arc development from high voltage surfaces exposed to vacuum, even if the surface is insulation, was discovered in T15 in the 1980s with long electrostatic discharges from the coil surfaces where no ground plane was implemented.

ITER was careful to ensure proper ground planes and insisted on Paschen testing of all components during manufacture and assembly (where multiple faults were found). The experiences of JT60SA in this respect (where no Paschen tests were performed in manufacturing or assembly) are a clear warning, with plasma operation interrupted by several years. It is likely that ITER still needs to apply precautions in this area.

Two developments were implemented to support the HV insulation system:

- Development of cyanate ester-based resins which give improved strength and substantially increased nuclear radiation resistance.
- Development of high voltage (20-30kV) pre-impregnated systems suitable for cryogenic use and hand application, incorporating polyimide films and requiring curing with minimal gas content, to complete local insulation on cooling pipes, joints and terminals.

This last item is a particular challenge and has caused failures on the ITER first of a kind coils, with the need to avoid direct tracking paths through resin and glass (which can crack) still not fully recognized. Short-cuts in manufacturing have proved more expensive to correct than implementing proper solutions at the start. The problem is to maintain the polyimide layers in place as the resin is applied and cured, since hand application of wet resin tends to allow wrapped layers of glass-polyimide to slide and ripple. The tracking length criteria has proved robust when properly implemented.

The original insulation systems for ITER, devised in 1994-5 and tested in the toroidal field model coil (TFMC), were laminates consisting of combined Kapton–H foil/boron-free glass fibre reinforcement tapes, which were impregnated by the VPI process with Bisphenol A diglycidyl ether (DGEBA) epoxy systems (Araldite F type or MY 745). DGEBA-based insulation systems showed significant radiation-induced damage, especially under interlaminar shear load. Reductions of the interlaminar shear strength by up to 50 % were found after irradiation up to the ITER neutron fluence of $1x10^{22}nm^{-2}$ (see also the section on the Nuclear Load Specification).

Cyanate ester (CE) resins are well known for offering a broad spectrum of applications due to their enhanced hot/wet performance, low moisture absorption and mechanical strength, as well as good radiation resistance. Following an initiative in European industry in early 2000s, CE resins were investigated as possible improvements to the DGEBA systems for the TF coils. To allow their application as the electrical insulation of large superconducting fusion magnets, they had to be compatible with the impregnation methods (basically vacuum-pressure impregnation) used for such coils. Low viscosity and a long pot life are important for a proper impregnation over large areas.

Initial investigations, Figure 6.1-68, showed that CE-based insulation systems offered excellent properties in relation to the ITER TF magnet design, with no loss of interlaminar shear load up to $4x10^{22}nm^{-2}$ and with initial values over 33% higher than the DGEBA resins. A mixing ratio of 40% CE and 60% of the original DGEBA turns out to be the best compromise between radiation resistance and costs, i.e. employing a relatively low amount of the far more expensive CE AroCy-L10.

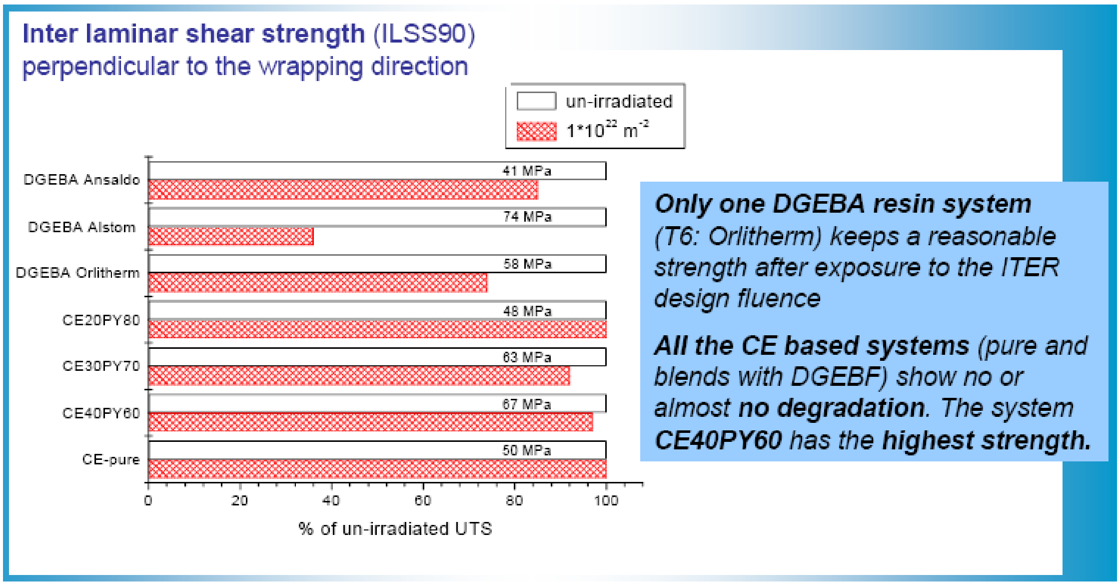

Fig. 6.1-68: Insulation Radiation Resistance.

The CE resins are cured by addition of a catalyst, and the process is exothermic, with a tendency to run out of control if not adequately cooled. Industrialization of the use of the resin required addressing not only the control of the curing, but also identification of new catalysts that allowed a suitably long pot life and which were acceptable under international health and safety regulations since some are characterised as endocrine disruptors. International export of the chemicals used in the resin systems proved almost impossible and local suppliers had to be identified to provide nationally approved equivalents. This complicated the ITER qualification processes since they had to be repeated for each local variant.

As well as resins for the coil impregnation, an insulation system was also required for the Feeders. In the PA, the original specification was for a vacuum impregnation, but this is impractical in view of the need for moulds and compression of the insulation. Instead, ITER assisted ASIPP/CNDA to develop a pre-impregnated system for the feeders. The challenge in a pre-preg is to achieve a low gas content during curing as gas bubbles degrade the insulation life. Eventually a pre-preg supplied by the company Gurit was chosen, with a textured surface that seemed to assist in gas evacuation between the layers (<3% being achieved). Curing takes place in a vacuum bag with heat shrink tape to provide compression. The pre-preg has a relatively short shelf life which has caused issues because of the ITER project delays (life of 2 years when in freezer, 6 months at room temperature), requiring a continuous re-supply. It is cut into strips, and a polyimide layer is added before respooling. It has been successfully applied to the feeders as manufactured and for assembly in the ITER cryostat, also for some repairs to PF coils.

6.1.10.2.2 HV wire exits

Although the coil internal insulation system has been successfully manufactured and qualified, many difficulties have been found (Figure 6.1-69) with the high voltage wire exits from the ground insulation, which provide the (critical) quench protection system. The regulatory requirements for materials in the cryostat prohibit the use of halogen containing materials. The cryostat pumping system is connected to the tritium recovery system (in case of leaks from the VV) and halogens would poison the tritium recovery beds. This restricted the choice of HV wires to an insulation of extruded polyimide. Such wires are extremely stiff and difficult to handle and have been found to be sensitive to Environmental Stress Corrosion from some of the coil resins. If the resin in liquid form touches the surface of the wire, it causes cracks due to a chemical attack as it cures.

Unfortunately, the wide variability of coil resins being used (each supplier is different, partly because of national H&S regulatory approval of only local resins, section 3.5 and Figure 6.1-38) has made it difficult to control this issue. Several elaborate wire exit designs have been produced, all aiming to keep liquid resin off the wires and most suffering from unpredictable failures (especially after thermal cycles) probably because of the amount of expert hand work required to make them.

The HV wire exits probably present the largest risk of failure to an ITER coil. The CS has experienced the most failures (possibly because it has done the most testing) but there are concerns with EU-DA and JA-DA wires in the PF and TF systems too (especially for TF coils that have not been thermally cycled). Mitigation and testing actions are possible but as of 2024 have not been implemented.

Some lessons learned for the future:

- Relax the ban on halogens if HV wires are kept as is, otherwise not practical to achieve the required flexibility and chemical immunity with industrially available wires.
- Reduce the number of HV wires (or eliminate, with alternative QD systems such as fibre optic).
- Standardise the design of the HV wire exits and pre-fabricate/test them on pipes outside the cryostat (the pipes are later welded and the local insulation built up at the weld area, as implemented by EU-DA).
- Reduce the voltages.

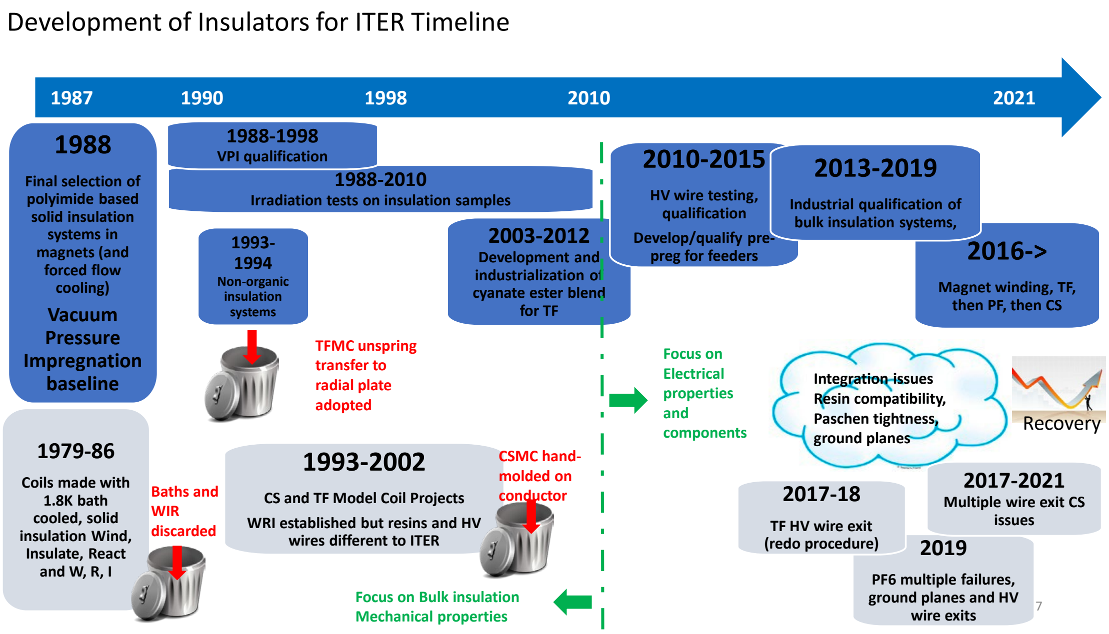

Fig. 6.1-69: History of ITER Insulation Development.

6.1.10.3 Structural Materials and Structure Fabrication

ITER relies on large quantities of structural steels to react the magnetic forces, with a total weight of >7500t. Attempts were made in the past to develop special alloys with enhanced properties, to reduce the amount of steel required (and, of course, the space the structural steel occupies) in critical regions of the tokamak. These attempts failed and, by the start of ITER construction in 2005, the design relied on high strength austenitic steels, basically 316LN, with one minor exception (the nose of the TF coils) where a special steel developed in the Japanese fusion program was retained.

Structural steels tend to be thought of as conventional materials and there is a tendency to push to extremes in the choice of required properties, based on highly specific compositions or special compositions lying ‘just outside the experience box’, perhaps overestimating the extent to which properties can be controlled in industrial production involving thousands of tonnes. It has been obvious, as the structural steel production for ITER coils and supports has proceeded, that achievable bulk properties were significantly overestimated in 1990 and production experience necessitated a series of reductions in performance specification. For example, the yield stress requirement for the highest performance stainless steel in the TF structures is 900 MPa and the fracture toughness is 180 MPam$^{1/2}$, compared to a targeted development activity, in 1990, of 1200 MPa and 200 MPam$^{1/2}$, values originally thought to be attainable Figure 6.1-70.

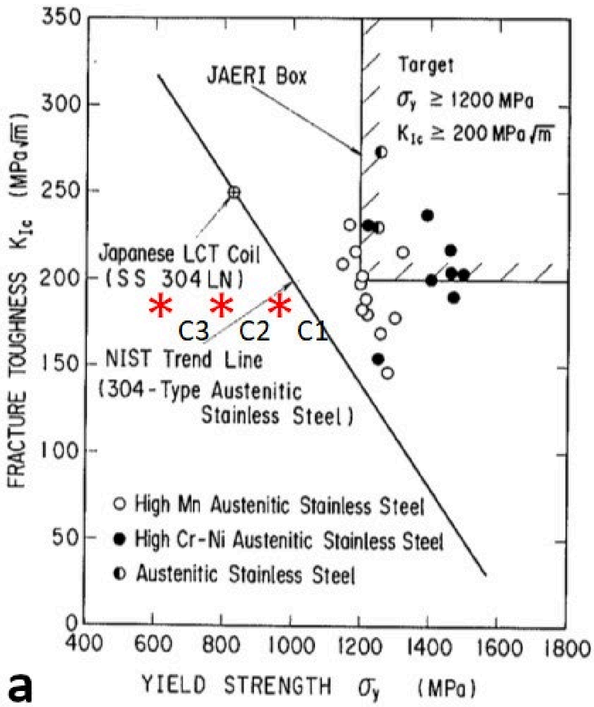

JCS	C	Si	Mn	P	S	Ni	Cr	Mo	N	Others
CSUS-JN1	0.026	0.99	4.2	0.026	0.002	14.74	24.2	—	0.34	
CSUS-JKA1	0.023	0.42	0.49	0.006	0.001	14.0	25.0	0.68	0.268	
CSUS-JN2	0.050	0.34	22.4	0.010	0.002	3.22	13.4	0.70	0.24	V: 0.30
CSUS-JK2	0.05	0.36	21.79	0.013	0.005	4.94	12.82	—	0.212	Cu: 0.70
CSUS-JJ1	0.046	0.44	9.74	0.020	0.002	11.92	12.21	4.89	0.203	

b

*Fig. 6.1-70: Attempt to develop high strength steels. a) the relation between fracture toughness and yield strength of the JCS at 4 K. * indicates the 3 ITER material grade specifications used in 2009 C1, C2, C3 ; b) chemical compositions of the JCS.*

6.1.10.3.1 Base Materials for Structures

Basic material research was launched in 1988 at the start of the ITER CDA, with the perception that higher structural metal properties could bring saving in overall machine cost. The program launched in JA, EU, and RF. Success was claimed in the mid-1990s in laboratory scale research but there was universal failure on an industrial scale. Problems of production of highly composition specific alloys was underestimated (and the willingness of steel suppliers to become involved in such a long term and small-scale development). The development also neglected issues such as welding, forging, and corrosion, so that reasonable behaviour in these areas was sacrificed to achieve a high toughness and yield.

By 2008, only JJ1 remained (TF coil nose) at C1 level and steel properties were at same level as obtainable industrially in the 1980s.

However, this reduction in required properties to levels that were already available industrially in 1990 hides the major achievements of the magnet structural steel procurement for ITER. It is not only the intrinsic material properties that have to be considered, but also forming, joining, machining and (completely entwined with these last two) the final tolerances that can be achieved. Broadly, the stronger the steel the more difficult it is to form and to weld, and considerable resources have had to be used to develop, for example, the basic forms for the CS tie plates and the TF coil sections, in particular to minimize the machining costs after forging and to reduce welding (which apart from reducing the bulk material properties and adding inspection challenges, also adds extra machining due to distortion). ITER has achieved local tolerances of under ±1mm in specific areas, and overall tolerances within a few mm, for coils with weights of 300t and characteristic dimensions of ~12m.

6.1.10.3.2 Large coil task on TF structures, forging and casting

One of the ITER large projects initiated in the EDA was the production (within the TF model coil task) of large structural sections of TF cases. This work was partly completed after the end of the EDA in 2001 and is not well reported.

Figure 6.1-71 shows various forged sub-sections of the ITER TF coil case, showing the complexity of the forged forms. Top: seamless TF case (of course, cut to insert the winding but then with matching surfaces), bottom, seamless radial plate for TFMC and casting for TF outer intercoil structure.

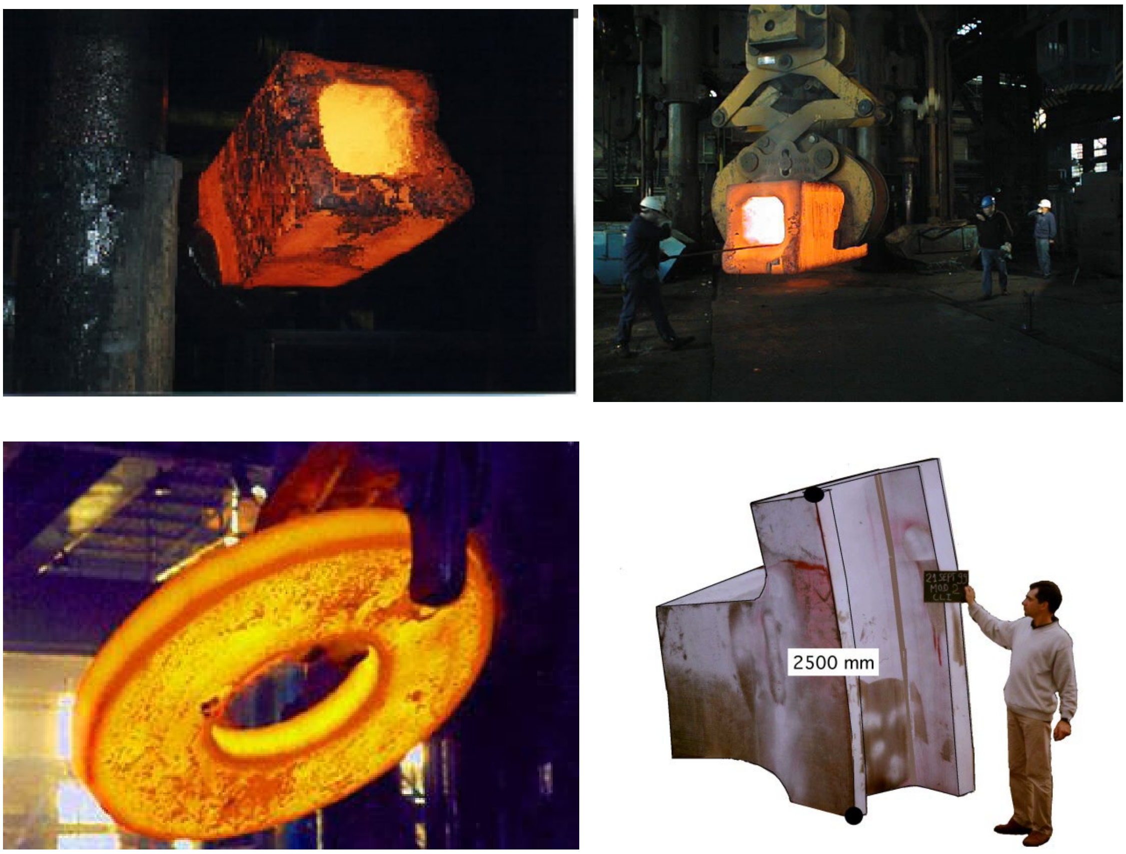

Fig. 6.1-71: Forging and Casting trials on Austenitic Steels, 2000-2005.

Casting was rejected because of poor properties (low modulus, low strength) and defects (voids) which were impossible to repair. The know-how obtained by the forging company (Kind) was used in the period 2012-2018 to produce almost all the forgings for the TF coil cases and VV under contracts with EU, KO and JA.

6.1.10.3.3 Structural Design

Due to complex load conditions, effective structural design is necessary and was difficult to achieve in the ITER environment since the design needs to match the manufacturing route and this was not known until the DA tried to place contracts. The magnet structures use a defect-based design and defects are associated with welds. Minor areas can dominate performance, with large volumes not near critical stresses, and critical stresses in local areas well below those achieved in the base material. These areas are typically welds but not just weld defects but also the achievable weld layout. It was found in 2015 that the structure supplier could not (at reasonable cost) achieve full penetration welds in many of the structural attachments, and such welds must be treated as a defect according to the codes. The ITER magnets were not very well designed in this respect. They were essentially designed by structural analysts, with poor consideration of the manufacturing constraints (shaping, joining and inspection) and overall, a very inefficient utilisation of material. Figure 6.1-72 shows the huge number of attachments and assembly welds in a single coil case. Figure 6.1-73 shows the main segments under manufacture, with a lack of consideration of worker access and weld angle resulting in multiple time-consuming movements of the subsectors during welding.

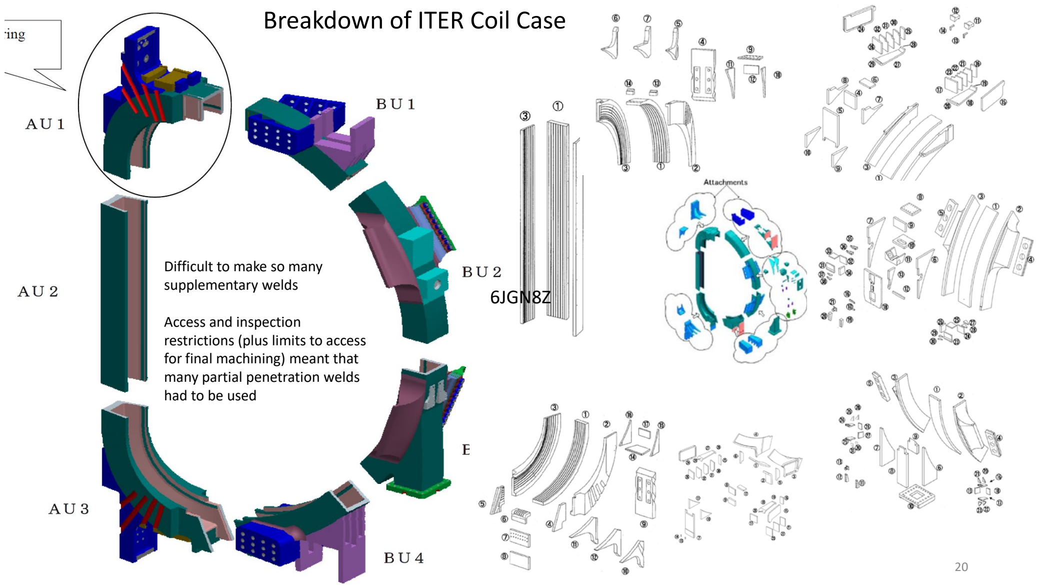

Fig. 6.1-72: Sub-components making up a TF coil case.

Fig. 6.1-73: Main TF Case Segments under Manufacture.

6.1.10.3.4 Maintaining Tolerances

A crucial step, as a component is built up, is maintaining tolerances. Weld distortions are the main source and can be minimised but rarely eliminated. These tolerances are not just related to the final component but for alignment of weld interfaces for the next manufacturing step. Machining of course has its own tolerance limits (vibration and temperature control are critical) but generally weld distortions can only be recovered by leaving an extra thickness which can be (non-uniformly) machined to recover the correct dimensions.

This machining may occur in several steps, and the over-metal must match the expected distortions. For cost reasons, it is better to limit final machining to essential interface regions. As the component gets larger, so, generally, do the machine tools and the difficulty to achieve tight machining tolerances. As an example, EU-DA did extensive weld distortion simulations and verified them by welding trials, before selecting the over-metal thicknesses shown in Figure 6.1-74.

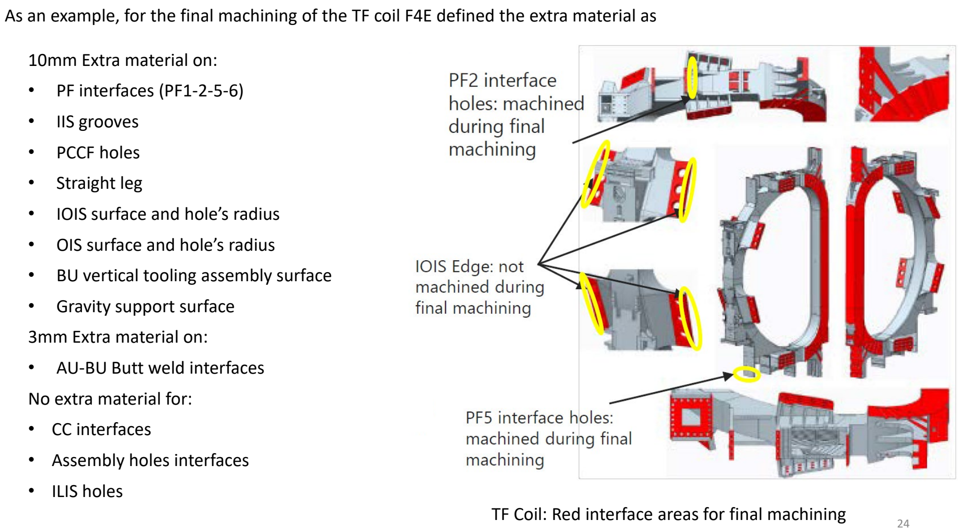

Fig. 6.1-74: Over-metal regions in the TF coil.

Although not originally intended, both JA-DA and EU-DA used large gantry machines for a final machining of the coils, as shown in Figure 6.1-75.

Fig. 6.1-75: TF coil on the Super Miller at MHI

The magnet structures turned out to be one of the most difficult procurements, from a combination of sophisticated technical requirements not fully anticipated by the DAs involved (nor by the IO) and the ITER procurement sharing. The technical requirements and the intricate interfaces to the coils were complicated by a further 'deal' between JA and EU because of the host site selection. This was poorly negotiated (with a lack of a common understanding) and took years to resolve.

JA did not have sufficient steel suppliers willing (or with the capacity) to forge high strength austenitic steels using high quality refined ingots (ESR). In the end much of the supply was subcontracted to Kind (in EU) by the JA prime contractor MHI. JA-DA had problems to identify industries willing to dedicate their machining capability to machine the large subsections to the schedule required so most of the work was subcontracted by MHI to HHI in KO (who were substantially a ship building company, although working also on the ITER VV segments). There were problems with environmental control of machine tools and on accuracy of the metrology. There were many negotiations with JA-DA and MHI about performing fitting tests on the 4 final subsections before shipping them to EU for casing the EU windings, and 'arrangements' involving ITER in order to persuade the suppliers and QST to implement what IO viewed as proper quality controls.

6.1.10.3.5 Conclusions, Magnet Structures

Finally, the required quality was achieved but the schedule was longer than foreseen, and the cost was much higher. The supply route followed, with the multiple subcontractors 'persuaded' to become involved, and quality disputes suggests that the suppliers were not really under the control of QST and certainly not EUDA. It was difficult to engage interest of heavy industry (for raw materials, forgings, machining) for a single very special supply. Low priority was given to the work and there were queues for occupancy of furnaces, presses, machine tools. There are problems in non-standard materials (even for the ITER austenitic 316LN with a request for ESR refining and monitoring of low level of trace elements) as these can require special cleaning of refining furnaces to avoid contamination, with disruption to established industry supply chains which is not popular.

For the future (next time), for structural quantities at the ITER level (>5000t):

- Use standard materials.
- Start manufacturing design early and work with suppliers to simplify manufacturing design.
- Ensure multiple suppliers to remove bottlenecks.
- Aim to limit tight tolerances to interfaces, not to the whole coil. And note that shimming is generally cheaper than overmetal and machining, although less robust.

6.1.10.4 Quality Experiences

In 2007, with the start of the construction, there was a wide-ranging review of the engineering status by ITER and the DAs. Unfortunately, the opportunity to realistically assess the engineering status and particularly the technical and manufacturing readiness was missed. At this review, the assessment level in many areas was that of a Conceptual Design Review and it was obvious that major central team resources would be needed to provide a build to print design to suppliers. This became immediately demonstrated in the buildings where a huge construction design effort had to be implemented. In magnets there was sufficient in-house experience to launch the conductor procurement very rapidly while keeping manufacturing divergence under control, but a major design effort was supplied by the DAs to start the coil & feeder procurements. In magnets, this allowed manufacturing designs to be achieved within about 3 years, in parallel with tooling design and manufacture but it also meant that ITER could not coordinate coil manufacturing processes, each DA/supplier essentially choosing their own. Divergence of processes (and a resultant unpredictable variability in the final product details, especially in areas like tolerances) was kept to an acceptable level by coordination groups and much argument.

A second major issue has been quality management. The original agreement between the ITER participant on quality management during construction was made in Dec 2005 and runs:

For all procurements, the ITER Organization shall be responsible for controlling and integrating the design, technical requirements and specifications; establishing and ensuring the schedules for delivery; managing overall assembly of ITER; establishing quality requirements for each procurement; and verifying capability of suppliers and monitoring their technical and schedule progress mainly through the use of Field Teams located in the territories of the Parties.

In fact, the field teams were not implemented, and the choice of suppliers (and monitoring them) was left in the hands of the DAs, with highly variable results. The ITER central team lacked by far the appropriate manpower resources to monitor such a diverse procurement and generally did not have access to the cost information which the DAs used to select suppliers, along with strategic political considerations. In magnets, it meant that initial product qualification, by testing of sub-components and by final acceptance tests (such as cold testing), has been generally inadequate. The consequences of this have yet to fully appear but will probably manifest themselves in 10-15 years' time during commissioning. At this point it will be difficult to separate out the direct manufacturing faults from aging, leaving responsibility open, and any warranty period will be long expired. More dramatic consequences such as the Thermal Shield corrosion, can be attributed to the weak quality controls from an under resourced central team, unsupported by the DA.

The third major issue has been interfaces. The procurement sharing within magnets was based on DA political strategy and resulted in a maximisation of interfaces between suppliers. For example, the separation of the 19 TF coils between three suppliers, while two others produced the cases and a third assembled the casing on 10 of the coils, could not have been better chosen if the object was to allow suppliers excuses to deny responsibility for problems (this can be seen in the NCRs raised in the coil case manufacture and in the casing operations). It meant that implementation of changes (inevitable given the unfinished state of the design) became a complicated negotiation process with delays and a tendency to try to bypass the configuration control (itself a heavy and bureaucratic process), often successfully as can be seen in the multiple examples of undocumented changes in the sections above.

6.1.11 Magnet Technology Development Beyond ITER

The design of the ITER magnets was substantially completed by 2001 and was, therefore, based on the magnet technology of the 1990s, together with assessments of what technical progress in supply chains could reasonably be expected during manufacturing (anticipated to be 2000-2010). The main risk (as seen in 2001) was the selection of Nb_3Sn for the TF coils (and to a lesser extent the CS since the material need was much lower and the schedule longer). The material was qualified by the CS and TF model coils, but these did not verify the Nb_3Sn supply chain, nor the large-scale manufacturing problems caused by the Nb_3Sn heat treatment, the high operating voltages and the huge steel forgings and very exact tolerances.

By 2004, new superconducting materials were becoming available, in the form of the HTS range. There were only a few niche applications suitable for the low production capacity. ITER exploited these in the form of HTS based current leads, introduced in 2004 and providing a 20% saving on cryogenic power. The Nb_3Sn supply chain had to be established (very successfully, as described elsewhere in this chapter) using the groundwork carried out for the model coil production. Although Nb_3Sn had minimal other applications, the ITER supply chain was sufficiently valuable (and national political support sufficiently strong) to allow multiple suppliers to become engaged.

Although often neglected, insulation technology also advanced in this period with the introduction of radiation resistant cyanate ester resins, qualified and adopted between 2005 and 2009. Another little noticed area was in the structural steels, where continuous gradual progress from the mid-1990s to 2015 (when most of the ITER structural steel was procured) enabled what would otherwise have been impossible in the 1990s. Steel refining, material quality and impurity control, forging and welding (especially low distortion EB and laser based), multi-axis NC machining and defect identification and sizing all enabled the ITER structural material tolerances and defect elimination to reach their specifications by 2019, which would not have been possible in 2001.

Of course, magnet technology did not freeze after 2015 but the subsequent advances could not be exploited in ITER. Now in 2024-5, we can consider how the ITER coils would look if the FDR were to be 25 years later. The most obvious is the industrial availability of coated HTS conductors, REBCO tapes. These offer higher field/temperature performance and their industrial supply chains are as well established as Nb_3Sn in 2001, and with more diverse customers. They eliminate the high temperature heat treatment required for Nb_3Sn and have the potential to start replacing this material within a few years once the associated technology issues (mostly quench protection) can be resolved.

In a 2024 ITER FDR, HTS REBCO would be a contender to replace the Nb_3Sn in the TF and CS coils (and would provoke much discussion). HTS REBCO is sometimes labelled as a 'base enabler' for magnetic fusion since it allows ultra-high field and therefore compact devices to be built. However, for fusion power plants, with neutron fluence on the in-vessel components the main design driver, the ultra-high field capabilities cannot be so easily exploited due to the extreme nuclear fluence on the plasma facing components (and of course the large increase in the magnetic forces). The real advantages of HTS REBCO at ITER field levels are likely to be in an elevated operational temperature >30K, even >40K (reducing cryogenic power and/or allowing higher heat loads, allowing for example a simplification of the TF case inner cooling design) and more stable superconducting operation.

This high stability results in difficulties of quench detection due to slow propagation and is an area where development is still needed, especially in pulsed coils. For a 2024 HTS application to ITER TF and CS coils (replacing Nb_3Sn in the same configuration), conductor-in-coil qualification is required which could be carried out using single layer inserts tested in the CSMC facility at 13T (as was done for revised CS and TF Nb_3Sn conductors 2013-2018 for ITER). The issues would be similar, mechanical degradation of the superconductor under loads, stability (i.e. lack of quench) especially under fast ramping, and quench detection/protection. The ITER CS and TF coils are substantially limited by stresses and HTS REBCO would not enable significant improvements in the coil configuration.

Beyond ITER-type devices, HTS REBCO is coils are being used in attempts to reduce operational voltage levels, with the ITER problems well recognised. The first steps in this have been seen in the last 5-7 years with the introduction of small and medium size non insulated coils (non-insulation means a low resistance metal barrier between conductor turns) for steady state coils like the TF, always with HTS REBCO (although NI LTS coils are also possible). Such coils were hoped initially to be fully self-protecting in the event of a quench but this seems difficult to realise as size increases from small test coils (depending on what quench initiating events are foreseen). NI coils come with the disadvantage of a slow current ramp up and an impossibility to implement a fast discharge in the event of quench. Medium size NI coils now use quench detection and heaters to enhance quench propagation. It seems likely that the traditional insulated conductor route will persist for some time yet.

HTS REBCO also allows non-helium cryogens to be considered, especially when operated at ITER field levels up to 13T. Research into Hydrogen and Neon is ongoing, although not near implementation in a coil.

Joinable coils (LTS or HTS) are also appearing in reactor concepts (such as UK STEP, CFS ARC and Gauss Fusion GIGA) where the importance of coil repairability and improvement in maintenance access to the in-vessel components is being recognised

HTS based coils may improve the superconducting part of the magnet design. However, magnetic forces remain the same and in ITER, the magnet structures occupy much more space than the superconducting part of the magnet and cost significantly more. Structural materials have made large improvements in the last 20 years (as demonstrated in the ITER coils) but the engineering achievable parameters now come close to the inherent material parameters, and the rate of improvement cannot be maintained. The next large steps in magnet technology need to come in improving / optimising the design of the magnet structures, supporting the magnet forces.

Finally, on magnet analysis and digital twins. ITER parameters were selected using primitive systems codes and the extent of internal optimisation of systems like the magnets was very low. Details like the location/extent of the IIS, OIS and IOIS were arrived at by inspiration rather than methodology, and then confirmed by analysis that in 2001 was undeveloped compared to 2024 expectations (although it can be noted that the JET magnet analysis basis from 1979 looked pre-historic compared to the ITER FDR in 2001 and the device still worked, well, for 40 years). A digital twin of ITER magnets that had sufficient parameterisation to allow design optimisation would still be challenging today, but at least the elements (programs) to do it are now available with now more confidence in their accuracy and their ability to represent the non-linearities present. This is likely to be another area of magnet improvements in the next 10 years.

Abbreviations and Glossary

CC	Correction Coils
CS	Central Solenoid
CSM	CS Module
CSPCS-CS	Pre-Compression Structure
DP	Double Pancake
ECC-ELM	Control Coils

EF	Error Field
FD	Feeders
FPA	Flexible Plate Assembly
FSP	Flexible Suspension Plates
FS	Flux Swing
GS	Gravity Support
HP	Hexapancake
HTSCL	High-Temperature Superconductor Current Leads
HS	Hoop Stress
ILIS	Inner Leg Intercoil Structure
IIS/OIS/IOIS	Inner/Outer/Intermediate Intercoil Structures
IB	Insulating Breaks
ICS	Intercoil Structures
KB	Key Blocks
OPF	Out-of-Plane Forces
OM	Overturning Moment
PJ	Pancake Joints
PF	Poloidal Field Coils
PFSS	PF3–PF4 Strut System
PFCS	PF Coil Supports
PE	Poisson Effect
PCR	Pre-Compression Rings
QP	Quadpancake
RP	Radial Plate
SPSJ	Six-Petal Splice Joint
SCH	Supercritical Helium Cooling
TFCC	TF Coil Case
TFC	Toroidal Field Coil
TB	Thermal Barrier
TP	Tie Plates
TIHW	Two-in-Hand Winding
VDE	Vertical Displacement Event
VSC	Vertical Stability Coils
WTD	Wedged TF Design
WL	Winding Lock
WP	Winding Pack

References

[1] L. Bottura, N. Mitchell, and J. V. Minervini, “Design criteria for stability in cable-in-conduit conductors,” *Cryogenics*, vol. 31, no. 7, pp. 510–517, Jul. 1991.

[2] D. Bessette *et al.*, “Test results from the PF conductor insert coil and implications for the ITER PF system,” *IEEE Trans. Appl. Supercond.*, vol. 19, no. 3, pp. 1521–1526, Jun. 2009.

[3] N. Mitchell, “Summary, assessment and implications of the ITER model coil test results,” *Fusion Eng. Des.*, vols. 66–68, pp. 971–993, Sep. 2003.

[4] A. Devred *et al.*, “Status of conductor qualification for the ITER Central Solenoid,” *IEEE Trans. Appl. Supercond.*, vol. 23, no. 3, pp. 6001208–6001208, Jun. 2013.

[5] N. Martovetsky *et al.*, “ITER Central Solenoid insert test results,” *IEEE Trans. Appl. Supercond.*, vol. 26, no. 4, pp. 1–5, Jun. 2016.

[6] N. Mitchell, M. Breschi, and V. Tronza, “The use of Nb_3Sn in fusion: lessons learned from the ITER production including options for management of performance degradation,” *Supercond. Sci. Technol.*, vol. 33, 054007, 2020; M. Breschi *et al.*, “Impact of mechanical and thermal cycles at different operating conditions on the ITER toroidal field coil conductor performance,” *Supercond. Sci. Technol.*, vol. 34, 085021, 2021.

[7] M. S. Lubell *et al.*, “The IEA large coil task test results in IFSMTF,” *IEEE Trans. Magn.*, vol. 24, no. 2, pp. 1180–1183, Mar. 1988.

[8] J. L. Young, T. L. Vota, and S. K. Singh, “Manufacturing development of the Westinghouse Nb_3Sn coil for the Large Coil Test Program,” *J. Phys. Colloques*, vol. 45, no. C1, pp. C1-145–C1-150, Jan. 1984 (Proc. 8th Int. Conf. Magnet Technology).

[9] ITER Organization, *ITER Documentation Series*, no. 26.

[10] L. Maqueda *et al.*, “Feasibility evaluation and pre-conceptual design of the ITER Tokamak systems monitor,” *Fusion Eng. Des.*, vol. 205, 113435, 2023. doi: 10.1016/j.fusengdes.2023.113435.

[11] P. Barabaschi *et al.*, “ITER progresses into new baseline,” *Fusion Eng. Des.*, vol. 215, 114990, 2025.